National Library of Canada
Acquisitions and Bibliographic Services Branch
395 Wellington Street
Ottawa, Ontario
K1A 0N4

Bibliothèque nationale du Canada
Direction des acquisitions et des services bibliographiques
395, rue Wellington
Ottawa (Ontario)
K1A 0N4

Your file Votre référence

Our file Notre référence

NOTICE

The quality of this microform is heavily dependent upon the quality of the original thesis submitted for microfilming. Every effort has been made to ensure the highest quality of reproduction possible.

If pages are missing, contact the university which granted the degree.

Some pages may have indistinct print especially if the original pages were typed with a poor typewriter ribbon or if the university sent us an inferior photocopy.

Reproduction in full or in part of this microform is governed by the Canadian Copyright Act, R.S.C. 1970, c. C-30, and subsequent amendments.

AVIS

La qualité de cette microforme dépend grandement de la qualité de la thèse soumise au microfilmage. Nous avons tout fait pour assurer une qualité supérieure de reproduction.

S'il manque des pages, veuillez communiquer avec l'université qui a conféré le grade.

La qualité d'impression de certaines pages peut laisser à désirer, surtout si les pages originales ont été dactylographiées à l'aide d'un ruban usé ou si l'université nous a fait parvenir une photocopie de qualité inférieure.

La reproduction, même partielle, de cette microforme est soumise à la Loi canadienne sur le droit d'auteur, SRC 1970, c. C-30, et ses amendements subséquents.

Canada

University of Alberta

GEOLOGY, GEOCHEMISTRY AND Nd ISOTOPIC STUDY OF THE HANIKAHIMAJUK LAKE AREA (NTS 86I/1,2; 86H/14,15) NORTHERN POINT LAKE VOLCANIC BELT, SLAVE STRUCTURAL PROVINCE, NWT

by

Joanne Elana Jensen

A thesis submitted to the Faculty of Graduate Studies and Research
in partial fulfilment of the requirements for the degree of
Master of Science

Department of Geology

Edmonton, Alberta

Fall, 1995

National Library
of Canada

Acquisitions and
Bibliographic Services Branch

395 Wellington Street
Ottawa, Ontario
K1A 0N4

Bibliothèque nationale
du Canada

Direction des acquisitions et
des services bibliographiques

395, rue Wellington
Ottawa (Ontario)
K1A 0N4

Your file Votre référence

Our file Notre référence

THE AUTHOR HAS GRANTED AN IRREVOCABLE NON-EXCLUSIVE LICENCE ALLOWING THE NATIONAL LIBRARY OF CANADA TO REPRODUCE, LOAN, DISTRIBUTE OR SELL COPIES OF HIS/HER THESIS BY ANY MEANS AND IN ANY FORM OR FORMAT, MAKING THIS THESIS AVAILABLE TO INTERESTED PERSONS.

L'AUTEUR A ACCORDE UNE LICENCE IRREVOCABLE ET NON EXCLUSIVE PERMETTANT A LA BIBLIOTHEQUE NATIONALE DU CANADA DE REPRODUIRE, PRETER, DISTRIBUER OU VENDRE DES COPIES DE SA THESE DE QUELQUE MANIERE ET SOUS QUELQUE FORME QUE CE SOIT POUR METTRE DES EXEMPLAIRES DE CETTE THESE A LA DISPOSITION DES PERSONNE INTERESSEES.

THE AUTHOR RETAINS OWNERSHIP OF THE COPYRIGHT IN HIS/HER THESIS. NEITHER THE THESIS NOR SUBSTANTIAL EXTRACTS FROM IT MAY BE PRINTED OR OTHERWISE REPRODUCED WITHOUT HIS/HER PERMISSION.

L'AUTEUR CONSERVE LA PROPRIETE DU DROIT D'AUTEUR QUI PROTEGE SA THESE. NI LA THESE NI DES EXTRAITS SUBSTANTIELS DE CELLE-CI NE DOIVENT ETRE IMPRIMES OU AUTREMENT REPRODUITS SANS SON AUTORISATION.

ISBN 0-612-06485-9

Canada

I, James Gebert, hereby grant Joanne Jensen permission to use the map and accompanying sample overlay, EGS 1995-3 1:50 000 Scale Geological Map of the Hanikahimajuk Lake Region as part of her Master of Science thesis.

James S. Gebert

University of Alberta

Library Release Form

Name of Author: Joanne Elana Jensen

Title of Thesis: Geology, geochemistry and Nd isotopic study of the Hanikahimajuk Lake area, (NTS 86I/1,2; 86H/14,15), northern Point Lake volcanic belt, Slave Structural Province, NWT

Degree: Master of Science

Year this Degree Granted: 1995

Permission is hereby granted to the University of Alberta Library to reproduce single copies of this thesis and to lend or sell such copies for private, scholarly, or scientific research purposes only.

The author reserves all other publication and other rights in association with the copyright in the thesis, and except as hereinbefore provided, neither the thesis nor any substantial portion thereof may be printed or otherwise reproduced in any material form whatever without the author's prior written permission.

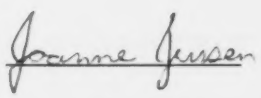

Joanne E. Jensen
155 Oakside Circle S.W.
Calgary, Alberta,
T2V 4H3

Submitted May 31, 1995

University of Alberta

Faculty of Graduate Studies and Research

The undersigned certify that they have read, and recommend to the Faculty of Graduate Studies and Research for acceptance, a thesis entitled Geology, Geochemistry and Nd Isotopic Study of the Hanikahimajuk Lake Area (NTS 86I/1,2; 86H/14,15) Northern Point Lake Volcanic Belt, Slave Structural Province, NWT. submitted by Joanne Elana Jensen in partial fulfilment of the requirements for the degree of Master of Science.

Supervisor - Dr. R. A. Creaser

Chairman - Dr. T. Chacko

Committee member - Dr. R. A. Burwash

Committee member - Dr. M. Sharp

Date Approved: May 31/95

To Mom and Dad

Thanks for all the support and encouragement.

I would like to acknowledge the financial and field support provided by the Canada-NWT Mineral Initiatives Office (1991-1996). I would especially like to thank Jamie Gebert for all of his help and support throughout this project. I thank Rob Creaser for taking me on as his student and for his supervision. Taro Yamashita is thanked for his time and effort put in providing the Nd isotopic analyses for the samples in the area. Steve Grant suffered through the first version of each chapter and is thanked for his reviews and suggestions.

ABSTRACT

This study indicates that the Hanikahimajuk Lake area is more complex than previously thought, both geologically and geochemically, and does not fit well within the geological and tectonic classifications that have been proposed for the Slave Province. The area is a continuation of the Point Lake volcanic belt to the south and a northeast trending, felsic volcanic arm, the Amooga Booga volcanic belt (ABVB) possibly has links to the Central Volcanic Belt in the east. There are two mafic volcanic types, a stratigraphically lower arc-related type, displaying relatively flat REE traces (type I), and a younger calc-alkaline sequence with LREE enriched signatures similar to intermediate volcanics in the area (type II). The felsic volcanics occur in two areas in the central part of the study area. The felsic volcanics are slightly LREE enriched with large negative Eu anomalies and have patterns similar to those associated with VMS deposits in the Abitibi Subprovince, Ontario. The Nd isotopic analyses indicate that the mafic volcanics were derived from a juvenile mantle source with little or no older crustal contamination, whereas the felsic and most of the intermediate volcanics were contaminated during petrogenesis by an older continental crustal component. The ϵNd_T values for synvolcanic diorite complexes bordering the volcanic belt (1.1 to -2.2) generally overlap those of the felsic to intermediate volcanics. The diorites have REE patterns similar to the intermediate volcanics, suggesting that these rocks are the plutonic equivalents of the volcanic rocks.

Three localities comprising older basement (>3.0 Ga) complex have been identified to the north of the ABVB. Geochemical results show that the basement tonalites have REE signatures unlike that of synvolcanic and postvolcanic granitoids that also occur in the region. Nd isotopic analysis on tonalite samples from the complex have $\epsilon Nd_{(2.7)}$ values ranging from -4.1 to -10.5.

TABLE OF CONTENTS

Page No.

CHAPTER 1 INTRODUCTION

1.1 PURPOSE 1
1.2 LOCATION AND ACCESS 1
1.3 PHYSICAL FEATURES 2
1.4 GEOGRAPHIC NAMES AND NOMENCLATURE 2

CHAPTER 2 GEOLOGICAL SETTING

2.1 THE SLAVE STRUCTURAL PROVINCE 3
2.2 REGIONAL GEOLOGY 4
2.3 LOCAL GEOLOGY 8
2.3.1 Basement Complex 9
2.3.2 Volcanic Rocks 9
2.3.3 Metasedimentary Rocks 12
2.3.4 Synvolcanic Complex 13
2.3.5 Granitoids 14
2.4 STRUCTURE 15

CHAPTER 3 PETROGRAPHY

3.1 BASEMENT COMPLEX 17
3.2 VOLCANIC ROCKS 18
3.3 METASEDIMENTARY ROCKS 20
3.4 SYNVOLCANIC COMPLEX 21
3.5 GRANITOIDS 22

CHAPTER 4 GEOCHEMISTRY

4.1 INTRODUCTION 23
4.2 MAJOR ELEMENT ANALYSES 24
4.3 TRACE ELEMENT ANALYSES 27
4.4 RARE-EARTH ELEMENT AND EXTENDED PLOTS 29
4.4.1 Basement Complex 29
4.4.2 Mafic and Intermediate Volcanic Rocks from the ABVB 29

Page No.

4.4.3 Felsic Volcanics from the ABVB 32
4.4.4 Metasediments from the ABVB 33
4.4.5 Mafic Volcanics from the PLVB 33
4.4.6 Felsic Volcanics from the PLVB 33
4.4.7 Amphibolites from the PLVB 33
4.4.8 Synvolcanic Complexes 34
4.4.9 Granitoids 34
4.5 SUMMARY 35

CHAPTER 5 Nd-Sm ISOTOPES

5.1 BASEMENT COMPLEX 36
5.2 VOLCANIC ROCKS 37
5.3 SYNVOLCANIC COMPLEX 38
5.4 METASEDIMENTS 38
5.5 GRANITOIDS 39
5.6 SUMMARY 39

CHAPTER 6 DISCUSSION

6.1 COMPARISONS WITH OTHER ARCHEAN BELTS 40
6.1.1 Archean Average Compositions 40
6.1.2 Hackett River and Yellowknife type classifications for the Slave Province 41
6.1.3 Abitibi Greenstone belt, Superior Province, Canada 43
6.1.4 Pilbara Block, Western Australia 45
6.2 RELATIONSHIP BETWEEN THE SYNVOLCANIC DIORITES, VOLCANIC ROCKS AND ASSOCIATED VMS DEPOSITS 46
6.3 TECTONIC MODELS 49
6.3.1 Collisional - accretionary models 50
6.3.2 Intracratonic models 52
6.3.3 Possible implications 53

CHAPTER 7 CONCLUSIONS 55

BIBLIOGRAPHY 98

APPENDIX A GEOCHEMICAL DATA 104

APPENDIX B UTM COORDINATES FOR THE SAMPLE LOCATIONS 121

LIST OF FIGURES

Page No.

Figure 1. Study area and Slave Structural Province Location Map 59

Figure 2. Slave Province greenstone belt location map. 60

Figure 3. Map area extent and scope of previous work. 61

Figure 4. Thin section photomicrograph of tonalite basement sample, JG91-1754 62

Figure 5. Thin section photomicrograph of gabbro, JG91-1758, from the mixed basement complex 62

Figure 6. Thin section photomicrograph of an ultramafic dyke sample (JG91-1659). 63

Figure 7. Thin section photomicrograph of an intermediate pillow lava, JG92-2495. 63

Figure 8. Thin section photomicrograph of a mafic pillow lava sample, JG92-2931. 64

Figure 9. Thin section photomicrograph of a laminated intermediate volcanic rock, JG92-3284. 65

Figure 10. Thin section photomicrograph of a tuffaceous felsic volcanic rock, JG91-1666. 65

Figure 11. Thin section photomicrograph of a quartz wacke, JG92-2006. ... 66

Figure 12. Thin section photomicrograph of an iron formation sample, JG92-2481. 66

Figure 13. Thin section photomicrograph of JG91-414, a diorite from the northern stock. 67

Figure 14. Thin section photomicrograph of JG92-3339, a diorite from the southern stock. 67

Figure 15. Thin section photomicrograph of JG92-2279, a gabbro. 68

Figure 16. Thin section photomicrograph of a sample of Tak Granite, JG91-1663. 68

Page No.

Figure 17. Thin section photomicrograph of the Rim Granite, JG91-1510. . . 69

Figure 18. Thin section photomicrograph of amphibolite bordering the PLVB, JG93-5719. 69

Figure 19. Thin section photomicrograph of the hornblende pyroxene igneous cumulate, JG93-5228. 70

Figure 20. Thin section photomicrograph of a pegmatitic dyke, JG91-1657. . 70

Figure 21. Thin section photomicrograph of a Mackenzie diabase dyke, JG91-79. 71

Figure 22. AFM diagram showing volcanic rock distribution. 72

Figure 23. Jensen plot. 72

Figure 24. Frequency vs silica histogram. 73

Figure 25a). Harker diagrams (see figure 25b) for legend of symbols). 74

Figure 25b) Harker diagrams continued. 75

Figure 26. QAP normative diagram. 76

Figure 27. MgO-FeO*-Al_2O_3 diagram. 76

Figure 28. MnO-TiO_2-P_2O_5 diagram. 77

Figure 29. Nb vs. Y plot. 77

Figure 30. Rb vs. Nb+Y plot. 78

Figure 31. Zr-Ti/100-Y*3 plot. 78

Figure 32a). REE diagram for the tonalite from the basement complex. 79

Figure 32b). REE diagram for the gabbro from the basement complex. 79

Figure 33a). REE diagram for mafic volcanics exhibiting type I patterns. 80

Page No.

Figure 33b). REE diagram of small mafic pillowed lavas showing the type I pattern. 80

Figure 33c). REE diagram for the large pillowed lavas with quartz and plagioclase phenocrysts and thick selvages (type I pattern). 81

Figure 33d). REE diagram showing the type I pattern displayed by plagioclase porphyritic pillowed lavas. 81

Figure 33e). REE diagram for the laminated mafic volcanics occurring in the ABVB. 82

Figure 34. REE diagram for pillowed lavas mapped as mafic and displaying type II patterns. 82

Figure 35. REE diagram for intermediate pillowed volcanics displaying patterns that fall between type I and type II. 83

Figure 36a). REE diagram of massive intermediate flows (type II). 84

Figure 36b). REE diagram of the laminated intermediate volcanics interlayered with the felsic volcanics in the eastern ABVB (type II). 84

Figure 37. Extended plot of the type I and type II intermediate and mafic volcanic rocks. 85

Figure 38. REE diagram of felsic volcanics from the ABVB. 86

Figure 39. REE diagram for the metasediments from the ABVB. 86

Figure 40a). REE diagram for mafic volcanics from the PLVB displaying type I patterns. 87

Figure 40b). REE diagram for mafic volcanics from the PLVB displaying type II patterns. 87

Figure 41. REE diagram for the felsic volcanics from the PLVB. 88

Figure 42. REE diagram of the amphibolites from the PLVB. 88

Figure 43. REE diagram for the synvolcanic diorites exhibiting type I patterns. 89

Page No.

Figure 44a). REE diagram for the synvolcanic diorites exhibiting type II patterns. 89

Figure 44b). REE diagram for the gabbros from the synvolcanic complex exhibiting type II patterns. 90

Figure 45. REE diagram for the type III pattern synvolcanic diorites. 90

Figure 46. REE diagram for gabbros from the synvolcanic complex displaying patterns similar to the type I mafic volcanics. 91

Figure 47. REE diagram of type I granitoids. 91

Figure 48. REE diagram of granites with large negative Eu anomalies. 92

Figure 49a). REE diagram of the type II granites. 92

Figure 49b) REE diagram of tonalites having type II granitic patterns. 93

Figure 50. ϵNd vs. time plot. 94

Figure 51 Proposed tectonic models for the Slave Structural Province 95

LIST OF TABLES

Page No.

Table 1. Preliminary U-Pb geochronological data (granted from S. Bowring, unpublished). 96

Table 2. Comparison table of Condie (1981) Archean average compositions and Hanikahimajuk Lake area averages. 97

LIST OF MAPS

EGS 1995-3 1:50 000 SCALE GEOLOGICAL MAP OF THE HANIKAHIMAJUK LAKE REGION AND SAMPLE OVERLAY

LIST OF ACRONYMS

PLVB	Point Lake Volcanic Belt
ABVB	Amooga Booga Volcanic Belt
SSP	Slave Structural Province
YKSG	Yellowknife Supergroup
CVB	Central Volcanic Belt
GSC	Geological Survey of Canada
DIAND	Department of Indian Affairs and Northern Development
MIO	Mineral Initiatives Office (Northwest Territories)
ARFZ	Avaarvik River Fault Zone
LOI	Lost on Ignition
REE	Rare-earth Element
HFSE	High-field Strength Element
CHUR	Chondritic Unfractionated Reservoir
MORB	Mid-ocean-ridge Basalt
VMS	Volcanogenic Massive Sulphide

CHAPTER 1. INTRODUCTION

1.1 Purpose

The Hanikahimajuk Lake area was mapped at a 1:50 000 scale in the summers of 1991, 1992 and 1993 with follow up work done in 1994, as part of the Canada-NWT Mineral Initiatives 1991-1996. This area straddles isotopic boundaries determined by Davis and Hegner (1992) for Nd and by Thorpe *et al.* (1992) for Pb. As well, in the first field season, three large areas of basement (>3.0 Ga) complex were found. The Hanikahimajuk Lake area was found to be unique in its proportions of volcanic rock types as compared to the rest of the Slave Structural Province and the fact that two, large synvolcanic dioritic complexes occur along the margins of the volcanic belt. This thesis was undertaken to constrain the geochemical and Nd isotopic relationships of the geology in the area, and to determine how a detailed localized study of a volcanic belt compares with regional geological and tectonic studies previously done in the Slave Structural Province.

1.2 Location and access

The study area is located in the Hanikahimajuk Lake (aka Amooga Booga Lake) region to the southeast of Napaktulik (formerly Takijuq) Lake (figure 1). The area is located along the western margin of the Slave Structural Province (SSP), contained in map sheets NTS 86H/14,15 and 86I/1,2, approximately 425 kilometers north of Yellowknife. Access to the Hanikahimajuk Lake area is possible by ski and float equipped aircraft from Yellowknife. The study area is

approximately 75 kilometers northwest of an airstrip at the Lupin Mine and 45 kilometers north of an airstrip at the Izok Lake exploration camp. Winter road access exists between the Lupin Mine and Yellowknife and a proposed extension to this road from Izok Lake to Coppermine would cross the southwestern portion of the study area.

1.3 Physical features

The topography of the study area is controlled by the lithology. Erosionally resistant metavolcanic rocks, diorites and granites form an elevated flat highland composed mainly of exposed bedrock. There is a marked difference between this type of topography and the northerly trending valley and ridge topography of the Wopmay Orogen to the west, and the glacial drift covered lowlands south of Itchen Lake, an area underlain predominantly by less resistant metasedimentary rocks.

There is approximately 70% of outcrop exposure in the study area, however, mapping is locally hampered by glacial drift and lichen obscures most rock faces, further impeding mapping. Valleys, commonly the site of geological contacts or faults in the area, are usually filled with drift.

1.4 Geographic names and nomenclature

Due to a lack of formally named lakes in the study area, it is difficult to assign names to the map units. Changes in the lake names can also cause confusion. For example, the largest lake in the area was originally named Buffalo Lake by Samuel Hearne in 1771 and has since been called Takijuq Lake (also spelled Takiywak, Takiyuak, or Takijuk) and is now called Napaktulik Lake. For

the purpose of this study, informal lake names (written in italic-type) and lake elevations have been used to identify areas.

Bostock (1980) classified the volcanic rocks in the Point-Contwoyto Lakes area as the Point Lake Formation (figure 2). He subdivided the volcanic belt into the Central Volcanic Belt (also known as *Olga Lake* Volcanic Belt) and the *Western* Volcanic Belt, the latter has since been replaced as the Point Lake Volcanic Belt (PLVB). The northeast trending arm of the PLVB north of Itchen Lake is informally referred to as the *Izok Lake* Volcanic Belt. In the Hanikahimajuk Lake area, the volcanic belt has been called the Amooga Booga Volcanic Belt, Takiyuak Volcanic Belt, and the South Segment of the Takijuq Supracrustal Belt. North of the Hanikahimajuk Lake area the belt has been named Takijuq Lake Volcanic Belt, Hood River Volcanic Belt, Hawk Lake Supracrustal Belt, Hood River-Takijuq Lake Supracrustal Belt, and Napaktulik Volcanic Belt. For the purposes of this study, the belt for NTS 86I/1,2 and 86H/15 will be referred to as the Amooga Booga Volcanic Belt (ABVB) and the belt in NTS 86H/14 will be referred to as the Point Lake Volcanic Belt (PLVB) (figure 2), although it should be remembered that the two are continuous, and not separate entities.

CHAPTER 2. GEOLOGICAL SETTING

2.1 The Slave Structural Province

The Slave Structural Province (SSP) (figure 1) is situated in the northwestern part of the Canadian Shield and is approximately 600 kilometers wide and 700 kilometers long. The majority of the rocks in the SSP are Archean

in age (3.1-2.6 Ga). To the east it is bordered by the Proterozoic Thelon Tectonic Zone and to the west; by the Proterozoic rocks of the Wopmay Orogen. The Slave differs from other Archean provinces in that the dominant supracrustals are turbidite metasediments, not volcanic rocks, and plutonic granitoid complexes make up less than 50% of the SSP. The ultramafic volcanic units, which include komatiites, typically found in Archean provinces, are rare, and have not yet been described in detail. Two distinct types of volcanic belts have been classified in the SSP, 1) Yellowknife-type, dominated by a thick lower basaltic unit with small amounts of felsic volcanics near the top and 2) Hackett River-type, dominated by felsic volcanic units with only minor amounts of basalt commonly occurring near the top of the stratigraphic column (Padgham 1985). Collectively, the volcanic rocks and the turbidite metasediments have been classified as the Yellowknife Supergroup (Henderson 1970, 1981).

2.2 Regional Geology

For the purposes of this study, it is important first to review the general geology of the Point-Contwoyto Lakes area because the geology is similar and can be compared to that of the study area. As well, recent geological mapping supported by geochronology is available from these areas.

The pre-YKSG basement, termed Anton Terrane by Kusky (1989), lies to the west of the PLVB in the vicinity of Point Lake (figure 2). Easton (1985) divided the basement into five separate units: three older orthogneiss units, an older migmatitic gneiss and a younger orthogneiss. The classic basement exposure of Augustus Granite is seen in the Keskarrah Bay area of Point lake and is

actually a structural inlier of foliated granodiorite to monzogranite within the PLVB. This granodiorite was dated at 3155+/-3 Ma by Krogh and Gibbins (1978). The gneisses located east of the PLVB range in age from 2.9 to 3.2 Ga.

Bostock (1980) subdivided the PLVB into six units. A high strain zone locally containing mylonites forms the western contact with the basement gneisses. The western portion of the PLVB is composed mainly of banded mafic rocks termed the Perrault Fm. (Henderson, 1988); these were previously mapped as mafic tuffs but could in fact be mafic mylonites. The western part of the PLVB is overlain by both massive and pillowed mafic flows with felsic volcanics becoming more abundant to the east. Gabbro sills commonly occur near the contact between the banded and massive mafic volcanics. For the most part, the mafic and felsic volcanics are broadly coeval; however, the earliest and latest phases of volcanism are mafic (Bostock, 1980).

In the area north of Itchen Lake, the northeast trending segment of the PLVB has been called the *Izok Lake* Volcanic Belt (figure 2). This portion of the PLVB youngs to the southeast towards the Itchen Lake sedimentary basin. Felsic volcanics make up the lowest preserved stratigraphic layer along the northwestern margin. The felsics are overlain by mafic to intermediate volcanics which represent the second volcanic cycle in the area (the *Izok Lake* cycle). The cycle is then capped by mafic breccias which in turn have been overlain by the metasedimentary rocks of the Itchen Lake Basin.

The Central Volcanic Belt (CVB) (figure 2) is a two-pronged volcanic belt exposed between Itchen and Contwoyto Lakes. The CVB youngs towards the

southeast and is composed of a thin lower massive mafic flow overlain by thick intermediate to felsic volcanic fragmentals and is capped by mafic to intermediate flow rocks. The CVB was included in the Point Lake Fm. by Bostock (1980); however, Davis and Hegner (1992) showed it to be geochemically distinct from the rocks in the PLVB.

Above (and sometimes interfingered with) the PLVB, along the margin of the Itchen Lake sedimentary basin, lies the Contwoyto Formation. It is composed primarily of thinly bedded greywackes and mudstones and is characterized by the occurrence of discontinuous bands and lenses of iron formation. Bostock (1980) subdivided the formation into two units: a unit composed of oxide iron formation in the Keskarrah Bay area and a larger unit locally containing lenses of sulphide- and silicate-facies iron formation.

The Itchen Formation is composed of thickly-bedded greywackes and mudstones and can be distinguished from the Contwoyto Fm. by the lack of iron formation. Towards the center of the Itchen Lake sedimentary basin, the Itchen Formation becomes progressively more metamorphosed and migmatized until it grades into a paragneiss unit.

The Keskarrah Formation is composed mainly of polymictic para-conglomerate with minor greywackes. This unit lies unconformably on top of the basement rocks of the Augustus granite and locally intercalates the mafic volcanics of the Point Lake Fm. Several interpretations have been made concerning the origin of this conglomerate. Bostock (1980) interpreted the unit as a submarine fan or deltaic deposit that formed during the later stages of Point

Lake volcanism. Henderson and Easton (1977a) suggested that the Keskarrah Formation was deposited during a stage of rifting. Kusky (1987) proposed that the conglomerate is a syn-thrusting molasse formed during regional deformation.

The plutonic rocks of the Contwoyto Lake region have been subdivided into six intrusive episodes, C1 to C6 (King *et al.*, 1989). The C1 phase is made up of synvolcanic hornblende gabbros and diorites. The C2 unit comprises of synvolcanic quartz porphyritic felsic dykes and trondhjemites. Late synvolcanic biotite tonalites to monzogranites make up the C3 phase. The first three units were dated as intruding between 2667-2650 Ma by van Breemen *et al.* (1989). C4 and C5 are syndeformational and consist of calc-alkaline intrusions, C4 is made up of diorites to granodiorites intruded between 2608 and 2585 Ma and C5 is comprised of tonalites to monzogranites. Syn- to post-deformational peraluminous granites (C6) intruded between 2585 and 2581 Ma. These younger granitoids have been further separated into C6b (Yamba Suite) comprising biotite granodiorite to syenogranites and C6a (Contwoyto Suite) made up of two mica granodiorite to syenogranite (King *et al.*, 1989).

The Point-Contwoyto Lakes area is transected by several north-trending boundaries that mark isotopic sub-divisions in the SSP. Thorpe *et al.* (1992) determined that there is a lead isotopic boundary through the area, with higher $^{207}Pb/^{204}Pb$ ratios existing to the west (Hood, Izok and Point deposits) and lower $^{207}Pb/^{204}Pb$ ratios to the east (Gondor deposit). This implies that the western deposits were derived from sources containing a component of ancient upper

crustal material, whereas in the east, deposits were likely derived from a mantle source or juvenile crust. Davis and Hegner (1992) defined a Sm-Nd boundary parallel to, but 100 kilometers east, of the lead isotope line with negative ϵNd_T granitoid rocks to the west and positive ϵNd_T to the east. In the west, therefore, the granitoids are interpreted to contain an ancient crustal component in their genesis, whereas the eastern granitoids were derived from juvenile sources. Both boundaries roughly coincide with the presently known extent of pre 2.7 Ga rocks within the SSP. As well, the boundaries lie close to a north-trending zone of discontinuously exposed quartz arenites, orthoconglomerates, and ultramafic intrusive rocks that underlie the bulk of the YKSG.

2.3 Local Geology

The study area was first mapped in 1960 as part of a helicopter reconnaissance project at 1:506 880 scale by Fraser, as part of Operation Coppermine by the Geological Survey of Canada (GSC Map 1960-1; Fraser, 1960). Fraser mapped out the extent of the YKSG rocks in the region but did not separate the volcanic rocks from the sediments in the study area. In 1966, Bostock included the southeastern portion of the study area as part of a 1:250 000 map of the Itchen Lake area, and in 1980 published a GSC report on this map area (GSC Map 1473A; Bostock, 1980). The Hood Cu-Zn deposits were discovered in 1972 for Texasgulf by Laplante and Money. Several thesis projects were subsequently funded in the area by Texasgulf. Gill (1976) looked at the stratigraphy, structure and petrology of the sulphide deposits and the host rocks in the study area. Rockingham (1979) focused on the metamorphism and metal

zoning of the Hood 41 deposit. Several mapping projects have been conducted by DIAND in the study area (figure 3), Hyde *et al.* mapped NTS 86I/1,2 at 1:50 000 and produced an accompanying report (EGS 1976-17,18; Hyde *et al.*, 1976), Bau mapped NTS 86H/14,15,16 at 1:50 000 in 1978 (EGS 1978-4; Bau *et al.*, 1976).

2.3.1 Basement Complex (map units 1-2)

In the region north of Hanikahimajuk Lake, the volcanic rocks are bordered by a mixed intrusive unit composed primarily of tonalitic and gabbroic rocks with minor amphibolite and leucogabbro. The tonalite from this unit has been dated at 3.35 Ga (table 1) (Bowring, unpublished); the gabbros are in tectonic contact with the tonalites and have not yet been dated. Locally the tonalitic rocks display a strong foliation becoming progressively gneissic. The texture in both the gabbros and tonalites ranges from fine to coarse grained. Orange-weathering ultramafic dykes intrude the basement complex locally. The contacts between the mafic volcanic belt rocks to the south and the intrusive unit are ambiguous. In places, the basement complex is in fault contact with the mafic volcanics. Ultramafic dykes which cut through the basement complex do not penetrate the belt rocks. However, at other locations the basement complex contains patches of amphibolite which may have been volcanic in origin and the belt appears to grade into the older mixed unit. This suggests two generations of amphibolite, a possible older phase and one that is the same age as the belt.

2.3.2 Volcanic Rocks (map units 3-5)

Several different varieties of mafic to intermediate volcanic rocks occur in the belt. To the north of Hanikahimajuk Lake, mafic pillowed flows with a light

orange-weathered surface, medium-green, fresh surface, thin pillow selvages (one to two centimeters) and small pillow outline (averaging forty centimeters) occur. Near lake *441* along the southwestern margin of the belt, slightly plagioclase porphyritic and glomeoporphyritic massive and pillowed flows occur. The mafic pillowed flows in the study area are commonly variolitic with small, less than one centimeter, varioles. Massive mafic flows and minor mafic pillowed lavas comprise the eastern portion of the PLVB in NTS 86H/14.

Intermediate pillowed flows are well exposed along the eastern end of lake *429*. These pillows are light green to gray on the weathered surface, with small quartz phenocrysts, have very large irregularly shaped outlines (up to one meter) and have thick (3-4 centimeter) selvages. The intermediate pillow lavas have variolitic textures but commonly the varioles have amalgamated to form entities larger than three centimeters.

Foliated dark-green, massive mafic rocks rich in chlorite and not displaying any volcanic textures occur along the edges of the volcanic belt at the contacts with the surrounding granitoid rocks. As well, massive mafic flows occur as interlayers within the felsic volcanic flows.

Laminated mafic rocks underlie the western portion of the northern PLVB and the westernmost portion adjacent to Napaktulik Lake in the Hanikahimajuk Lake area. The laminations in these rocks are the result of the alternate layering of amphibole and plagioclase. Bostock (1980) considered these rocks to be a mafic volcaniclastic unit that had been subjected to subsequent mylonitization along the PLVB western boundary.

Laminated intermediate rocks consisting of volcaniclastic sediments occur as interbeds with the felsic volcanic rocks in the eastern portion of the ABVB. These rocks are grey on the weathered surface and display geochemical signatures distinct from those of the felsic volcanics.

A zone dominated by primarily felsic volcanic rocks (2675 Ma, Bowring, unpublished, table 1) exists in the central portion of the Hanikahimijuk Lake area. This zone is cutoff to the west by the Avaarvik River fault zone (ARFZ) and to the east by the granitoid rocks of the Rockinghorse Batholith. Two large accumulations of felsic volcanic flows occur within this region, possibly marking volcanic centres. The western accumulation is situated at the southwest corner of Hanikahimijuk Lake near the Hood 10 Cu-Zn deposit. The other accumulation lies roughly in the center of the belt approximately two kilometers east of Hanikahimijuk Lake. Between the two centres, the felsic volcanic rocks are interbedded with mafic and intermediate volcanics.

In the easternmost portion of the felsic zone, the felsic volcanic flows are interlayered with intermediate rocks. Fragmental volcaniclastic rocks occur here but the fragments are mainly less than ten centimeters in length. The laminated intermediate rocks are interpreted as reworked volcanic sediments. The central portion of this zone is underlain by metasedimentary rocks which become thicker towards the east. The rock types in this portion of the ABVB suggest that this area was a more distal volcanic environment than the western portion of the belt.

To the south, near lake *485*, a thinner zone of mixed intermediate and felsic volcanic rocks exists. As well, lenses of felsic rock up to 20 meters in

thickness exist in the northern portion of the PLVB, but unlike in the ABVB, the felsic volcanic rocks do not form thick centres.

2.3.3 Metasedimentary Rocks (map unit 6)

Metasedimentary rocks border the ABVB west and northwest of the Hanikahimijuk Lake area. These rocks grade up to amphibolite facies and locally contain large (1-4 centimeter) garnets, andalusite (1-6 centimeter) and small sillimanite crystals. The metasedimentary rocks in this area are very close in appearance to the laminated mafic rocks and can easily be confused with the mafic volcanics. Small bodies of fissile iron formation (ten meters thickness on average) also occur in this area.

In the eastern portion of the ABVB, fine-grained metasedimentary rocks are interbedded with intermediate volcanic tuffs, becoming increasingly thicker towards the east. A magnetite-bearing siltstone, locally becoming iron formation, can be traced up to two kilometers in this zone. A similar iron formation is exposed seven kilometers west along strike and the two may be part of the same unit.

Along the northwest margin of the PLVB several conglomerates and associated wackes and mudstones are exposed. A quartz-pebble conglomerate with grain sizes ranging from pebble to cobble makes up the most extensive unit, traceable along strike for approximately five kilometers and in some places is up to twenty meters thick. It is composed primarily of 30% or more white quartz pebbles contained in a quartz-wacke matrix but can in places contain volcanic fragments as well. This conglomerate is interbedded with, and fines upwards into,

the quartz wacke that makes up its matrix. Younging directions determined from crossbedding were towards the northwest.

A western conglomerate outcrops in a doubly plunging syncline. This conglomerate has a siltstone to mudstone matrix and contains a wide variety of different pebble types and sizes ranging from felsic to mafic in composition and pebble to cobble in size. As well, the conglomerate contains approximately 10% of the quartz pebbles that are seen in the eastern conglomerate. The western conglomerate appears to overlie the eastern conglomerate as indicated by the younging directions. A large valley separates the two units, but the conglomerates may be in structural contact with one another.

2.3.4 Synvolcanic Complex (map units 7 and 8)

To the north and south, the ABVB is bordered by the mafic intrusive rocks of Bostock's Western Pluton (1980). Hyde *et al.* (1976) referred to each body as a separate stock which he termed stock A, B and C. The northern stock was dated by U-Pb methods and gives a preliminary age of 2673 Ma (Bowring, unpublished, table 1). The southern stock gives a preliminary U-Pb age of 2680 Ma (Bowring, unpublished, table 1).

The main portion of this mafic plutonic complex is made up of coarse grained to pegmatitic rock composed mainly of amphibole and plagioclase with accessory quartz, given the field name "black and white diorite". Rock containing dark-green amphibole, pyroxene and plagioclase, given the field name gabbro, also occurs but to a lesser extent. Gabbro is most commonly found north of Hanikahimajuk Lake and field relationships suggest that the gabbros are an

earlier phase than the diorite. In some regions along the perimeter of the northern diorite stock, breccias composed of gabbro (dark-green) intruded by diorite (black and white) occur. As well, gabbroic xenoliths are commonly found enclosed in the diorite.

2.3.5 Granitoids (map units 9, 10, 11, 12)

Surrounding and intruding both the belt rocks and synvolcanic mafic intrusives are later granitoid rocks. The Tak granite (Padgham, 1985) is a porphyritic granite that borders the ABVB to the northwest (>2420 Ma, Bowring, unpublished, table 1). A phase of strongly foliated porphyritic rapakivi Tak granite makes up a zone approximately one kilometer wide at the margin of the belt. To the south, the ABVB is bordered by the red-weathering Rim granite, ca. 2550 Ma (Bowring, unpublished, table 1) of Hyde *et al.* (1976). He named this granite because it forms a rim between the volcanic rocks and the diorite intrusion. Along the contacts, the Rim granite becomes bleached and very similar in appearance to the felsic quartz-eye rhyolites, making it difficult, in some areas, to distinguish between these two units. Further to the south, the Rim granite begins to lose its characteristic red-weathering and begins to resemble the regional granodiorites.

On a local scale, the granites in the study area can be separated and classified as distinct units. However, on a regional scale context it appears that the granites in the study area are related.

In the southwest region of the map area a hornblende- and pyroxene-cumulate intrusion occurs. In the field this intrusion appears gabbroic but

contains potassium feldspar rather than plagioclase which would suggest a more alkaline nature. This is not, however, borne out in the complex's chemistry which shows the samples to have approximately 12% MgO and to plot within the basaltic komatiite field on a Jensen (1976) diagram.

To the west of the PLVB, south of the eastern portion of the ABVB and along the eastern margin of southern Napaktulik Lake, amphibolitic intrusive rocks occur. Most likely, these rocks were derived from the synvolcanic mafic intrusive stocks, but their age relationships are not certain. They are generally composed mainly of biotite, hornblende and plagioclase with some minor quartz.

Most of the units in the study area have been intruded by quartz and alkali feldspar bearing pegmatite dykes. These dykes range in size but on average are thirty centimeters wide.

Four different episodes of diabase dykes (map unit 14) intrude the area. The majority are the strongly magnetic north to northwest trending Proterozoic Mackenzie dykes. Nonmagnetic dykes trend towards the north and northeast. Plagioclase porphyritic dykes have an easterly trend. Four large diabase sills outcrop in the northwest portion of the map area.

2.4 Structure

The SSP has experienced several different phases of deformation. The first phase of regional folding did not generally impart a penetrative fabric on most areas in the SSP. The second phase of folding did result in a strong foliation, generally the primary regional foliation. A third phase of folding produced folds that occur on map scale and is locally expressed as crenulation cleavage. As well,

in some of the sedimentary terranes in the SSP two later crenulation cleavages can also be found (Padgham and Fyson, 1992).

Generally, metavolcanic belts do not record the structural history as well as sedimentary terranes, and this is the case in the Hanikahimijuk Lake area. For the purposes of this study the first foliation measured is generally the regional foliation, keeping in mind that this fabric was probably actually due to a second phase of deformation in the SSP.

In previous studies, a northeast trending synclinal fold axis was interpreted to run through *Shetland* Lake as the conglomerate units to the north were thought to be roughly coeval to the felsic volcanics to the south. However, geochronological data has shown that there is a 100 Ma gap (table 1) between these two units. This would indicate that these units are not coeval and that the conglomerates are in fact younger than the felsic volcanics.

Due to a lack of good top indicators for most of the ABVB and owing to the fact that thick lichen growth hampers mapping in the area, stratigraphic interpretation within the ABVB is problematic. For these reasons the placement of large scale belt folds, which rely on stratigraphy and top indicators, is also uncertain.

The majority of top indicators that were found indicate that the ABVB is younging towards the northwest. A reversal of this trend occurs at the east end of lake *429* and defines a northeast trending synclinal fold axis.

In the western portion of the ABVB, a northerly trending structure termed the Avaarvik River fault zone (ARFZ) separates the felsic volcanic rocks to the

east from the laminated mafic volcanics and metasedimentary rocks to the west. Similarly, this zone separates rocks with differing degrees of deformation. West of the ARFZ the rocks display a strong foliation that has been refolded by a second deformation and locally have crenulation cleavage. East of the ARFZ, the rocks of the ABVB have a northeast trend in contrast to a more northerly trend to the west. As well, there is flattening parallel to the regional foliation in both the mafic pillowed flows and the felsic volcanic clasts.

At the eastern end of the ABVB the metasedimentary rocks interbedded with the felsic and intermediate volcanics locally display a strong penetrative foliation which in some cases has been refolded. Small lenses of iron formation in this area have also been isoclinally folded. The surrounding volcanic rocks appear unfolded and do not display the same fabrics as the metasedimentary rocks.

CHAPTER 3. PETROGRAPHY

3.1 Basement Complex

A mixed unit consisting of weakly- to moderately-foliated tonalite, gabbro and leucogabbro yielded the oldest known date in the map area. The unit is located approximately one kilometer north and northwest of Hanikahimajuk Lake, and has a maximum exposed thickness of 2.5 kilometers. Rocks in this area are mainly tonalitic, mixed with leucogabbro and are cut in places by gabbroic dykes. U-Pb dating (table 1) from slightly discordant zircons taken from sample JG91-1660, a tonalite, gave an age of 3350-3400 Ma (Bowring, unpublished), no dating was done on the gabbros in the same unit. In thin section, the tonalite (eg.

sample JG91-1754) consists mainly of large (5mm), subhedral, corroded plagioclase crystals (60%) and smaller, clear, anhedral quartz crystals (25%). As well, corroded, subhedral crystals of alkali feldspar (5%); euhedral crystals of chlorite showing anomalous blue birefringence (5%); calcite occurring between crystal contacts (2%); anhedral crystals of opaque minerals (2%); and euhedral apatite crystals (1%) occur in sample JG91-1754 (figure 4).

Sample JG91-1758 is a gabbro from the mixed intrusive unit. In thin section (figure 5), this sample contains slightly pinkish, subhedral crystals of clinopyroxene (augite) averaging 5mm in size (40%); corroded anhedral to subhedral plagioclase crystals 2 to 5mm in size (30%); pleochroic green to brown, subhedral crystals of hornblende (20%); smaller anhedral olivine crystals (2mm) (5%); and anhedral to subhedral opaque grains (pyrite).

Red-weathering, northwest-trending ultramafic dykes cut the mixed intrusive unit. The dykes are made up of magnetic peridotite, which is serpentinized in some places along small shear zones. Sample JG91-1659 consists of slightly greenish, anhedral crystals of orthopyroxene (enstatite) (35%), anhedral olivine crystals (30%), clinopyroxene (augite) crystals with subhedral shape (15%) and euhedral to subhedral opaque crystals, most likely chromite (Cr is 3200 ppm for this sample) and magnetite (20%) (figure 6).

3.2 Volcanic Rocks

The volcanic rocks can be separated into three distinct groups: mafic, intermediate and felsic, based on field data, thin section analysis and geochemical data. In some parts of the map area, the mafic and intermediate volcanics are

difficult to divide in the field and are, therefore, classified together on the map.

In the northern portion of the map area, the volcanic rocks are deposited along a northeast trending zone which at its widest is 8 kilometers thick. Mixed mafic and intermediate rocks flank the zone, and toward the center of the zone massive intermediate and felsic flows up to 2 kilometers wide occur.

The undivided mafic and intermediate rocks consist of both pillowed (variolitic and non-variolitic) and massive flows, which are light to dark-green weathering in outcrop. Sample JG92-2495 (figure 7) is an example of an intermediate pillowed lava from the area just south of *Flat Cat* Lake. This sample consists of 70% subhedral crystals of corroded plagioclase, occurring as both large (3mm) and small (<1mm) crystals, 15% small crystals of green pleochroic hornblende, 3% quartz occurring as veins and as small (1mm) amygdules, small, anhedral opaque minerals, possibly pyrite (4%) and 2% small chlorite crystals. Sample JG92-2931 is a mafic pillow lava from the area west of *Not Point* Lake. From the thin section (figure 8), this sample has 70% pleochroic green laths of clinopyroxene (augite), small crystals of plagioclase surrounding the clinopyroxene (25%), anhedral quartz crystals occurring as veins (5%), large (5mm) phenocrysts of fractured olivine (5%), and small anhedral opaques (5%). These two rock types are extremely difficult to divide based on field observations alone, however, there is a notable difference between them in terms of their petrographic and geochemical characteristics.

In the middle of the zone the volcanic rocks can be divided into intermediate and felsic flows. The intermediate volcanics consist of pillowed,

massive and volcaniclastic units, which are light-green or light-gray weathering in the field. JG92-3284 is an example of a laminated intermediate volcanic rock from the *Flat Cat* Lake area (SiO_2 52.9%). Plagioclase, which occurs both as large, and slightly corroded crystals 2 to 5mm in size displaying carlsbad twinning (20%) and as matrix <1mm (30%), is the main component of this rock. Quartz occurs as anhedral crystals (20%). A large amount (15%) of calcite occurs a amygdules and as veins. Sericite occurs as ribbons around the phenocrysts (10%) and some opaques also occur (figure 9).

Two large areas of felsic volcanic rocks exist, one is located to the west and southwest of Hanikahimajuk Lake and the other is approximately 2 kilometers from the eastern edge of Hanikahimajuk Lake. The felsic volcanics in these areas consist of massive, fragmental and tuffaceous rocks. Sample JG91-1666 (figure 10) is characteristic of the tuffaceous felsic volcanic rocks from the eastern center. It consists of quartz, both as matrix (70%) and as larger, 3mm, eyes (5%) and biotite occurring as brown ribbons around and interlayered with the quartz. As well, there is a large portion of opaques, probably pyrite, averaging 2mm in size (10%), and a few (<5%) corroded plagioclase phenocrysts.

3.3 Metasedimentary Rocks

Interbedded with the intermediate volcanic rocks in the eastern portion of the ABVB are metasedimentary rocks. Sample JG92-2006 is a quartz wacke from this area composed primarily of large 5mm subhedral quartz clasts (30%) and potassium feldspar clasts which have a dirty appearance and have tartan twinning (10%) contained in a quartz and sericite matrix (figure 11).

An iron formation in the eastern portion of the ABVB can be traced for approximately two kilometers along strike. In thin section (figure 12), the iron formation has alternating layers of magnetite (dark) and quartz (light-gray), some biotite also occurs within the quartz-rich layers. The individual layers average 1mm in width and both the magnetite and quartz are fine-grained (<0.1mm).

3.4 Synvolcanic Complex

A synvolcanic mafic plutonic complex borders the belt rocks to the north and south. Sample JG91-414 is an example (figure 13) of the northern diorite stock, consisting of extremely corroded anhedral plagioclase crystals (50%) and anhedral to subhedral pleochroic green hornblende crystals (30%). The hornblende has been altered to biotite in some places, recognizable by it's bird's eye extinction. Some quartz crystals are also present (10%) and can be distinguished from the plagioclase by their clear appearance and undulatory extinction. Apatite and opaques occur as well but make up <5% of the rock.

Sample JG92-3339 is part of the southern stock of diorite (figure 14). This rock consists of 30% corroded, anhedral to subhedral, large (5mm) crystals of plagioclase, green to brown pleochroic hornblende crystals with 120° cleavage (30%), subhedral, clear quartz crystals (20%), 3mm laths of biotite (5%), chlorite displaying anomalous blue birefringence and sericite with high order birefringence (4%) and euhedral, small crystals of apatite (2%). Pyrite makes up 10% of this sample occurring as subhedral 2 to 4mm opaque crystals in thin section.

Gabbroic rocks also occur as part of the mafic plutonic complex. In thin section, (JG92-2279) the gabbros contain 30% anhedral to subhedral, pleochroic

green clinopyroxene (augite) crystals, 40% corroded plagioclase crystals, subhedral to euhedral large (5mm to 1cm) crystals of hornblende, 20%, biotite showing bird's eye extinction under crossed polars (5%) and opaques (2%) (figure 15).

3.5 Granitoids

Bordering the ABVB to the northwest, is the Tak granite (Padgham, 1985). An example of this granite is JG91-1663 which has 60% alkali feldspar occurring as large (up to 2cm), altered, twinned and myrmeketic crystals, clear anhedral quartz crystals (25%), pleochroic green to brown biotite (10%) and muscovite with clear to light green pleochroism (2%) (figure 16).

Bordering the ABVB to the south, is the red-weathering Rim granite (Hyde *et al.*, 1976). This granite (JG91-1510) consists mainly of altered anhedral to subhedral crystals of alkali feldspar (60%) and clear, large crystals of quartz (30%). Biotite occurs along the crystal contacts as alteration and also as larger, 2mm, laths (5%). Subhedral, 3mm opaque grains also occur throughout the thin section (5%) (figure 17).

On the southwest margin of the study area a large amphibolitic unit borders the PLVB. This rock (JG93-5719) has subhedral to euhedral large crystals of hornblende (40%), dirty, large subhedral crystals of plagioclase (40%), clear quartz crystals (10%), laths of pleochroic green biotite (3mm) with bird's eye extinction and 8% opaques (most likely pyrite) (figure 18).

Sample JG93-5228 comes from a plug of hornblende and pyroxene igneous cumulate in the southwest region of the study area. This rock (figure 19) is coarse grained and consists of strongly pleochroic hornblende crystals with 120°

and 60° cleavage (40%), equant euhedral green crystals of clinopyroxene (25%), alkali feldspar (25%) occurring as large, slightly corroded, anhedral crystals with tartan twinning, euhedral diamond shaped crystals or large anhedral granules of sphene (5%), and apatite (5%) with a clear appearance and high positive relief in plane polarized light.

Pegmatite dykes intrude most of the other units in the study area. In thin section (figure 20), the pegmatites (JG91-1657) are mainly composed of large (1 to 2cm) anhedral quartz crystals (50%) and large (up to 2cm) twinned alkali feldspar crystals (30%). Muscovite, clear with high order pink birefringence (8%) and pleochroic green biotite (2%) also occur.

Several later diabase dykes exist in the Hanikahimajuk Lake area. Sample JG91-79 is an example of a Mackenzie diabase (figure 21) with subhedral, twinned plagioclase crystals (50%), orthopyroxene with first order yellow birefringence (30%), titanaugite displaying hourglass zoning (10%), green pleochroic hornblende crystals (5%) and equant opaque crystals of magnetite and pyrite (5%).

CHAPTER 4. GEOCHEMISTRY

4.1 Introduction

Over three summer field seasons, 1991, 1992 and 1993, one hundred and thirty-one geochemistry samples were collected from throughout the study area. Samples were chosen so as to minimize the degree of weathering and alteration, and to be representative of rock types seen in the thesis area. The 1991 samples were sent out to Barringer Magenta Laboratories Ltd. of Calgary, AB and the

1992 and 1993 samples were analyzed by XRAL X-ray Assay Laboratories, Don Mills, Ont. The results and the methods used for the analyses are tabulated in Appendix A.

4.2 Major Element Analyses

When the samples are plotted on an AFM diagram (figure 22) there is a bimodal pattern exhibited, with the more mafic volcanics straddling and plotting above the tholeiitic-calc-alkaline line and the more felsic samples plotting in the calc-alkaline field. None of the samples are exceedingly MgO rich, even the basaltic samples have less than 10 wt% MgO compared to 32.5% MgO for sample JG91-1659, an ultramafic dyke. This supports the observed lack of komatiitic samples in the area. The majority of the felsic volcanic samples are $Na_2O + K_2O$ enriched.

On a Jensen (1976) plot (figure 23), the majority of the mafic volcanic samples plot within the high Fe tholeiite field (HFT). Additional samples plot in the high Mg tholeiite field (HMT), the calc-alkaline basalt (CAB) and tholeiitic andesite (TA) fields. The intermediate volcanics plot mainly in the high Fe tholeiite and along the borders of the calc-alkaline fields. The felsic volcanics fall mainly in the calc-alkaline rhyolite and dacite sections of the diagram.

A frequency vs. silica histogram (figure 24) of the igneous samples displays a strong bimodal distribution. Basaltic composition samples (<53% silica) are the most prevalent in the study area making up 44% of the samples collected. The other peak is of rhyolitic composition (>70% silica) and encompasses 30% of the sample suite. Andesitic (53-63% silica) and dacitic (63-70% silica) samples each

make up 13% of the samples, respectively.

Harker diagrams (figure 25a,b) show the spread of the various major elements in the samples. All of the samples show varying degrees of alteration both in thin section and geochemically (see fig. 25b LOI vs. SiO_2) which can be expected when studying Archean rocks. The samples in general become depleted in TiO_2 as their SiO_2 value increases. The exception to this is the ultramafic sample JG91-1659 which is depleted in both TiO_2 and SiO_2. A fairly consistent pattern of Al_2O_3 vs. SiO_2 exists for the sample suite although the diorite samples show slight Al_2O_3 enrichment, likely reflecting plagioclase accumulation in these samples. The ultramafic sample, JG91-1659 and the iron formation sample, JG92-2481, are both Al_2O_3 depleted. MgO and CaO content increase with decreasing SiO_2 content and JG91-1659 (ultramafic dyke sample) is extremely enriched in MgO but depleted in CaO. The plot of Na_2O vs. SiO_2 shows a wide range of scatter, the general trend is one of increasing Na_2O with increasing SiO_2 content. However, some of the felsic volcanics and all of the epiclastics are depleted in Na_2O, which indicates alteration has affected these samples. K_2O increases with higher silica contents reflecting an increase in alkali feldspar in these samples. The felsic volcanics and granitoid rocks are depleted in P_2O_5 whereas the mafic volcanics, gabbros and especially the diorites are enriched in P_2O_5 indicating a higher content of apatite in these rocks.

When the samples are plotted on a LOI vs. SiO_2 plot, the most altered samples are the laminated volcanics (open squares) and some of the mafic and felsic volcanics. This indicates that alteration has affected these rocks and that

their analyses may not be as accurate as samples plotting in the lower portion of the LOI diagram.

When the granitoid samples are plotted on a QAP normative diagram (LeMaitre, 1989) (figure 26) the samples all fall within the plagioclase enriched portion of the diagram. The granites plot in two distinct groups, group I plot within the monzogranite field and group II plot within the granodiorite field mainly. The diorites and gabbros plot in the tonalite, quartz monzodiorite, and quartz diorite fields. The samples mapped as tonalites fall into the granodiorite and tonalite fields on the QAP diagram.

Tectonic diagrams based on the major elements are difficult to apply to Archean greenstone belts because in most cases there has been some degree of mobility of the elements due to alteration (Pearce *et al.*, 1977). Therefore, the analyses based on these types of diagrams should be viewed with caution. When the volcanic samples with between 51 and 56% SiO_2 (andesitic samples) were placed on a MgO-FeO*-Al_2O_3 tectonic diagram (Pearce *et al.*, 1977) the samples plot in a somewhat linear fashion in mainly two groups in the orogenic field (island-arcs and active continental margins) and in the continental field (figure 27). The fields on this diagram are based on Cenozoic data and may not be applicable to Archean rocks (Pearce *et al.*, 1977). However, Pearce *et al.* (1977) did plot some Archean samples from the Abitibi Subprovince, Ontario, Canada, to test the diagram and comparisons can be made to these samples. The samples from the study area show similar trends to the Abitibi samples. The Lower Abitibi samples plot in the continental field and the Upper Abitibi samples plot in

the orogenic field. Pearce *et al.* (1977) state that the "continental" samples may be samples from within plate volcanism indicating possible early continental crust.

The volcanic samples ranging in SiO_2 from 45 to 54% can be plotted on a MnO-TiO_2-P_2O_5 tectonic diagram following Mullen's (1983) work on basaltic composition samples. This tectonic diagram is likely more robust than ones based on Mg and Fe, as Ti and P have less mobility than these elements during secondary processes. The samples from 1991 and 1993 (samples from 1992 were not analyzed for MnO) plot in two distinct groups (figure 28). The samples collected in 1991 fall into the calc-alkaline basalt (CAB) field and the 1993 samples fall into the island-arc tholeiite (IAT) field. None of the samples plot within the mid-ocean-ridge basalt (MORB) field. The segregation of these two suites of samples can be explained by the mafic affinities of each group. The IAT 1993 samples display more mafic characteristics generally than the CAB 1991 samples and have relatively flat tholeiitic type REE patterns. The CAB 1991 samples have a LREE enriched signature and their geochemistry indicates that these samples are more intermediate ($>K_2O$) than the 1993 samples. Both groups are depleted in TiO_2 relative to MnO which may indicate an early fractionation of magnetite such as occurs in a high fO_2 type of environment (Mullen, 1983). As well, the more intermediate nature of some of the samples is reflected in higher P_2O_5 contents.

4.3 Trace element analyses

The most effective trace elements other than REE's to study when trying to discriminate between the tectonic settings of granitoid rocks are Rb, Nb and Y

because alteration has minimal affect on the mobility of Nb and Y (Pearce *et al.*, 1984). When the 1991 and 1993 (for the 1992 samples Nb and Y were not analyzed) granitoid samples are plotted on a Nb vs. Y plot (Pearce *et al.*, 1984) the majority of the samples plot within the volcanic arc and syn-collisional granite field (figure 29). Some of the samples plot in or very near to the transitional zone between the within-plate granite and orogenic granite fields. If the same samples are plotted on a Rb vs. Nb+Y diagram (Pearce *et al.*, 1984) the majority plot within the VAG (volcanic arc granite) field and the rest plot in the WPG (within plate granite) field (figure 30). Sample JG91-1657, a pegmatite (cross) contains very few ferromagnesian minerals and is made up primarily of quartz, K feldspar, plagioclase and muscovite. This sample's high Rb content may be the result of K-silicate alteration (secondary muscovite) and also from fractionation (Pearce *et al.*, 1984). As well, the fields for both of the diagrams were based on Phanerozoic source granitoids. Pearce *et al.* (1984) note that in Archean samples the granitoids have higher Rb values and slightly higher (Y+Nb) values. The overall effect to the Pearce *et al.*, 1984 diagrams will be to blur the synCOLG/VAG discrimination and displace the boundaries to lower values of Y. Pearce *et al.* (1984) also cautioned that granitoids of similar age and location could plot in different fields as a result of several different related tectonic regimes.

A Zr-Ti/100-Y*3 plot (figure 31) following Pearce and Cann (1973) can be used to classify the basaltic and andesitic volcanics further. The mafic and

intermediate volcanics plot within the B and C fields on the diagram. The tectonic setting represented by these groups is comparable to modern calc-alkaline basalts. Once again caution must be applied in making a direct correlation between rocks of Archean age to modern examples as the environments in the Archean are not well known (Pearce and Cann, 1973), but these classifications back up the ones plotted on the P-Mn-Ti plot.

4.4 Rare-Earth Elements and Extended Plots

The rare-earth elements (REE) are probably the most useful tool to classify Archean rocks geochemically because they are relatively unsusceptible to alteration. Some of the high-field-strength elements (HFSE) are also relatively immobile and behave similarly to the REE and can therefore be used to further compare the samples.

4.4.1 Basement Complex

The basement tonalites display REE patterns that are unique compared to the synvolcanic plutons and to the younger granitoids (figure 32a). In particular, they show steeper LREE/HREE fractionation and HREE depletion relative to the 2.7Ga plutons. The gabbroic samples from the mixed basement unit show relatively flat patterns with minor LREE and HREE depletion (figure 32b).

4.4.2 Mafic and Intermediate Volcanics from the ABVB

The REE plots of the mafic to intermediate volcanic rocks of the ABVB show that there are two distinct types of samples. Type I (figure 33) shows a flat REE pattern with approximately 10 times chondrite and is similar to the TH1 tholeiite of Condie (1981). Type II (figure 34) shows LREE enrichment at 50 to

100 times chondrite similar to patterns in the intermediate volcanic rocks and to the TH2 classification of Condie (1981). Condie (1981) determined that there are mainly two distinct classifications of Archean tholeiites (TH1 and TH2). The TH1 group differs from TH2 by its TiO_2, K_2O, P_2O_5, V, Sr, Zr, Y and its lower CaO, Cr, FeO/Fe $_2O_3$ and Ti/Zr. TH1, which is similar to the type I pattern of the study area, constitutes the most common rock type in most greenstone belts, whereas TH2 (similar to the type II pattern) is found mainly in the higher stratigraphic levels of greenstone belts (Condie, 1981). Condie (1981) showed that the TH1 patterns were similar to the MORB and modern immature arc tholeiites and that the TH2 patterns were comparable to modern calc-alkaline tholeiites.

The patterns, for the most part, do not seem to be dictated by lithology or location of the samples. For example, pillowed flows mapped as mafic in the field have the LREE enriched patterns. As well, some of the pillowed samples north of Hanakihamijuk Lake, which were similar looking and close in proximity to one another, give both flat and LREE enriched patterns. However, there are some lithologic and spatial controls on the type of pattern observed. Mafic volcanic rocks located along the suspected base of the ABVB have flat type I patterns (figure 33a). Intermediate pillowed flows have type II patterns. The laminated mafic rocks from the western ABVB display the flat type I pattern, but the laminated intermediate rocks from the eastern ABVB display enriched LREE patterns. Plagioclase porphyritic pillow lavas from the eastern ABVB (samples JG92-2477, 2494, 2931, 2932 and 2933) show a type I pattern (figure 33d) with

slight positive Eu anomalies which are most likely due to the accumulation of plagioclase within these samples. Samples JG91-268 and JG91-1604 were mapped in the field as small mafic pillow lavas with thin selvages in the area north of Hanikahimajuk Lake and show the flat type I pattern (figure 33b), differing slightly from the plagioclase porphyritic samples in that they do not show an Eu anomaly and that they have slight Ce enrichment comparatively. The laminated mafic volcanic samples collected from the western portion of the ABVB (JG91-722, JG93-4691, 4692, 4693B and 4693C) display the flat type I patterns (figure 33e). Pillow lavas, originally mapped as mafic, collected throughout the ABVB display the type II pattern (figure 34) which could indicate that these samples have a more intermediate character than mafic as originally mapped.

Samples JG91-288 was mapped as an intermediate pillowed volcanic with large pillows containing both quartz-eyes and plagioclase phenocrysts and having thick selvages. This sample shows a REE pattern that falls between type I and type II (figure 35). This pattern is characterized by a slight LREE enrichment (but not as enriched as type II) and relatively flat HREE. Massive intermediate flows (JG91-1654, 1786, 1793 and 1439) plot as a type II pattern (figure 36a). The laminated intermediate volcanics that are interlayered with the felsic volcanics in the eastern portion of the ABVB also show type II patterns (figure 36b). The type II patterns of the intermediate volcanics closely match the group I Archean andesites of Condie (1981), these samples are somewhat analogous to modern calc-alkaline andesites.

Extended plots of the type I and type II mafic and intermediate volcanics

also show distinct differences between the two groups. The type I volcanics are less enriched in the HFSE than the type II, approximately 3x MORB compared to approximately 10x MORB (figure 37). The type I samples have patterns similar to those of Phanerozoic island-arc tholeiites (Pearce, 1983). These rocks are characterized by relatively flat patterns plot below MORB values with Th enrichment. The flat pattern is roughly parallel to MORB and plots below due to less fractional crystallization or more partial melting than modern MORB (Pearce, 1983). The Th enrichment may be explained by the transport of Th from a subduction zone to the overlying zone of mantle melting due to its low ionic potential (Pearce, 1983).

The type II patterns are comparable to modern calc-alkaline basalts (Pearce, 1983). These samples have more enriched patterns than the type I with negative Ti anomalies. Enrichment of these elements is most likely caused by contamination by subduction processes, however Th can also be enriched in basalts from crustal contamination (Pearce, 1983) but the degree of Th enrichment from a crustal component is difficult to distinguish in trace element plots.

4.4.3 Felsic Volcanics from the ABVB

The felsic volcanics show similar REE patterns throughout the ABVB (figure 38). Their pattern is characterized by LREE enrichment and large negative Eu anomalies. The Eu anomalies are probably due to the fractionation of plagioclase from the melt or from the presence of residual plagioclase if the original magma formed from a crustal melt.

4.4.4 Metasediments from the ABVB

The metasediments display a LREE enriched pattern similar to that of the intermediate and mafic volcanic type II style (figure 39). The metasediment pattern is similar to the Jackson Lake group A sediments by Yellowknife Bay (Taylor and McLennan, 1985). To obtain a sediment with the mineralogy necessary to create this pattern requires at least 50% mafic volcanic component mixed with a felsic volcanic or Na-granitic source (Taylor and McLennan, 1985).

4.4.5 Mafic Volcanics from the PLVB

The mafic volcanics of the PLVB display two types of patterns similar to those of the ABVB. Samples JG93-4237B, 5672, 5897, 4718, 5663 and 5159 have flat REE patterns similar to the type I of the ABVB (figure 40a). Samples JG93-5695, 5648, 4255, and 4742 display LREE enriched patterns similar to the type II of the ABVB volcanics (figure 40b).

4.4.6 Felsic Volcanics from the PLVB

The felsic volcanic rocks of the PLVB, although not as plentiful as in the ABVB, display a LREE enriched pattern with large negative Eu anomalies as are seen from felsics in the ABVB (figure 41). This suggests that these rock types have a similar composition and origin.

4.4.7 Amphibolites from the PLVB

The amphibolitic rocks to the west of the PLVB show a variety of REE patterns. These range from relatively flat (JG93-5726) to more LREE enriched traces with flat HREE (figure 42). The LREE enriched traces could be an indication of a source rock that contained more pyroxene than those with the flat

REE pattern.

4.4.8 Synvolcanic Complexes

The synvolcanic diorites and related rocks (ie. gabbros) show three general types of REE patterns. Type I diorites exhibit LREE enrichment with large positive Eu anomalies (figure 43). The samples in this group are characterized by a very coarse grained to pegmatitic texture and the Eu anomalies can, therefore, be attributed to plagioclase accumulation. The type II diorites show LREE enrichment with minor HREE depletion and have relatively smooth patterns (figure 44a) similar to the type II mafic and intermediate volcanics. The type III diorites are similar to the type II but have comparatively flat HREE (figure 45). Samples JG92-2383, 2279, 2590 and JG91-414 were mapped as gabbros but display type II diorite patterns (figure 44b) as compared to samples JG92-2538 and JG92-2493 (gabbros) which show patterns different to those of the diorites. Sample JG92-2538 has slight LREE enrichment and sample JG92-2493 shows a relatively flat pattern similar to the type I mafic volcanics (figure 46).

4.4.9 Granitoids

The granitoid rocks can be split into three groups based on their REE patterns. The first group, type I (figure 47), plot as mainly monzogranites on the QFP triangle and exhibit LREE enrichment, negative Eu anomalies and minor HREE depletion. The second group have LREE enriched patterns with large negative Eu anomalies, this group includes JG91-1510, a sample collected from the Rim Granite to the south of the ABVB (figure 48). The third group of granitoids (type II), plots mainly in the granodiorite field of the QFP diagram and

are strongly HREE depleted (figure 49a). The granitoids mapped as tonalites located to the east of the PLVB also show similar traces to the type II granites (figure 49b). The type I granites and the granites with traces similar to the felsic volcanics fall within Taylor and McLennan (1985) K granite classification. These late Archean potassium granites exhibit REE patterns caused by moderate degrees of partial melting of crustal material in which plagioclase is a dominant residual phase. The HREE depletion in the type II granitoids is most likely caused by the presence of garnet in the source region of these samples.

4.5 Summary

The basement tonalites display REE patterns that are unlike the synvolcanic diorites and younger granitoids. The geochemistry of the belt rocks show that the area consists of a bimodal succession with roughly equal mafic and felsic volcanic components. There are two distinct mafic volcanic units. Type I mafic volcanics have tholeiitic tectonic affinities and display flat REE patterns. Type II mafic volcanics display LREE enriched patterns that are similar to the diorites and to the intermediate volcanics and plot in calc-alkaline fields on the tectonic diagrams.

CHAPTER 5. Nd-Sm ISOTOPES

The elemental concentrations and isotopic ratios of samarium and neodymium have important applications when searching for the ages and origins of rocks. Sm/Nd fractionation is only affected by magmatism, unlike Rb/Sr, U/Pb and Th/Pb which can be affected by condensation and/or core formation (DePaolo, 1988). This means that Nd isotopic studies can provide information

about the crustal resisdence times. This is especially useful when looking at Archean rocks because the Sm/Nd ratios, unlike the Rb/Sr ratios are not as readily reset by metamorphism. The Sm-Nd isotopes of the supracrustal rocks in the Slave province have not been examined extensively to date. The Sm-Nd isotopes of the granitic rocks occurring in the Slave Province have been studied by Davis and Hegner (1992) and can therefore be compared to the results in this study.

The Hanakihamijuk Lake region straddles a Sm-Nd isotopic boundary proposed by Davis and Hegner (1992). This boundary separates granitoid rocks having positive ϵNd_T (ϵNd at time of emplacement) values between +0.3 and +3.6 in the central and eastern Slave Province from those in the west which have ϵNd_T values -1.0 to -4.6. The eastern and central granitoids are interpreted to have been derived from juvenile crust. The western granitoids, on the other hand, are interpreted as having intruded through exposed pre 3.1 Ga crust and therefore have been contaminated by an older crustal component.

Thirty-one samples deemed representative from the region were analyzed by K. Yamashita for Sm and Nd isotopes. The information presented in this chapter represents a collaborative effort between the author and K. Yamashita. ϵNd values for the samples are shown on figure 50, more detailed analyses are available from K. Yamashita (UofA Ph.D thesis, in preparation).

5.1 Basement Complex

The basement tonalite has an ϵNd_T value of 0 equal to that of CHUR, with a T_{DM} age of 3.5 Ga, which supports a preliminary U-Pb date of 3.35 Ga

(Bowring unpublished) (table 1). The $\epsilon Nd_{2.7}$ values are between -4.1 and -10.5.

These values are similar to those found by Bowring *et al.* (1989) for the Acasta Gneiss located to the southwest of the Hanikahimajuk Lake area. In their study, Bowring *et al.* (1989) analyzed two samples for Sm-Nd. They found that one sample (BGXM) had an $\epsilon Nd_{(3.7)}$ value of -4.8, $\epsilon Nd_{(2.7)}$ value of -23.5 and a T_{CHUR} age of 4.10 Ga and that the other sample (BGXM-M) had an $\epsilon Nd_{(3.7)}$ value of -2.6, $\epsilon Nd_{(2.7)}$ value of -21.2 and a T_{CHUR} age of 3.92 Ga. The minimum U/Pb age from BGXM determined was 3.842 Ga, supporting the Sm-Nd findings.

A Sm-Nd study of the southern Slave by Dudas (1989) determined $\epsilon Nd_{(2.6)}$ values from +0.7 to -7.1 for the major Archean lithologies. In the Sleepy Dragon Complex (near Cameron River) $\epsilon Nd_{(2.6)}$ values ranged from +3.8 to -7.1 and gave a T_{DM} of >3.1 Ga. In the southern pre-YKSG Anton Complex, west of Point Lake, $\epsilon Nd_{(2.6)}$ was +0.3 to -0.9 unlike the Sleepy Dragon Complex in the Cameron River area (figure 2), which indicates that these areas are actually separate entities and not parts of the same single older crustal block (Dudas, 1989). The Hanikahimajuk Lake area values seem to be more closely related to the Sleepy Dragon Complex rather than the Anton Complex.

5.2 Volcanic Rocks

The volcanic rocks show very little scatter in ϵNd_T ranging from -1.2 to 2.5. There is a general trend in the ϵNd_T values that shows lower ϵNd_T in progressively more felsic samples. Most of the mafic and intermediate volcanic rocks have positive ϵNd_T values which indicate derivations from a depleted mantle source with little to minor contamination by older crust. There does not

appear to be any correlation between Nd isotopic values and the two different REE patterns of the intermediate and mafic volcanics. The lower ϵNd_T for some of the intermediate and all of the felsic volcanics indicates that there was a component of older crustal material in their petrogenesis. The bimodal nature of the volcanic rocks indicates that there could be more than one type of source for these rocks.

Dudas (1989) found ϵNd_T values for the Kam Formation basalts in the southern Slave to be between -0.4 to -2.1. These values overlap those found for coeval or somewhat younger granitoids in the southern Slave ($\epsilon Nd = 0.7$ to -1.7). These values implicate the interaction of older sialic crust in the formation of these lithologies, which contrasts the findings for the basaltic samples from the Hanikahimajuk Lake area.

5.3 Synvolcanic Complex

The synvolcanic diorites have ϵNd_T values ranging from 1.1 to -2.2. These values overlap with the values from the intermediate and felsic volcanic samples, suggesting that the synvolcanic diorites are consistent with the isdea that they represent the plutonic equivalents of the volcanic rocks in the belt. The T_{DM} calculated are also supported by the preliminary U-Pb dates (Bowring, unpublished) these show that the ages for the diorites are coeval to those of the intermediate and felsic volcanics (table 1).

5.4 Metasediments

The metasedimentary samples have ϵNd_T values that range from -0.4 to -5.0 . This suggests that the basement and volcanic rocks were both contributing

to the detritus in the area and that the basement complex was, at least, partially exposed at the time of deposition.

5.5 Granitoids

The young granitoids have ϵNd_T values ranging from 0.2 to -1.6. These values fall within Davis and Hegner's (1992) classification of granitoids from the western Slave Province, indicating that there was an older crustal component involved in the petrogenesis of the granitoids. As well, there does not appear to be a sharp boundary between the granitoids showing positive ϵNd_T values and those that have more negative values, indicating a more gradational transition than that suggested by Davis and Hegner (1992).

5.6 Summary

The basement complex samples have negative $\epsilon Nd_{2.7}$ values ranging from -4.1 and -10.5 and a T_{DM} age of 3.5 Ga; these values are distinct from those in the volcanic belt (see below). The volcanics have ϵNd_T values ranging from -1.2 to 2.5. The mafic volcanics have positive values whereas some of the intermediate volcanics and all of the felsics volcanics have negative values. This indicates that the mantle-derived mafic volcanics were likely contaminated slightly by older crustal material and that the felsic and intermediate volcanics have a significant component of older crustal material in their petrogenesis. The sediments have Nd isotopic values that indicate that both the basement and the volcanic rocks were contributing detritus to these sediments, implying older basement material was exposed at the time of sedimentation. The synvolcanic diorites have Nd isotopic values that overlap the intermediate and felsic volcanic values suggesting that the

diorites are the plutonic equivalent of the volcanics. The younger granitoids show gradual Nd isotopic change from more negative ϵNd_T values in the west to positive values in the east; similar results were obtained by Davis and Hegner (1992) further supporting a fundemental difference between the eastern and western Slave Structural Province.

CHAPTER 6. DISCUSSION

6.1 Comparisons with other Archean belts

6.1.1 Archean Average Compositions

Condie (1981) extensively analyzed and classified the rocks contained within Archean greenstone belts using geochemical and stratigraphic constants. He separated each major rock type into groups based on their REE patterns and relationships within the belt. It is, therefore, useful to compare the sample averages from the study area to the average Archean compositions that Condie (1981) has proposed (table 2).

The mafic volcanic rocks are bimodal and seem to fit relatively well into Condie's TH1 and TH2 tholeiitic compositions. The main differences between the Hanikahimajuk samples and the average Archean samples are that the study area samples have greater REE concentrations and have considerably less (2 wt% for type I and 3 wt% for type II) MgO than the Archean averages. The higher apatite content of the mafic volcanics of the study area could be the reason for increased REE content in these rocks as opposed to the Archean average. The lower MgO is likely a result of the small amount of fractional crystallization in the Hanikahimajuk Lake samples.

The andesitic samples of the study area match well with the AI group of Condie (1981). The main differences between them are a higher MgO content in the Condie andesite and higher REE contents in the Hanikahimajuk average andesite, again, like the basalts.

The felsic volcanic average composition from the study area falls within the FII REE envelope proposed by Condie (1981). The average felsic volcanic composition from the Hanikahimajuk Lake area falls in between the compositions of Condie's dacite and rhyolite averages.

6.1.2 Hackett River and Yellowknife-type classifications for the Slave Province

In the past, the greenstone belts in the Slave Province have been separated into two types, the Yellowknife-type and the Hackett River-type (Padgham, 1985). Mafic dominated Yellowknife-type belts occur in the south-central and western portion of the Slave Province . These belts are rectilinear and characteristically have less than 25% felsic volcanics superimposed on top of tholeiitic mafic sequences. Gold is the primary economic mineral associated with the Yellowknife-type belts. Hackett River-type belts occur as mainly oblate calc-alkaline bodies in the north and eastern portion of the Slave Province. Volcanogenic massive sulphides are the main deposits in these belts. Below, I compare these subdivisions to those from the Hanikahimajuk Lake area.

The Hackett River greenstone belt in the northeastern portion of the Slave Province is characterized by predominantly intermediate- to felsic-composition volcanic rocks (Frith, 1987). The volcanics range in succession from 55% to 70% SiO_2 and the majority appear to have chemical compositions that somewhat

matches that of modern arc or continental calc-alkaline environments (Ewing, 1979). However, there is another calc-alkaline volcanic trend that does not fit any modern analogues that is lower in overall REE abundance and that has depleted HREE and Y (Ewing, 1979).

The Hanikahimajuk area also has large portions of intermediate to felsic volcanics, but there is also an almost equal amount of basaltic volcanics in the belt. The REE patterns for the Hanikahimajuk samples do not show two separate calc-alkaline trends as they do in the Hackett River area, the depleted calc-alkaline trend is absent in the Hanikahimajuk Lake area.

The Yellowknife-type belts show a bimodal volcanic succession with little or no intermediate SiO_2 composition volcanics present (Goodwin, 1988). The Yellowknife volcanics have been separated into the Kam Formation, the Duck Formation and the Banting Formation (Henderson, 1975).

The Kam Formation consists of mafic to intermediate pillowed and massive flows which display slightly LREE enriched REE patterns (Jenner *et al.*, 1981) similar to the type I mafic to intermediate REE patterns seen in the Hanikahimajuk Lake area. The Duck Formation is mainly composed of intermediate to mafic flows which are similar to the Kam Formation but which display greater LREE enrichment (100x chondritic) (Jenner *et al.*, 1981). The Duck Formation REE pattern is similar to the type II REE pattern displayed by some of the mafic and intermediate volcanics in the Hanikahimajuk area. The Banting Formation consists of porphyritic dacite flows, felsic agglomerate and andesites displaying REE patterns with HREE depletion and no Eu anomalies

(Jenner *et al.*, 1981). The Banting felsic volcanics do not have the same type of pattern as the Hanikahimajuk samples which do not show the HREE depletion and have slight negative Eu anomalies.

As can be seen from the above comparisons of the Yellowknife-type and Hackett River-type greenstone belts with the one in this study, the two-fold classification may be an oversimplification for the Slave Province. The geochemistry and the field data from the Hanikahimajuk Lake area do not fit well into either classification.

6.1.3 Abitibi Greenstone Belt, Superior Province, Canada

The Abitibi greenstone belt located in the Superior Province, Canada is the largest Archean greenstone belt in the world. Due to its large mineral wealth and easy accessibility it has been the focus of numerous geological, geochemical and geochronological studies and is, therefore, useful to compare to the Hanikahimajuk Lake area.

Broadly the Abitibi greenstone belt displays cycles of volcanism in sequences from basal komatiites successively overlain by tholeiitic, calc-alkaline and alkalic volcanics (Jensen, 1985). U-Pb dating on the volcanics has established the period of volcanism from approximately 2740 Ma to 2700 Ma (Krogh and Davis, 1974).

In the Hanikahimajuk Lake area, and the Slave Province in general, there are none of the basal komatiites that occur in abundance in the Abitibi. As well the upper alkalic volcanic sequences are absent in the Hanikahimajuk area. The REE patterns for the tholeiitic sequence of basaltic volcanics from the Abitibi

differs slightly from the type I found in the Hanikahimajuk area. The Abitibi pattern has the same relatively flat REE trace as the type I but also has slight negative Eu anomalies (Condie, 1981) which the type I Hanikahimajuk samples do not. The Abitibi andesites also show different REE patterns than the study area, with relatively flat REE traces and large negative Eu anomalies (Condie, 1981) compared to the LREE enriched patterns of the Hanikahimajuk Lake area samples. The rhyodacites from the Abitibi do, however, have similar REE patterns as the study area felsic rocks (Shirey and Hanson, 1986).

Sm-Nd studies for the Abitibi by Shirey and Hanson (1986) show that the ϵNd_T for all the igneous rocks is +1.9 and that the age is 2737+/-42 Ma. For the individual samples, the ϵNd_i results ranged from +3.3 to -0.4. Younger granitoids had lower ϵNd (+1.5 to -0.1) indicating the possible incorporation of older crustal material (Shirey and Hanson, 1986). The tholeiitic basalts and diorites on the other hand had higher ϵNd values (+3.3 to +1.0) indicating an uncontaminated mantle source for these rocks (Shirey and Hanson, 1986).

Further study in the Kamiskotia-Montcalm area of the Abitibi by Barrie and Shirey (1991) support the idea that portions of the Abitibi have been affected by crustal contamination whereas other sections have not. Barrie and Shirey (1991) determined ϵNd_T values of +2.2 to +2.6 for the bimodal successions of volcanic rocks in the Kamiskotia region, indicating derivation from a long-term, LREE-depleted mantle with no significant contamination by crustal material. However in the Montcalm area the gabbroic complex has ϵNd_t ranging from 2.8 to 1.0 indicating that there was contamination by a crustal component during its

petrogenesis. As well, granitoid rocks surrounding the greenstone belt have ϵNd values of +0.6 to -0.4 compared to ϵNd values of +2.5 to +3.8 for granitoids occurring within the belts. U-Pb data from an inherited zircon of 2926 Ma supports the presence of older sialic crust in the area.

Although the older crustal component in the Abitibi does not appear to be as old as the basement in the Hanikahimajuk area the relationships between the older crust and the supracrustal rocks appears to be similar. There seems to be at least two different sources of magma generation in both the Abitibi and in the Hanikahimajuk Lake area, one that has not been affected by older sialic crust and one that does have an older crustal component affecting its formation.

6.1.4 Pilbara Block, Western Australia

The Pilbara Block is located in the northwestern portion of Western Australia's Precambrian Shield. The rocks making up the area have been separated into pillowed and massive tholeiitic basalt, high-Mg komatiitic basalts, minor peridotitic komatiites and subordinate felsics, clastic sediments and cherts. This sequence has been overlain by dacitic agglomerates, tuffs and flows followed by another mainly mafic volcanic sequence with some felsic lenses and overlain by potassic rhyolites (Jahn *et al.*, 1982).

The REE pattern for the lower basalts are different from the type II patterns of the Hanikahimajuk Lake area in that although they display similar LREE enrichment they also display relatively flat HREE (Jahn *et al.*, 1982). The overlying dacitic rocks exhibit relatively similar patterns as the lower basalts and their relatively flat HREE patterns (Jahn *et al.*, 1982) differ from the

Hanikahimajuk Lake area intermediate volcanics. In the next sequence, the felsic lenses of mainly dacitic composition exhibit flat enriched REE patterns with positive Eu anomalies (Jahn *et al.*, 1982), whereas the felsic volcanics in the Hanikahimajuk Lake region although displaying flat enriched patterns have negative Eu anomalies. The subsequent potassic rhyolites have steep REE patterns with large negative Eu anomalies (Jahn *et al.*, 1982).

Jahn *et al.* (1982) interpret the source for the Pilbara Block intermediate to felsic rocks as that of a basaltic composition (i.e. amphibolite or eclogite). The Nd isotopic data show that these rocks are not derived from a much older crustal source ($\epsilon Nd = +0.33$). This contrasts with the Nd isotopic data from the Hanikahimajuk area that show that some of the rocks from that area have been affected by a much older crustal component during their petrogenesis. Therefore, the fundamental difference between the Hanikahimajuk Lake area and the Pilbara Block is that the Hanikahimajuk Lake area has a significant portion of older sialic crust affecting the magmatism in the area whereas the Pilbara Block originated from a basaltic composition oceanic crust. This could explain the absence of komatiitic volcanic rocks in the Hanikahimajuk Lake area due most likely to a higher degree of fractionation under a continent and the abundance of the same in the Pilbara derived from an oceanic crust.

6.2 Relationship between the synvolcanic diorites, volcanics and associated VMS deposits

In the Abitibi Province several studies have tried to establish if there is a

particular type of volcanic rock that hosts VMS (volcanogenic massive sulphide) deposits and also the nature of the heat source driving the formation of the VMS deposits (e.g. Campbell *et al.*, 1982; Lesher *et al.*, 1986; Barrie *et al.*, 1993). These studies were undertaken to establish traceable patterns in VMS-related host rocks. By comparing the results in the Abitibi with the volcanic rocks associated with the Hood VMS deposits in the Hanikahimajuk Lake area we can determine if the trends found to exist in the Abitibi are applicable to other Archean greenstone belts. What these studies determined is that most of the VMS deposits occur in and around felsic volcanic centres that are associated with bimodal volcanic sequences (Lesher *et al.*, 1986). As well, the heat source needed to generate the deposits comes from high-level, subvolcanic magma chambers. For example, in the Kamiskotia region, a underlying gabbroic complex in the deposit's footwall has U-Pb dates roughly coeval to the felsic volcanism, 2707 +/-2 Ma compared to 2705+/-2 Ma (Barrie and Davis, 1990) and the isotopic signature for these units is identical (Barrie and Shirey, 1991). The synvolcanic mafic intrusions generate the high heat flow necessary to produce an ore body by hydrothermal circulation.

The REE patterns for the felsic volcanics that host the majority of the VMS deposits in the Abitibi can be categorised as one distinct group having REE enriched relatively flat patterns with pronounced negative Eu anomalies (e.g. Group I of Barrie *et al.*, 1993 and FIII from Lesher *et al.*, 1986). Other felsic volcanics displaying LREE enriched REE patterns with weak or no Eu anomalies were shown not to be associated with base metal deposits.

In the Hanikahimajuk Lake area, the majority of the felsic volcanic rocks

occur at two centres, each of which is associated with Cu-Zn-Pb deposits. The REE patterns of these felsic volcanics match the FIII classification from Lesher *et al.* (1986) and Group I from Barrie *et al.* (1993). Surrounding the felsic centres are two synvolcanic diorite complexes. The preliminary U-Pb data (Bowring, unpublished) show the diorites to be the same age as the felsic volcanic rocks around the VMS deposits, 2673 Ma and 2675 Ma, respectively. As well, the Sm-Nd data from this study show that the diorites overlap the felsic and intermediate volcanic values. This supports the hypothesis that the diorite complexes are coeval and related to the belt volcanics and have acted as the heat source for the VMS Hood deposits. In order to produce the REE patterns with pronounced negative Eu anomalies Campbell *et al.* (1982) found that the felsic volcanics in the Abitibi had to undergo a high degree of fractional crystallization on their way to the surface. This further implies that there must have been a subvolcanic magma chamber present below the orebodies.

Synvolcanic mafic intrusions occur in association with other bimodal volcanic belts in the western Slave Province. The C1 phase intrusion (King *et al.*, 1989) in the Contowyto Lake region is a small synvolcanic gabbroic and dioritic complex occurring in close proximity to the Gondor VMS deposit in the Central Volcanic Belt. As well, a small amphibolitic intrusion borders the *Izok Lake* VMS deposit (Bostock, 1980). These may be other examples of synvolcanic mafic intrusions acting as the heat engine for base metal deposits. Geochemical and isotopic studies based on the Abitibi findings could lead to more VMS discoveries in the Slave Province.

6.3 Tectonic Models

Several attempts have been made to constrain the tectonic evolution of the Slave Province to some type of tectonic model. These models generally follow two types: 1. collisional - accretionary types involving island-arc and continent collisions (Kusky, 1989; Davis *et al.*, 1994), or Andean type margins (Fyson and Helmstaedt, 1988) and 2. intracratonic types where greenstone belts are interpreted to be formed by collapsing ensialic rifts and the surrounding granitoids are interpreted to be reactivated basement (Henderson, 1981; Easton, 1985).

In the Hanikahimajuk Lake region several criteria must be met to fit a tectonic model to the geology, geochemistry and isotopic data from the area. The Hanikahimajuk Lake area consists of a bimodal volcanic sequence with tholeiitic mafic volcanics overlain by felsic and intermediate calc-alkaline volcanics and then another cycle of calc-alkaline mafic volcanism occurred. From the geochemistry of the samples it can be seen that two phases of volcanism and magma generation have probably taken place. The mafic volcanic samples seem to belong in an oceanic island-arc setting (figure 27 and 28) whereas the felsic and intermediate volcanics plot in calc-alkaline continental environments. The granitoids in the area plot in volcanic arc (figure 30) and calc-alkaline (figure 31) environments. As well, from the Sm-Nd data, it is evident that the felsic volcanics and some of the intermediate volcanics have been contaminated by an older crustal component (negative ϵNd_T values) but the mafic volcanics (positive ϵNd_T) have not, or to a much smaller extent. The younger granitoids also display gradational ϵNd_T values ranging from +0.2 to -1.6 from east to west, respectively.

Therefore, any tectonic model applied to the Hanikahimajuk Lake area will have to account for the presence of older sialic crust through which the felsic and some of the intermediate volcanics erupted and likely interacted, and for mafic volcanism resulting from a depleted mantle source with little or no crustal contamination within close proximity to and at roughly the same time as felsic volcanism.

6.3.1 Collisional - accretionary models

Kusky's (1989, 1990, 1991) accretionary model (figure 51a) for the Slave Province separates the Slave into two tectonostratigraphic zones, the Anton terrane and the paired Contowyto terrane and Hackett River Arc. The Hackett River Arc is interpreted as an island-arc formed above an east dipping subduction zone at 2.7 to 2.67 Ga. Kusky interprets the Hackett River Arc to be an immature island arc based on the volcanic sequence, the development of caldera complexes and the overall size of the belt. The Contowyto terrane is similar to forearc accretionary complexes and Kusky (1989) believes the west verging folds and thrusts in this area are compatible with the east dipping subduction. As well, Kusky (1989) interprets the mafic volcanic belts in this terrane to be ophiolitic slivers scraped off the oceanic lithosphere. The Anton terrane represents the remnants of an older Archean continent. This terrane consists of gneiss >3.48 Ga deformed prior to the main orogenic event at 2.6 Ga.

The Hanikahimajuk Lake area is located on the border of the Anton terrane and Contowyto terrane of Kusky (1989, 1990, 1991). He interprets the mafic dominated (Yellowknife-type) greenstone belts of the western Slave

province to be ophiolite slivers of oceanic crust and explains the occurrence of felsic volcanic rocks in the area in terms of superimposed arc magmatism. This theory does not fit with the volcanic rocks of the Hanikahimajuk Lake area since the felsic volcanics have been contaminated by an older crustal component. Older crust is only known to occur in the western Slave province so the felsic volcanics must have originated close to or at their present location. As well, Kusky's model does not adequately explain the two trends of mafic volcanism occurring in close proximity throughout the area. The oceanic crust of Kusky (1989) has tholeiitic trends but does not account for the calc-alkaline type II REE mafic trends, absence of MORB type mafic volcanics and the fact that no ophiolitic sequences have been documented.

Davis *et al.* (1994) also believe an accretionary model best fits the geology of the Slave province. Their model (figure 51b) proposes the development of the early tectonostratigraphic assemblage in supra-subduction setting, which could include island-arcs, back arc basins and continental margin basins. This was followed by collision by the eastern volcanic and associated plutonic rocks onto the older rocks of the western Slave. Collision caused regional shortening and thickening of the lithosphere. Continued heating of the crust caused crustal melting and extension to occur which resulted in the intrusion of the young granitoids. This model like the one proposed by Kusky (1989) does not explain the crustal contamination involved in the petrogenesis of the felsic volcanics of the Hanikahimajuk Lake area. As well, the isotopic Sm-Nd boundary proposed by Davis and Hegner (1992) is interpreted in Davis *et al.* (1994) to be the suture

between the accreted terranes, but in the Hanikahimajuk Lake area this boundary is gradational rather than sharp as would be expected from a suture zone.

Fyson and Helmstaedt (1988) propose a tectonic model (figure 51c) that involves rifting of the older (>3.0 Ga) sialic crust to form the oceanic crust that makes up the Yellowknife type belts. This was followed by closure to the basin and obduction of oceanic crust in the western Slave Province and subduction and calc-alkaline magmatism in the eastern Slave Province. Then tectonic underplating by shallow subduction of the western Slave Province and westward migration of calc-alkaline magmatism occurred. This model does not account for the evidence of plutonism occurring simultaneously in both the western and eastern parts of the Slave Province (Davis *et al.*, 1994) and does not explain the two different types of mafic volcanic rock in the Hanikahimajuk Lake area. As well, there should be evidence of pre 3.0 Ga sialic basement existing in and underneath the eastern Slave Province and so far none of the isotopic data or geology supports this.

6.3.2 Intracratonic models

Henderson's (1981) model for the Slave Province proposes rifting and the opening of basins floored by sialic crust with the development of mafic volcanic greenstone belts forming along the basin margins. Felsic volcanics occur within and outside the basin and are a major contributor to the sediments. Felsic volcanism was most likely triggered by the same mechanism that caused extension (Henderson, 1981).

Easton (1985) elaborated on Henderson's (1981) model (figure 51d) saying

that the tectonic evolution of the Slave Province is similar to the Basin and Range Province in the western United States. Extension results from low angle normal faulting in the old (>3.0 Ga) sialic crust. Both calc-alkaline or tholeiitic magmatism could occur as a result. Turbidites would accumulate in the basins as submarine fan deposits. Normal faulting would position the supracrustal rocks next to metamorphic and granitic rocks from deeper crustal levels. Subsequent extension and crustal thinning would result in higher heat flow in the lower crust which would generate the later granitoid plutons.

These intracontinental models do not explain how mafic volcanics apparently derived from juvenile sources occur in the Hanikahimajuk Lake area. If the rifting occurred in the old sialic crust, the geochemical signatures of the volcanics should show contamination by this older crust. As well, the geochemical data from the Hanikahimajuk Lake area shows most of the samples to have a calc-alkaline or island-arc tholeiitic affinity as opposed to a mid-ocean ridge one that would be expected if rifting occurred.

6.3.3 Possible Implications

The geology of the Hanikahimajuk Lake area does not fit well into either type of model. This area's tectonic evolution was complex and most likely involved more than one event. This is supported by the generation of two types of magmatism in the area, a mafic dominated magma derived from a depleted mantle source and a felsic-intermediate magma that has been contaminated by crust. As well, the interrelationships and timing of the different types of magmatism in the area does not allow for large scale separate events to have

affected the area.

The generation of the mafic phase of volcanism originating from the depleted mantle may have happened in one of two ways. The magma may have erupted through the older sialic crust very quickly with a very short residence time so no contamination occurred. This may indicate the presence of a fracture, which could explain the linear nature of the greenstone belts in the western Slave. Or the magma may have erupted through juvenile crust separate from the older sialic block. This type of volcanism most likely occurred in a primitive arc setting.

The generation of the felsic and intermediate volcanic rocks occurred in a subvolcanic chamber with contamination from an older crustal component and then they erupted explosively as volcanic centres. The geochemical and Nd isotopic signatures of these rocks indicate that they most likely originated in a continental regime. The differences between the two types of magma generation and their tectonic affinities could indicate that an arc-continent collision has occurred in the Hanikahimajuk Lake area.

The PLVB forms a linear entity which seems to continue to the north as the Napaktulik belt and even perhaps with the Anialik River Belt, and to the south possibly with the Winter Lake Belt. The felsic east-west trending ABVB is closely related to the north-trending PLVB, and can be interpreted as a continuation of the PLVB. However, the ABVB is geologically similar to more felsic volcanic belts to the east and may have at one time been linked to the belts to the east but the links have been overprinted by later granitoid generation. Future studies looking at the Nd isotopic signatures and geochemistry of

supracrustal rocks from the Slave Province are needed to further constrain the timing and origin of magmatism of the greenstone belts throughout the Slave.

CHAPTER 7. CONCLUSIONS

1. Three localities of mixed tonalite and gabbro intrusives found to be basement (>3.0 Ga) have been found in the Hanikahimajuk Lake area. These intrusives are not as severely deformed as their counterparts in other portions of the Slave Province, and had been misinterpreted in previous studies as younger granitoids. More detailed studies and careful mapping of granitoids in other parts of the Slave may lead to new localities of pre-YKSG basement.

2. There is a bimodal sequence of volcanism with tholeiitic affinity mafic to intermediate volcanics overlain by calc-alkaline intermediate to felsic volcanics, followed by sedimentary deposition. The supracrustal rocks are surrounded by synvolcanic dioritic complexes to the north and south that have protected the stratigraphy of the supracrustals from severe deformation and metamorphism. The greenstone belt has been intruded by post-deformation granitoids.

3. The mafic volcanics have two distinct geochemical trends. The type I mafic volcanics display relatively flat REE patterns similar to the TH1 group of Condie (1981) (island-arc tholeiites). The type II mafic volcanics display LREE enriched patterns similar to the TH2 (calc-alkaline) group of Condie (1981).

4. The geochemical signatures of the rocks from the Hanikahimajuk Lake area show a more calc-alkaline affinity than that of MORB's. On various geochemical diagrams the rocks plot in fields associated with arc like environments.

5. Nd isotopic analyses indicate that two generations of magmatism have occurred in the area. The mafic volcanic rocks have ϵNd_T values that indicate that they formed from a depleted mantle source with little or no crustal contamination. The felsic volcanic rocks on the other hand have much lower ϵNd_T values indicating that there was an older crustal component affecting the petrogenesis of these rocks. The sediments have Nd isotopic values that are intermediate between those of the basement and the volcanic rocks indicating that both contributed detritus to the sediments. The younger granitoids show gradual Nd isotopic change from negative ϵNd_T in the west to positive ϵNd_T values to the east.

6. The Hanikahimajuk Lake area does not fit well into the two fold classification of greenstone belts proposed for the Slave Province (Padgham, 1985). The Hackett River-type (felsic) and Yellowknife-type (mafic) divisions are too broad to be used to classify the Hanikahimajuk Lake area which has an equal component of felsic and mafic volcanic rocks.

7. The Abitibi and Pilbara Block Archean areas are characterized by basal komatiitic sequences followed by mafic volcanism overlain by felsic volcanism. The basal komatiitic sequence is absent in the Hanikahimajuk Lake area. The Nd isotopic evidence from the Abitibi shows similarities to the Hanikahimajuk Lake area in that there appears to be some older continental crustal contamination in portions of the belt. The Pilbara Block, in contrast, does not exhibit contamination of an older continental component, but rather formed from a basaltic oceanic crustal source.

8. The felsic volcanic rocks in the Hanikahimajuk Lake area show similar REE patterns to the felsic volcanic rocks known to host VMS deposits in the Abitibi. Studies in the Abitibi have identified felsic volcanic rocks exhibiting flat enriched REE traces with negative Eu anomalies are more likely to host VMS deposits than other felsic volcanics that do not exhibit these types of patterns. To produce these types of REE patterns Campbell *et al.* (1982) determined that the felsic volcanics must have undergone a high degree of fractional crystallization prior to eruption, indicating that a subvolcanic magma chamber must have existed below the orebody. In addition, the subvolcanic magma would provide the heat needed to generate the VMS deposits. The synvolcanic dioritic complex in the Hanikahimajuk Lake area displays similar REE to the intermediate volcanic rocks and has ϵNd_T values that overlap those of the felsic to intermediate volcanic rocks. As well, preliminary U-Pb results show that the diorites are roughly coeval to felsic volcanics associated with the Cu-Zn-Pb deposits. This supports the hypothesis that the diorites formed as part of a high level subvolcanic complex and that they acted as the heat engine to form the VMS deposits.

9. The tectonic models (collisional-accretionary and intracontinental) proposed for the evolution of the Slave Province do not fully explain the rock generation in the Hanikahimajuk Lake area. The main problem is explaining the generation of a mafic volcanic sequence from a depleted uncontaminated mantle in close proximity to a felsic volcanic sequence that has been contaminated by an older crustal component.

10. The PLVB form a continual linear entity with the Winter Lake Belt to

the south and with the Napaktulik and perhaps Anialik River Belts to the north. The ABVB forms an east-west trending felsic arm of the PLVB and is similar to the felsic volcanic belts to the east, suggesting a possible link. Further isotopic studies on supracrustal rocks throughout the Slave Province may show this.

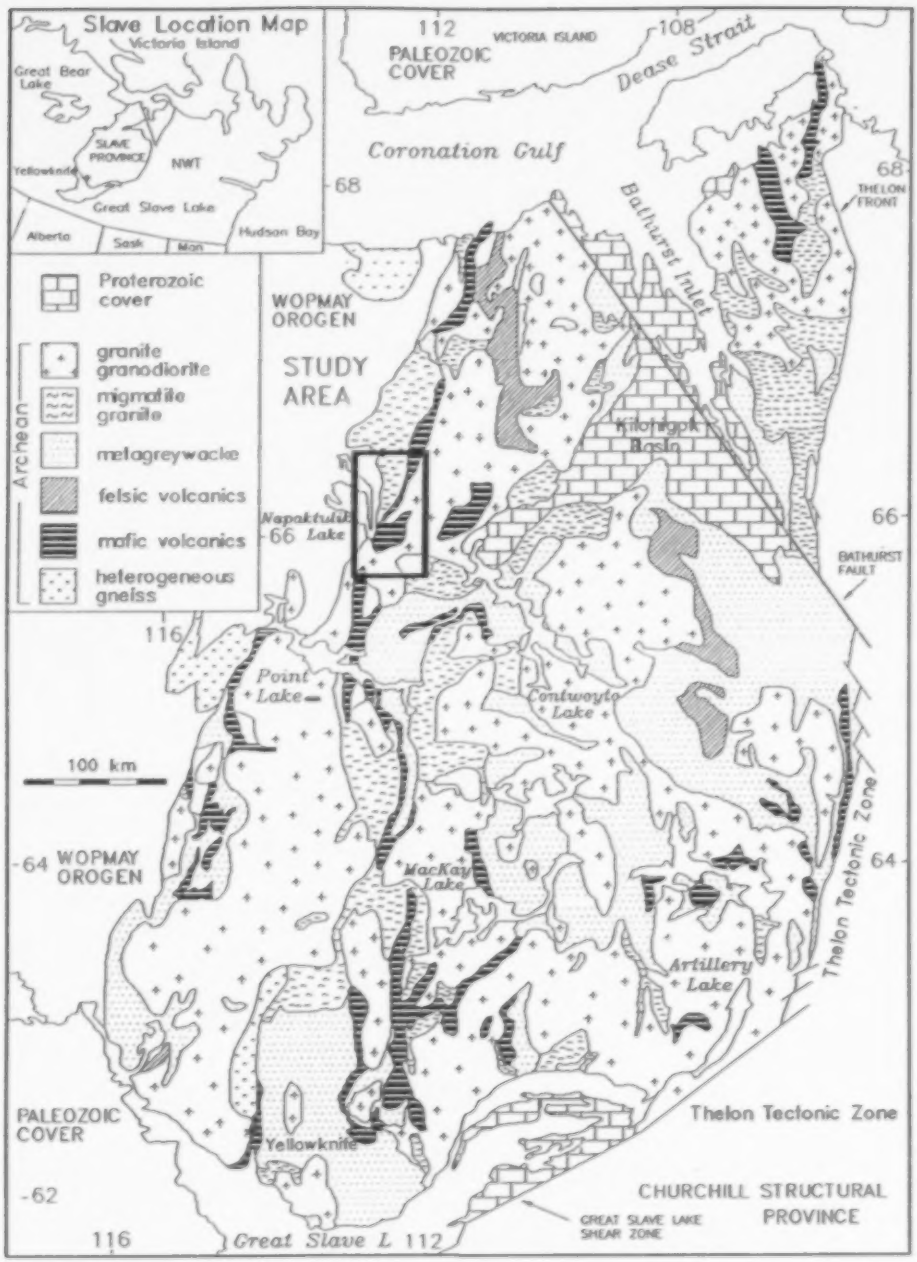

Figure 1. Study area and Slave Structural Province Location Map

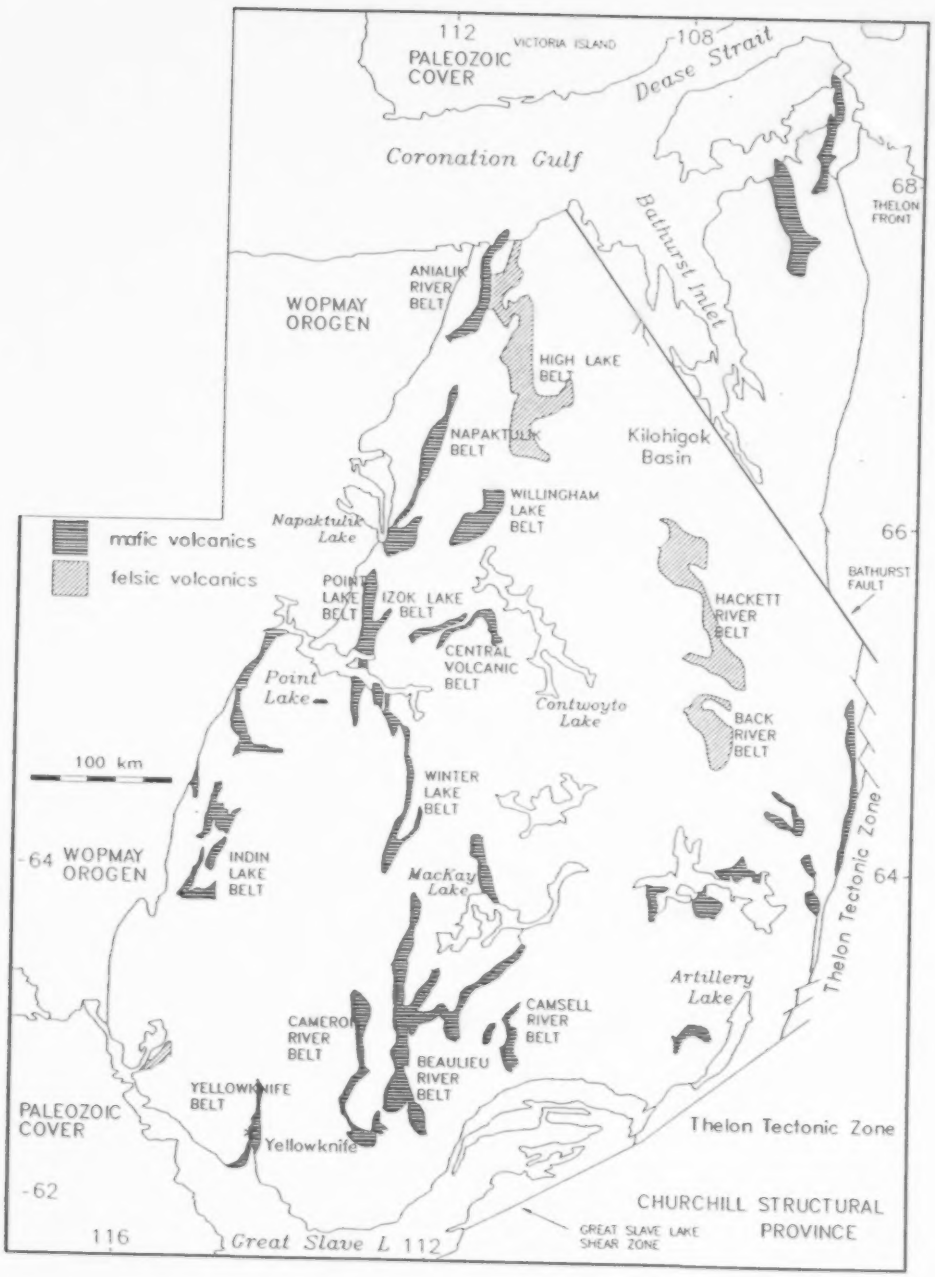

Figure 2. Slave Province greenstone belt location map.

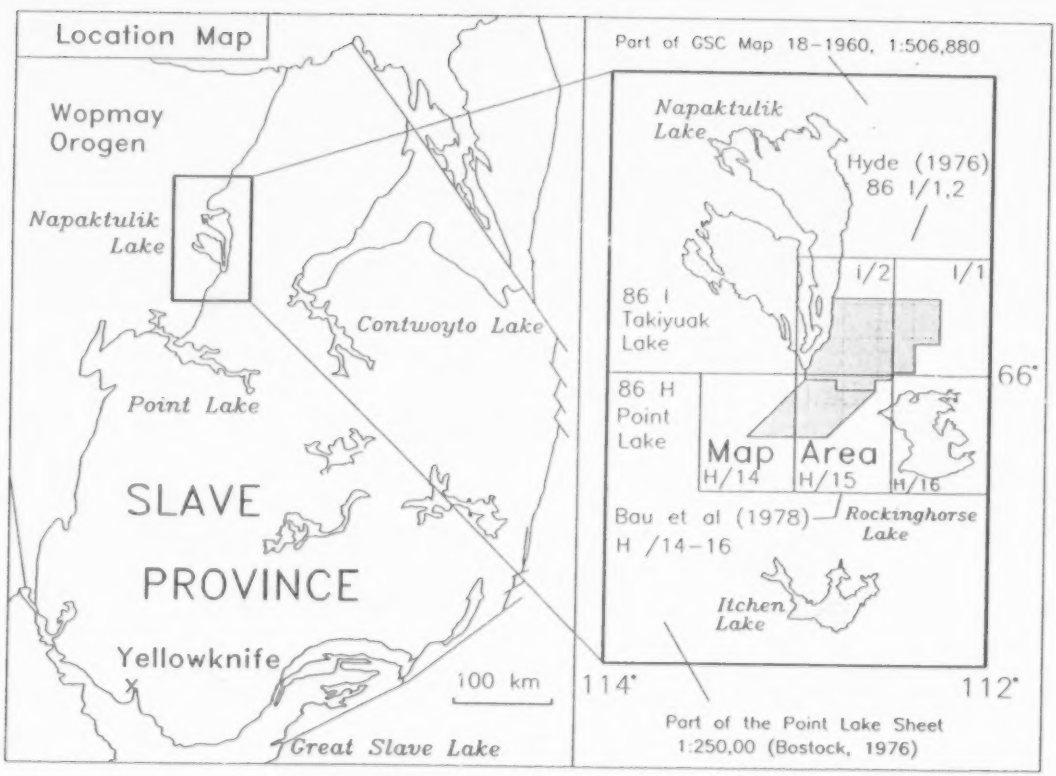

Figure 3. Map area extent and scope of previous work.

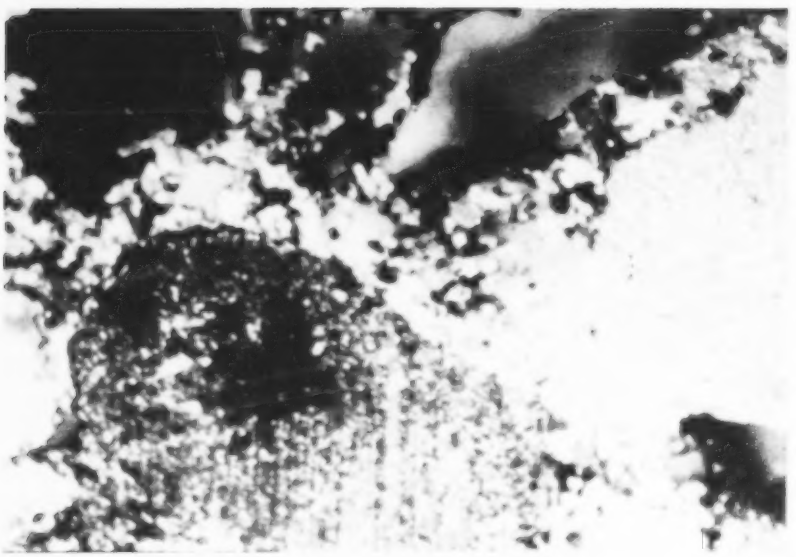

Figure 4. Thin section photomicrograph of tonalite basement sample, JG91-1754 (low power, field of view = 3mm, crossed polars).

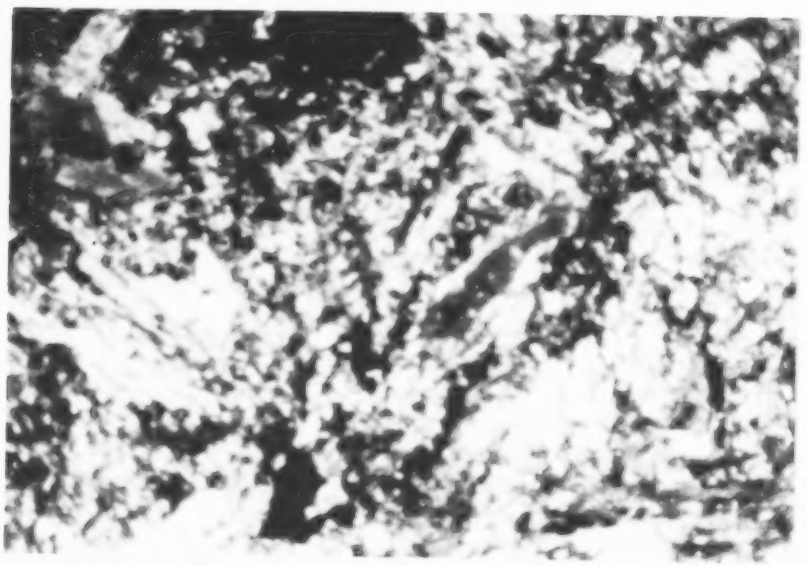

Figure 5. Thin section photomicrograph of gabbro, JG91-1758, from the mixed basement complex (low power, field of view = 3mm, crossed polars).

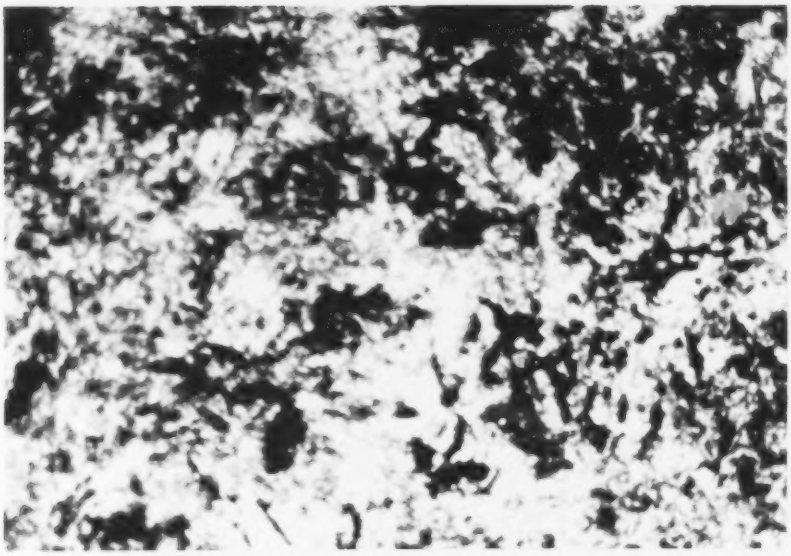

Figure 6. Thin section photomicrograph of an ultramafic dyke sample (JG91-1659) (low power, field of view = 3mm, crossed polars).

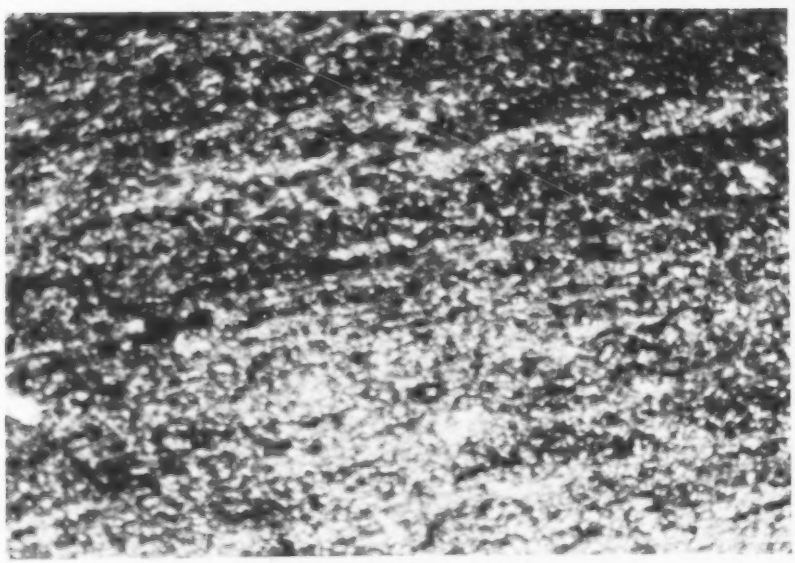

Figure 7. Thin section photomicrograph of an intermediate pillow lava, JG92-2495 (low power, field of view = 3mm, crossed polars).

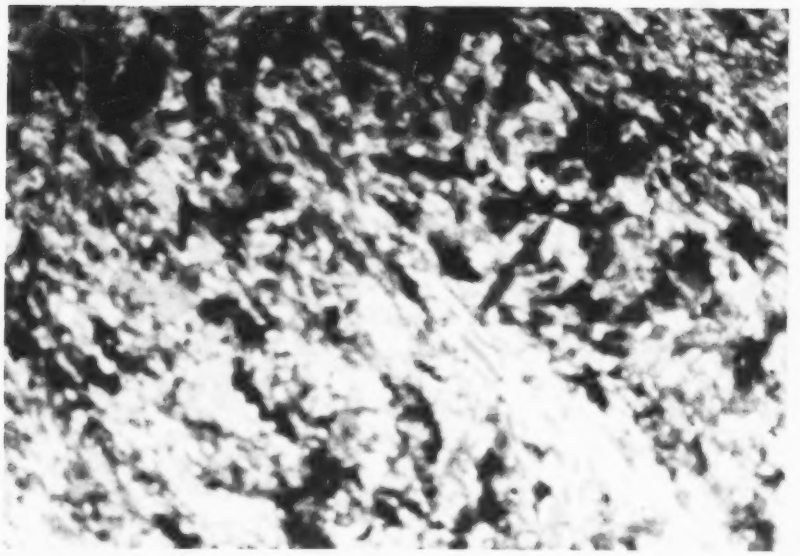

Figure 8. Thin section photomicrograph of a mafic pillow lava sample, JG92-2931 (low power, field of view = 3mm, crossed polars).

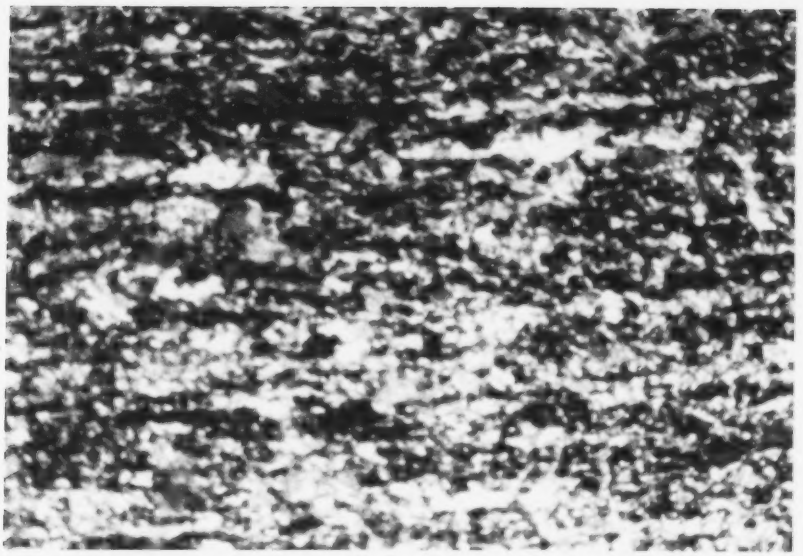

Figure 9. Thin section photomicrograph of a laminated intermediate volcanic rock, JG92-3284 (low power, field of view = 3mm, crossed polars).

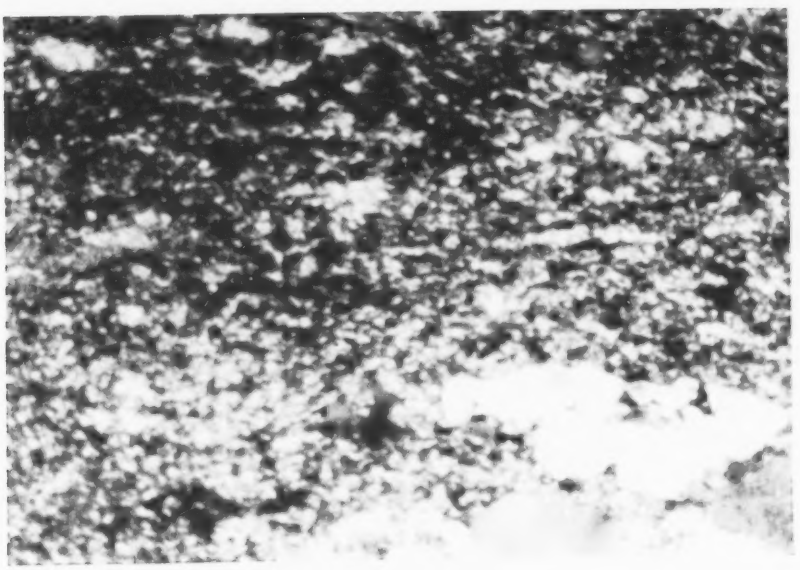

Figure 10. Thin section photomicrograph of a tuffaceous felsic volcanic rock, JG91-1666 (low power, field of view = 3mm, crossed polars).

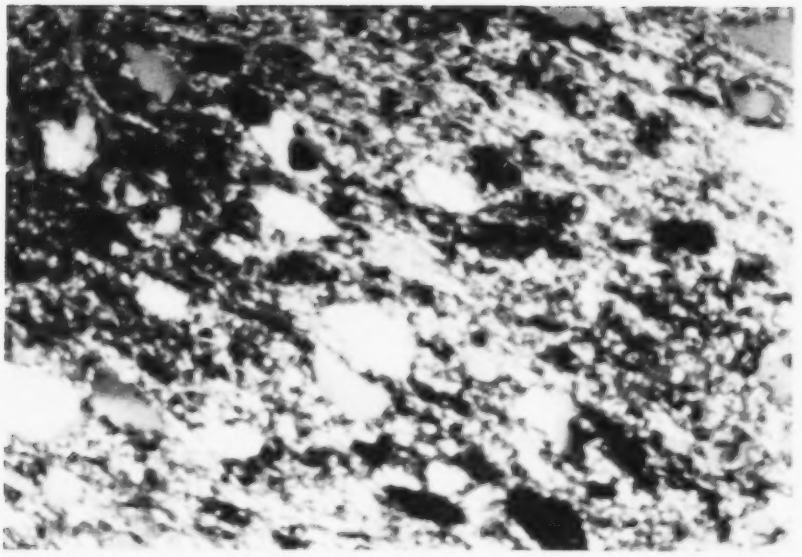

Figure 11. Thin section photomicrograph of a quartz wacke, JG92-2006 (low power, field of view = 3mm, crossed polars).

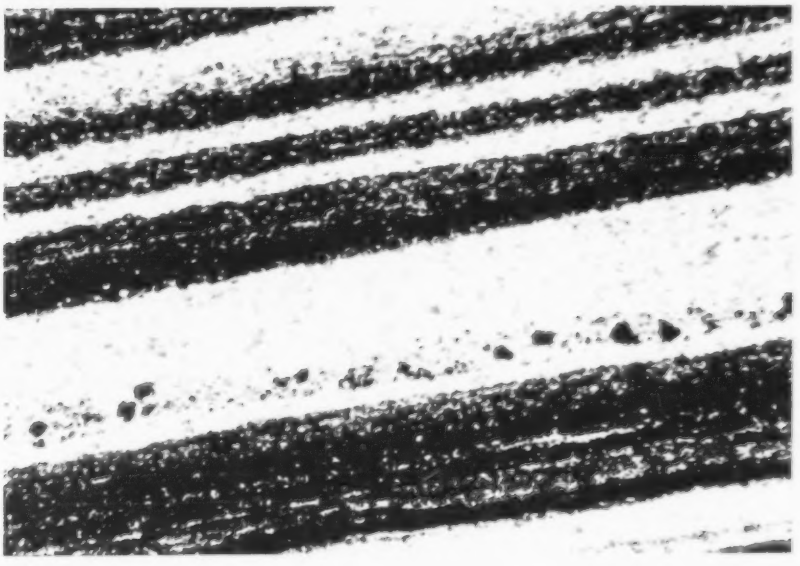

Figure 12. Thin section photomicrograph of an iron formation sample, JG92-2481 (low power, field of view = 3mm, crossed polars).

Figure 13. Thin section photomicrograph of JG91-414, a diorite from the northern stock (low power, field of view = 3mm, crossed polars).

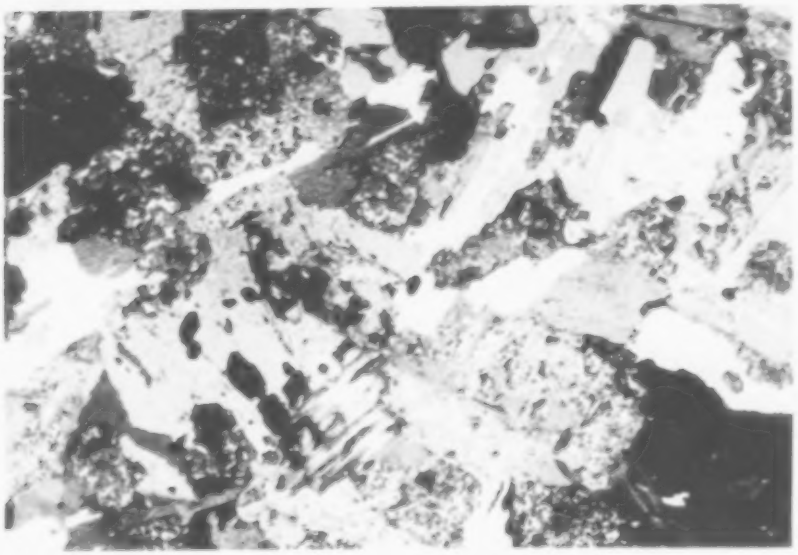

Figure 14. Thin section photomicrograph of JG92-3339, a diorite from the southern stock (low power, field of view = 3mm, crossed polars).

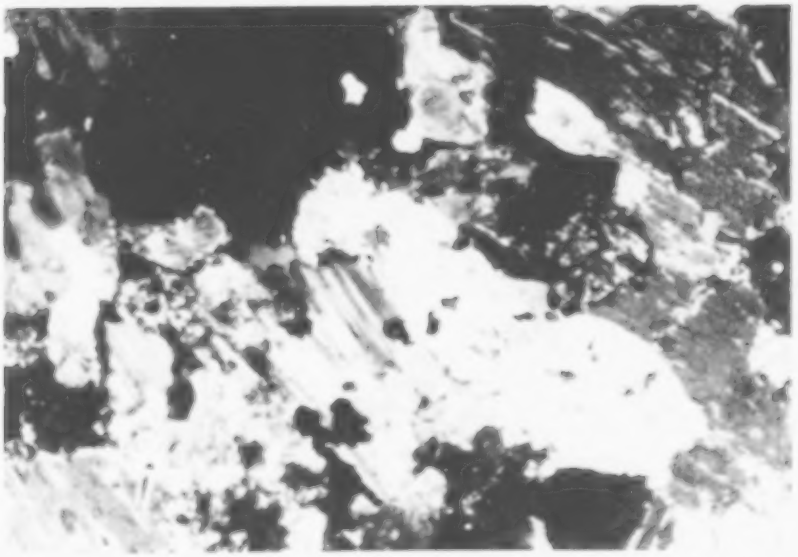

Figure 15. Thin section photomicrograph of JG92-2279, a gabbro (low power, field of view = 3mm, crossed polars).

Figure 16. Thin section photomicrograph of a sample of Tak Granite, JG91-1663 (low power, field of view = 3mm, crossed polars).

Figure 17. Thin section photomicrograph of the Rim Granite, JG91-1510 (low power, field of view = 3mm, crossed polars).

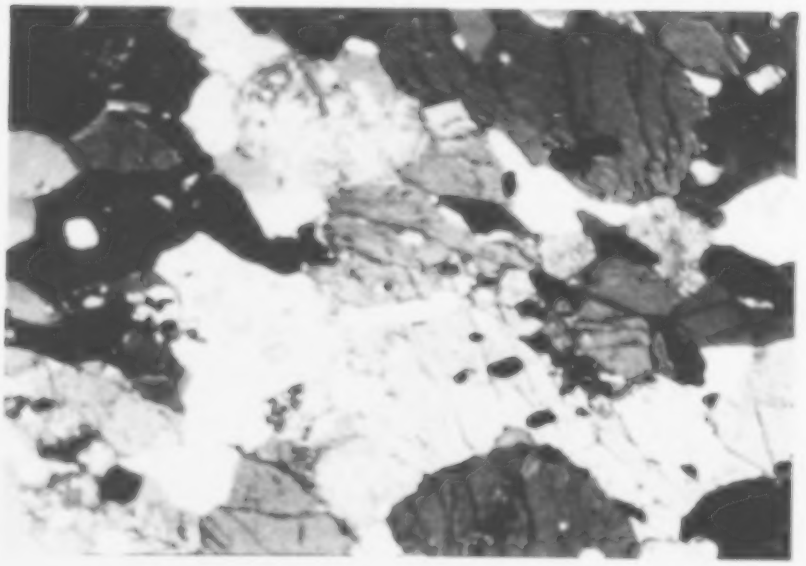

Figure 18. Thin section photomicrograph of amphibolite bordering the PLVB, JG93-5719 (low power, field of view = 3mm, crossed polars).

Figure 19. Thin section photomicrograph of the hornblende pyroxene igneous cumulate occurring in the southwest region of the study area, JG93-5228 (low power, field of view = 3mm, crossed polars).

Figure 20. Thin section photomicrograph of a pegmatitic dyke, JG91-1657 (low power, field of view = 3mm, crossed polars).

Figure 21. Thin section photomicrograph of a Mackenzie diabase dyke, JG91-79 (low power, field of view = 3mm, crossed polars).

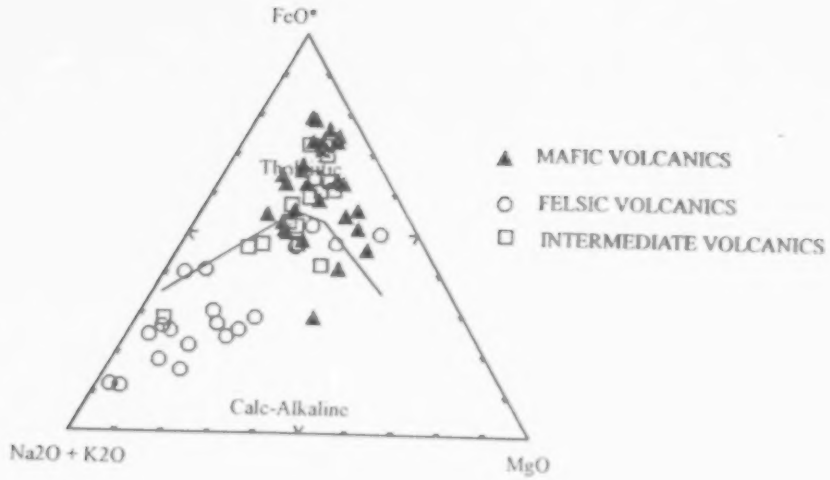

Figure 22. AFM diagram showing volcanic rock distribution.

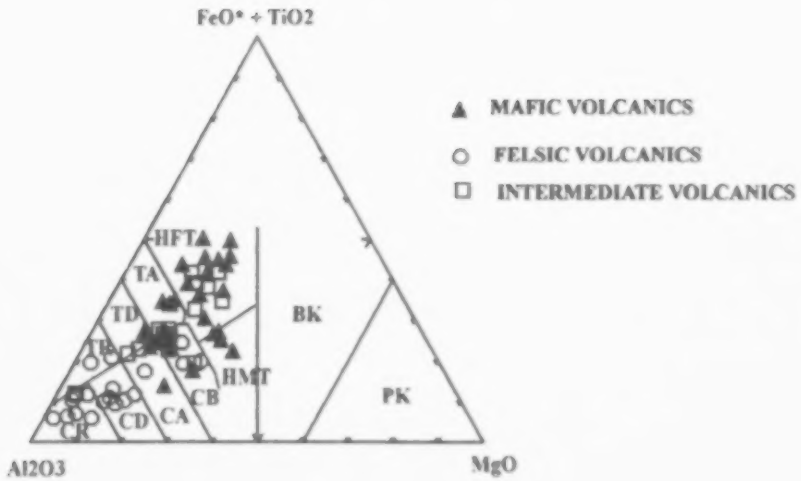

Figure 23. Jensen plot.

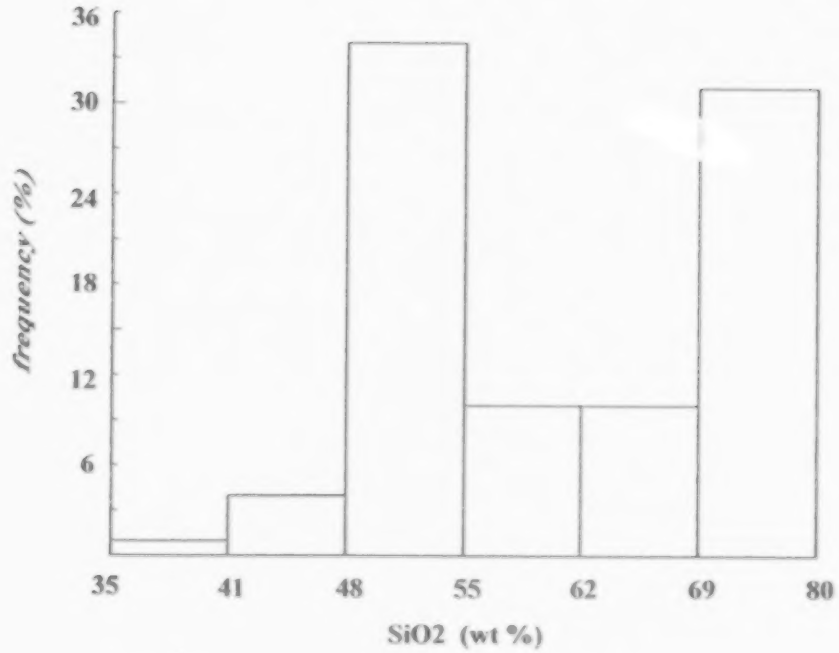

Figure 24. Frequency vs silica histogram.

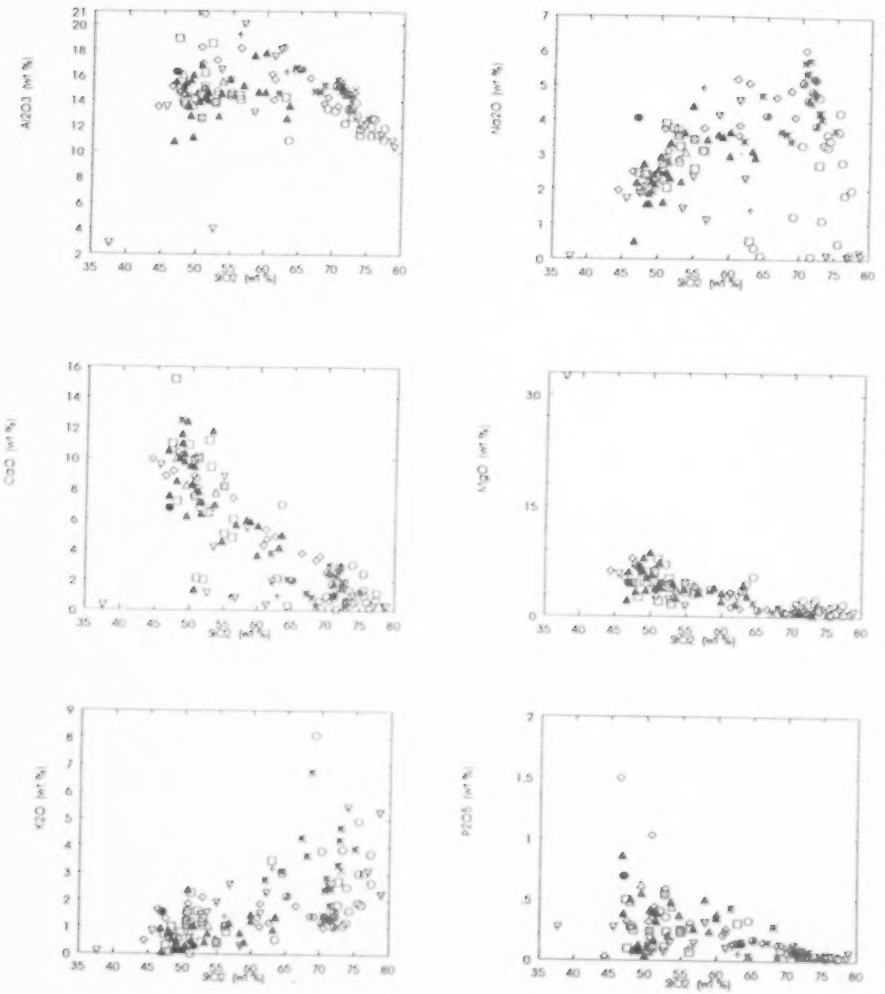

Figure 25a). Harker diagrams (see figure 25b) for legend of symbols).

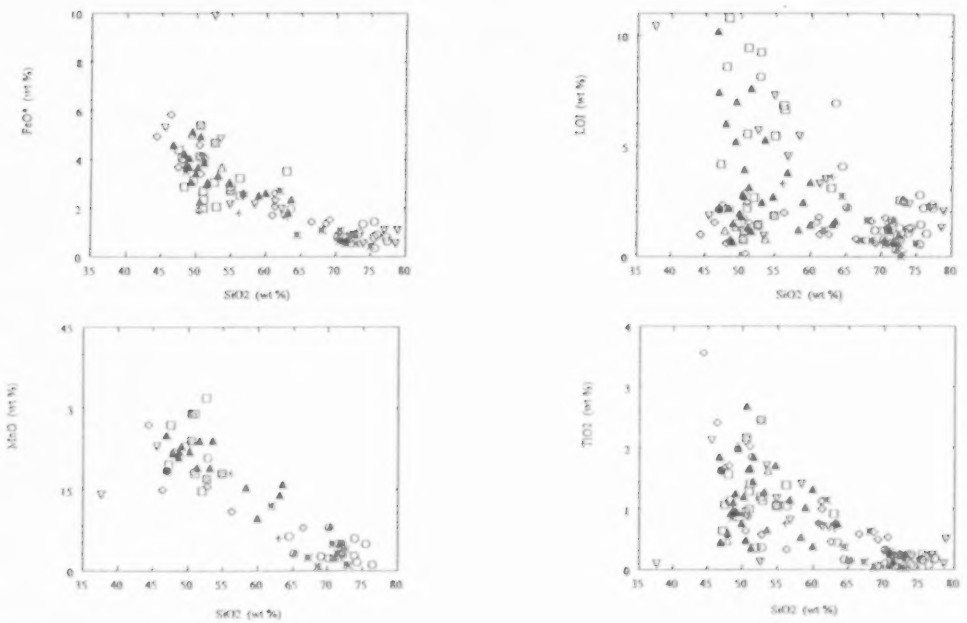

PLOT SYMBOL LEGEND

- DIABASE
- MAFIC VOLCANIC
- INTERMEDIATE VOLCANIC
- FELSIC VOLCANIC
- DIORITE
- GRANITE
- TONALITE
- AMPHIBOLITE
- GABBRO
- CONTACT ROCK
- SEDIMENT
- PEGMATITE
- ULTRAMAFIC

Figure 25b) Harker diagrams continued.

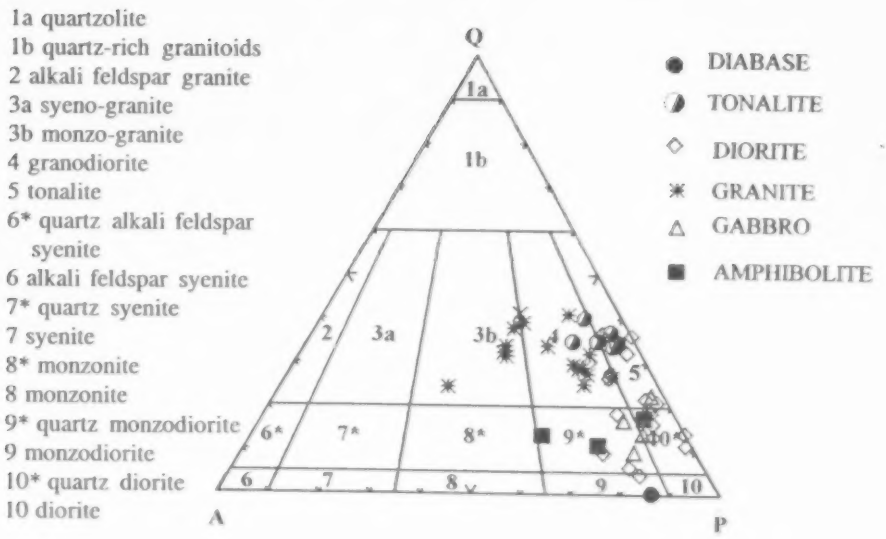

Figure 26. QAP normative diagram.

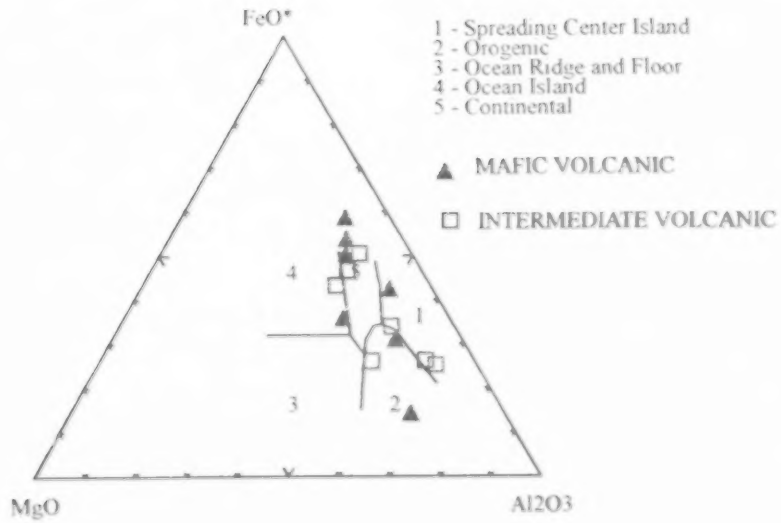

Figure 27. MgO-FeO*-Al $_2O_3$ diagram.

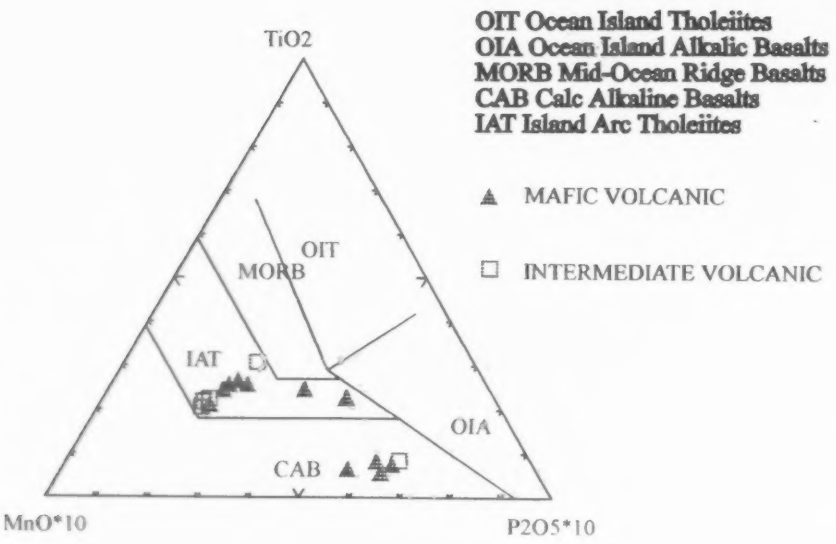

Figure 28. MnO-TiO $_2$-P_2O_5 diagram.

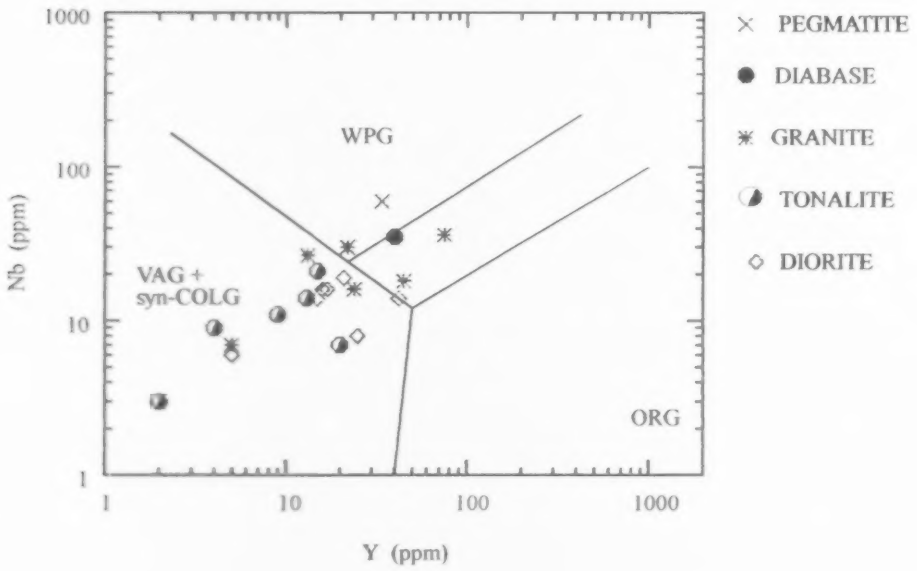

Figure 29. Nb vs. Y plot.

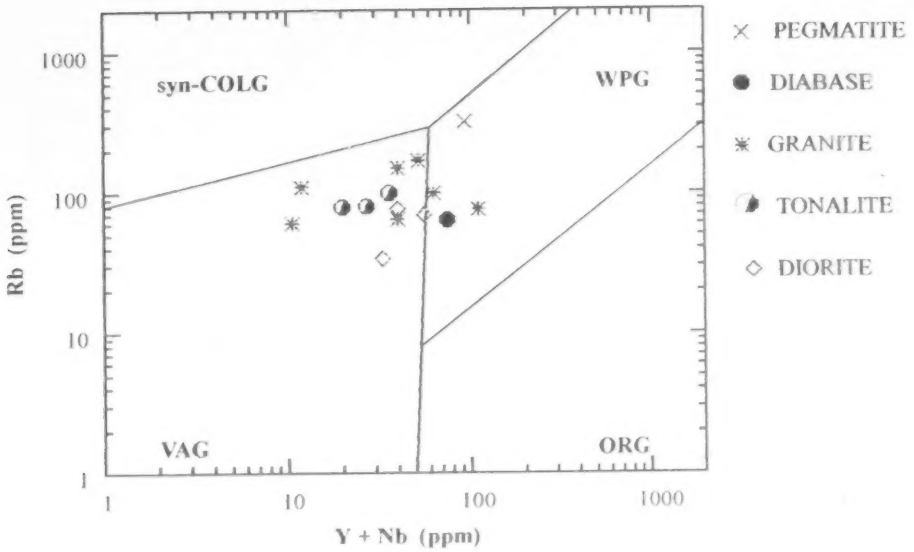

Figure 30. Rb vs. Nb+Y plot.

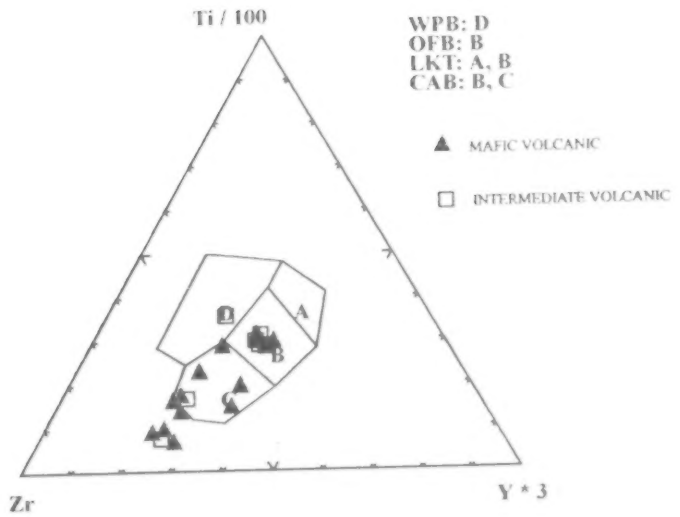

Figure 31. Zr-Ti/100-Y*3 plot.

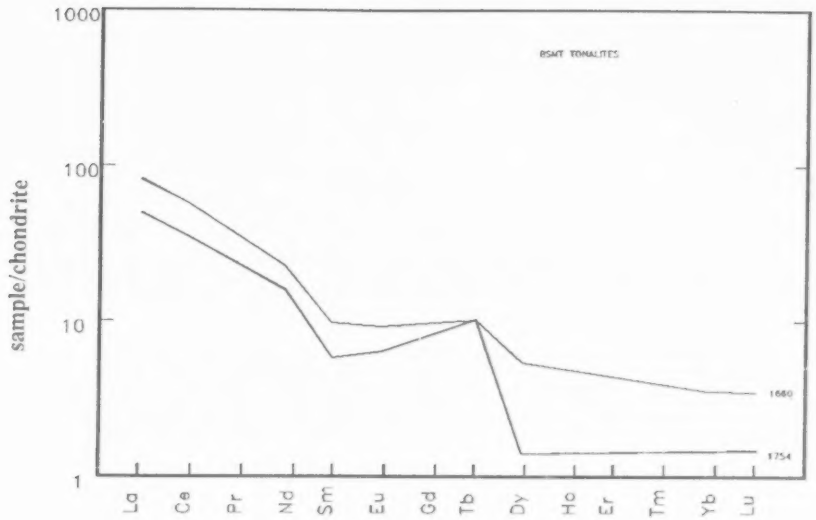

Figure 32a). REE diagram for the tonalite from the basement complex.

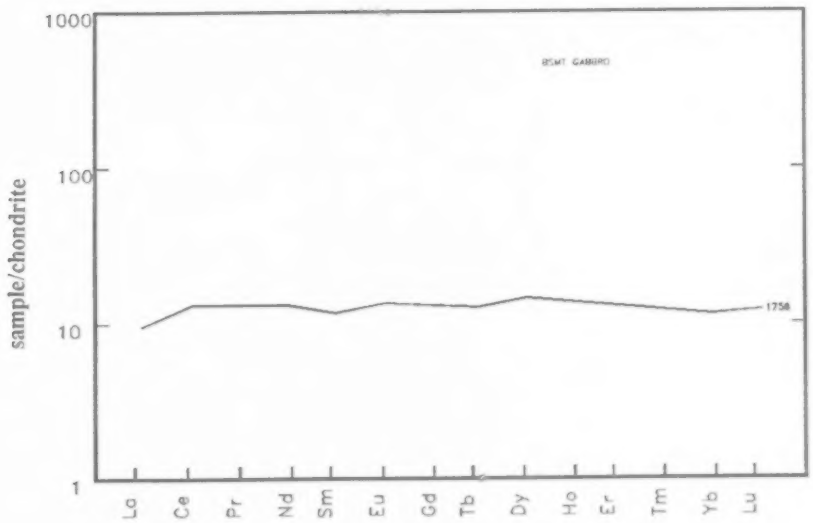

Figure 32b). REE diagram for the gabbro from the basement complex.

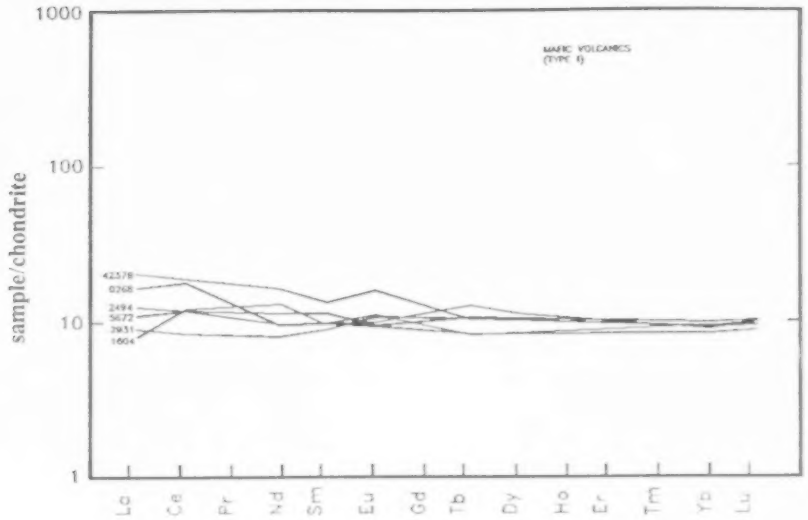

Figure 33a). REE diagram for mafic volcanics exhibiting type I patterns.

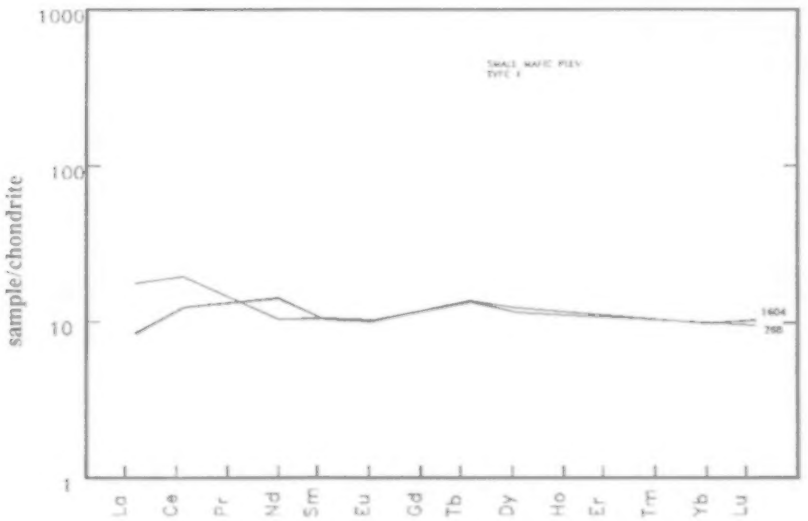

Figure 33b) REE diagram of small mafic pillowed lavas showing the type I pattern.

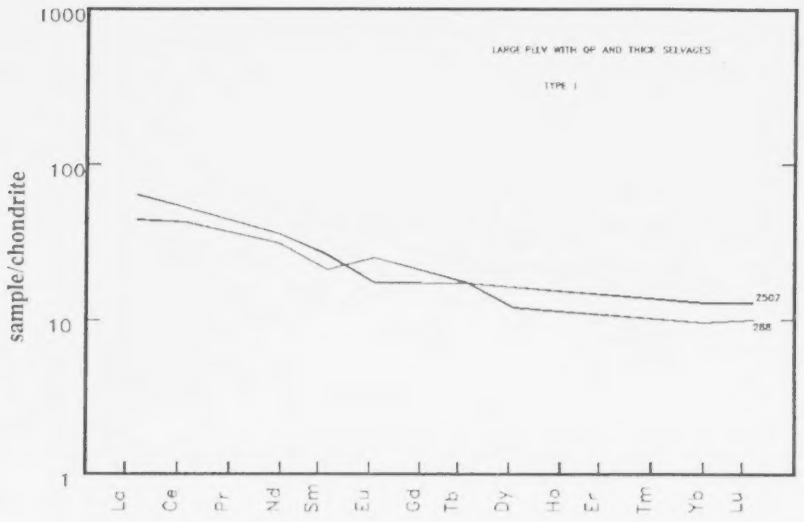

Figure 33c) REE diagram for the large pillowed lavas with quartz and plagioclase phenocrysts and thick selvages (type I pattern).

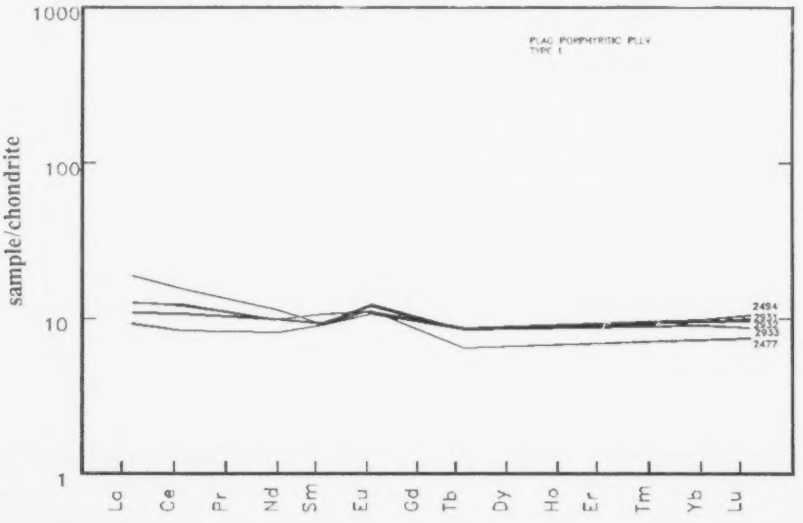

Figure 33d) REE diagram showing the type I pattern displayed by plagioclase porphyritic pillowed lavas.

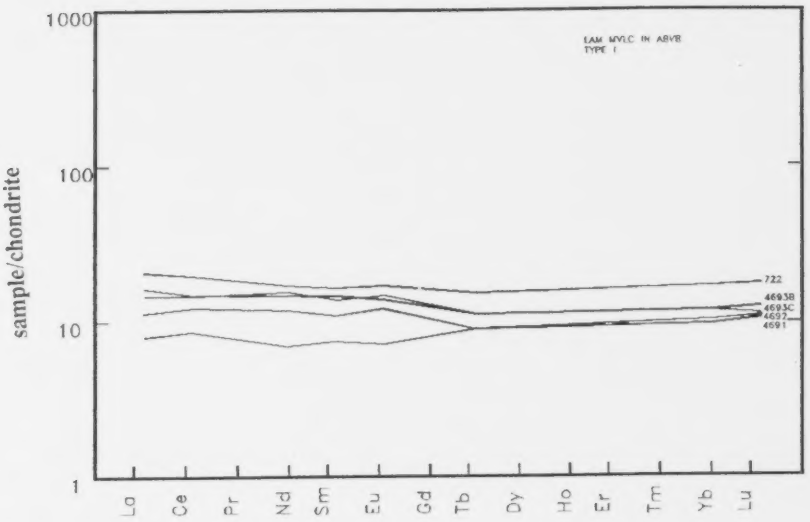

Figure 33e). REE diagram for the laminated mafic volcanics occurring in the ABVB.

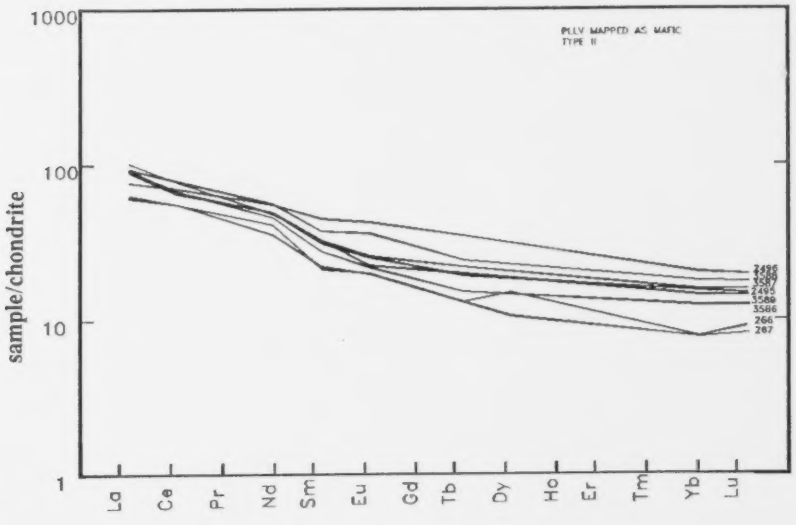

Figure 34. REE diagram for pillowed lavas mapped as mafic and displaying type II patterns.

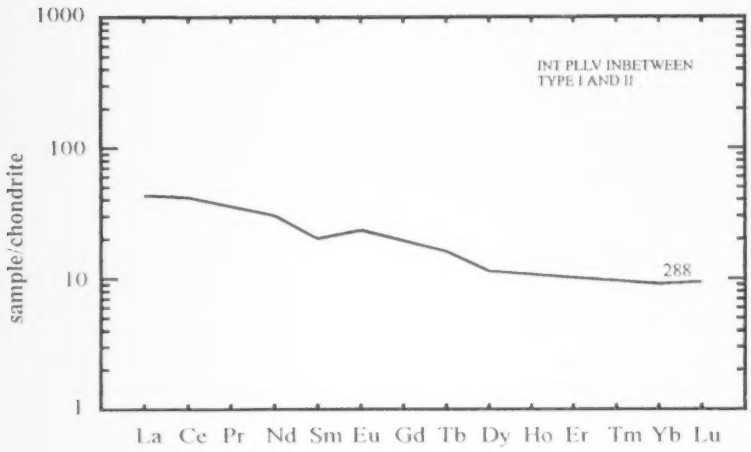

Figure 35. REE diagram for intermediate pillowed volcanics displaying patterns that fall between type I and type II.

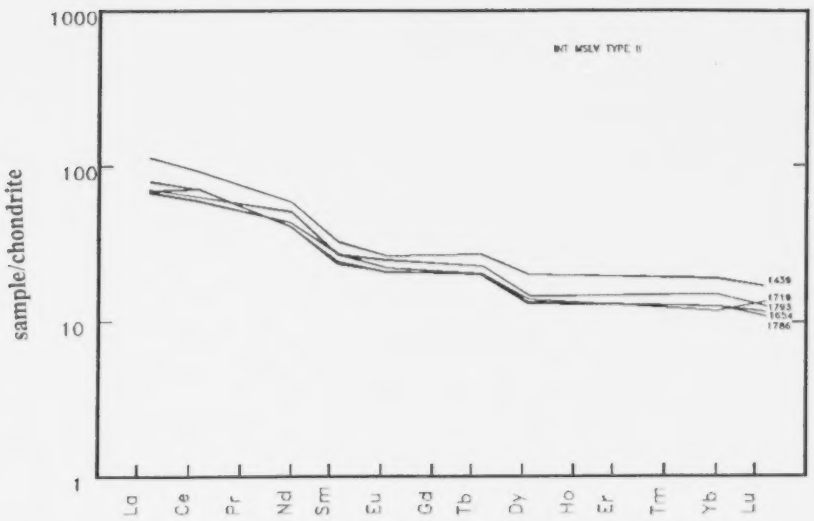

Figure 36a). REE diagram of massive intermediate flows (type II).

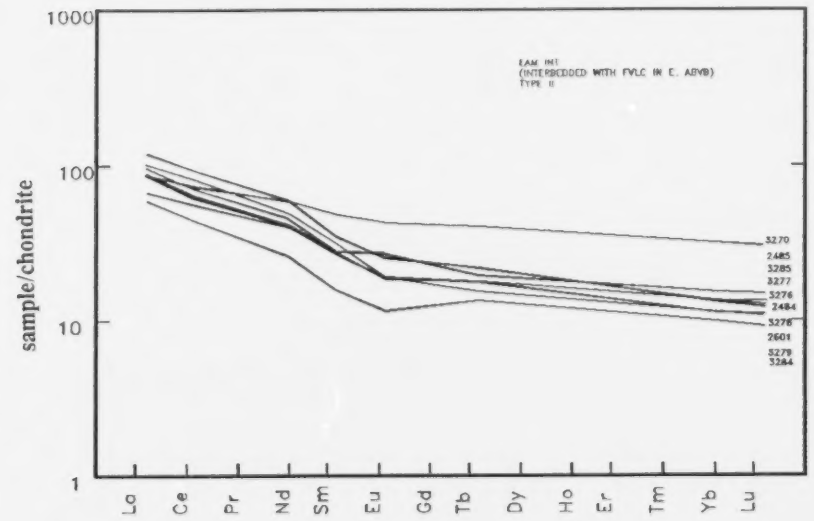

Figure 36b). REE diagram of the laminated intermediate volcanics that are interlayered with the felsic volcanics in the eastern ABVB (type II).

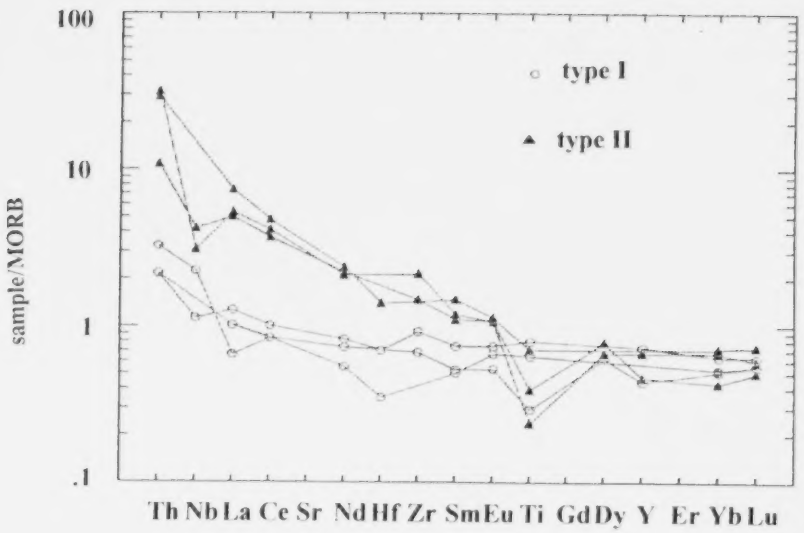

Figure 37. Extended plot of the type I and type II intermediate and mafic volcanic rocks.

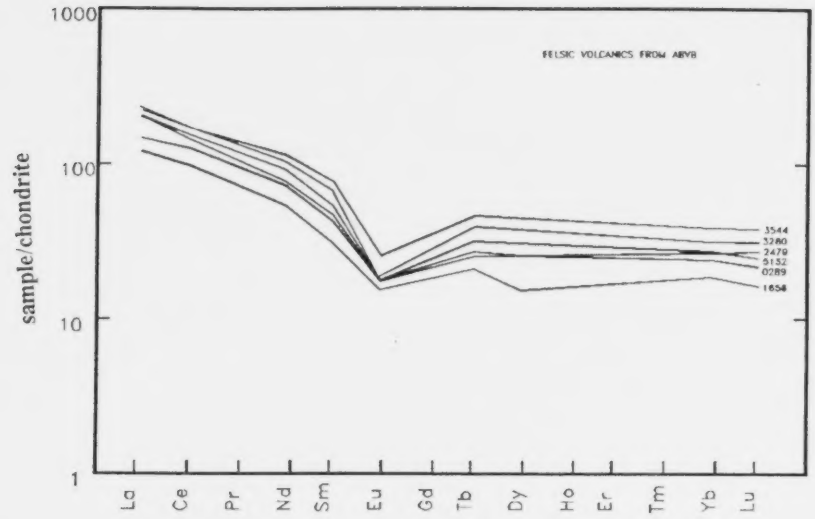

Figure 38. REE diagram of felsic volcanics from the ABVB.

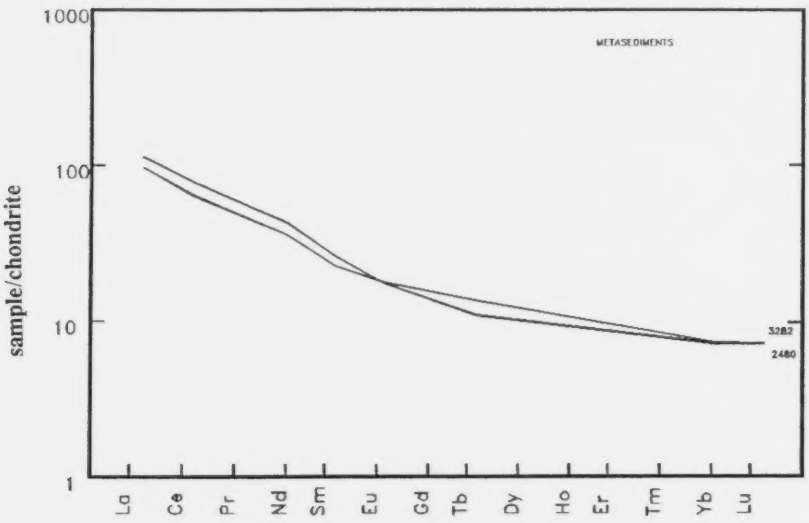

Figure 39. REE diagram for the metasediments from the ABVB.

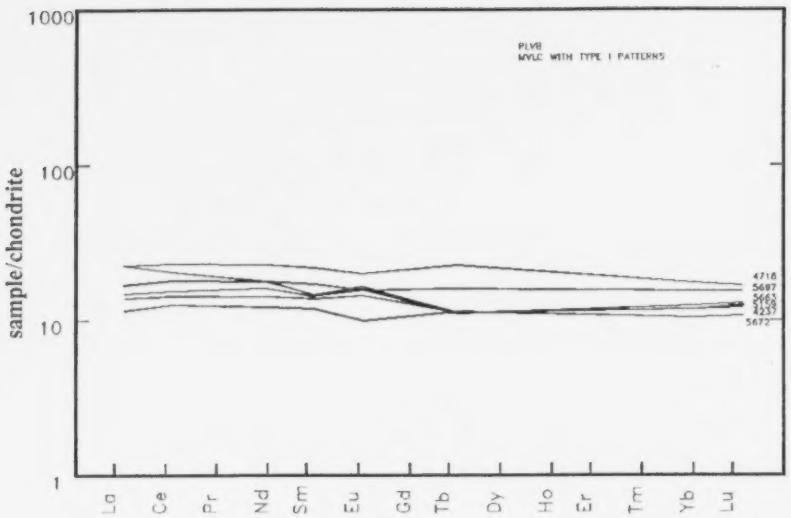

Figure 40a). REE diagram for mafic volcanics from the PLVB displaying type I patterns.

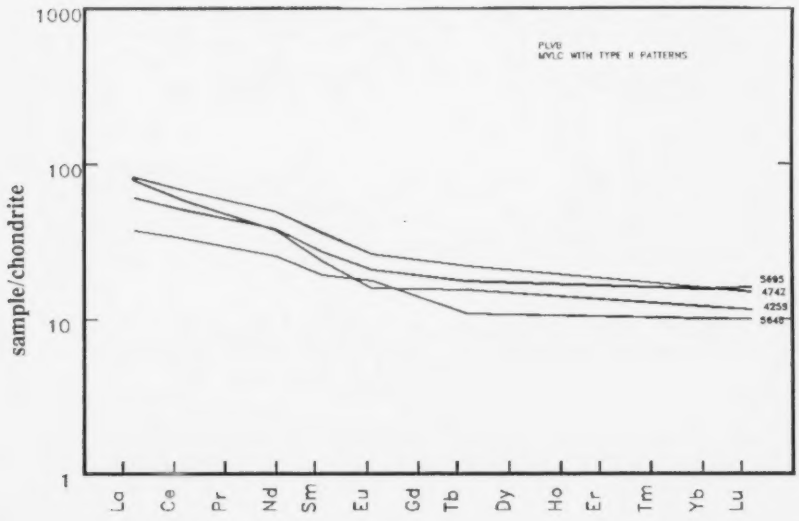

Figure 40b) REE diagram for mafic volcanics from the PLVB displaying type II patterns.

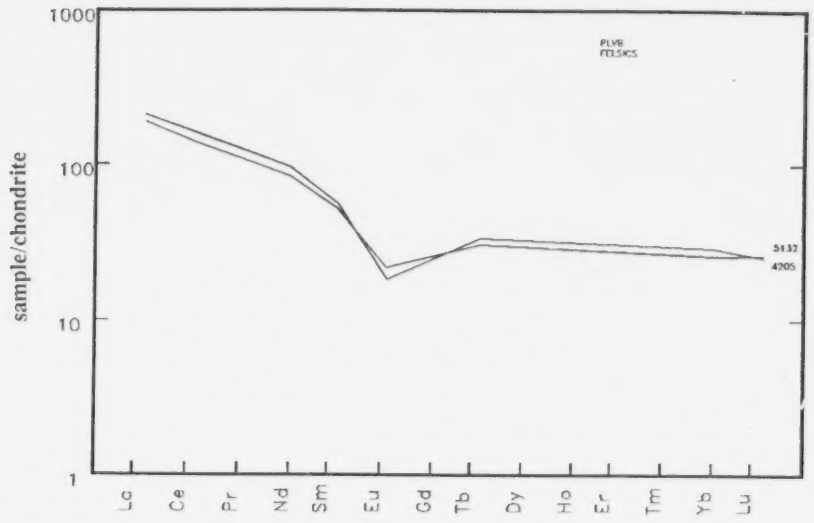

Figure 41. REE diagram for the felsic volcanics from the PLVB.

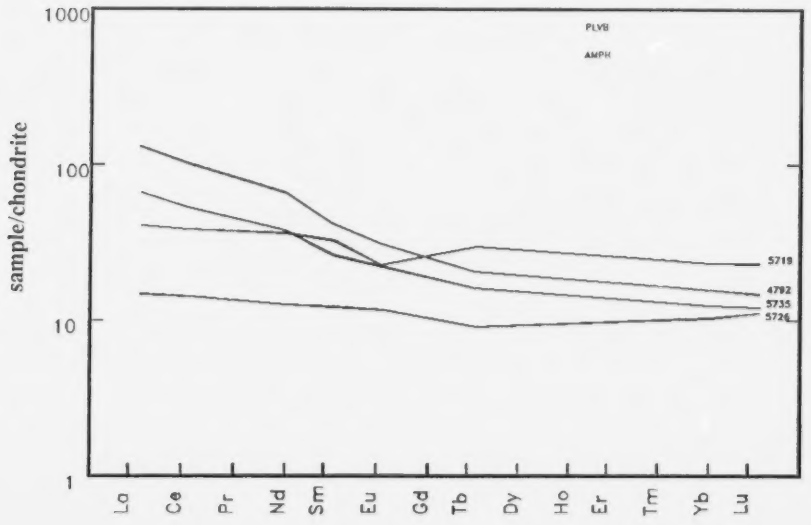

Figure 42. REE diagram of the amphibolites from the PLVB.

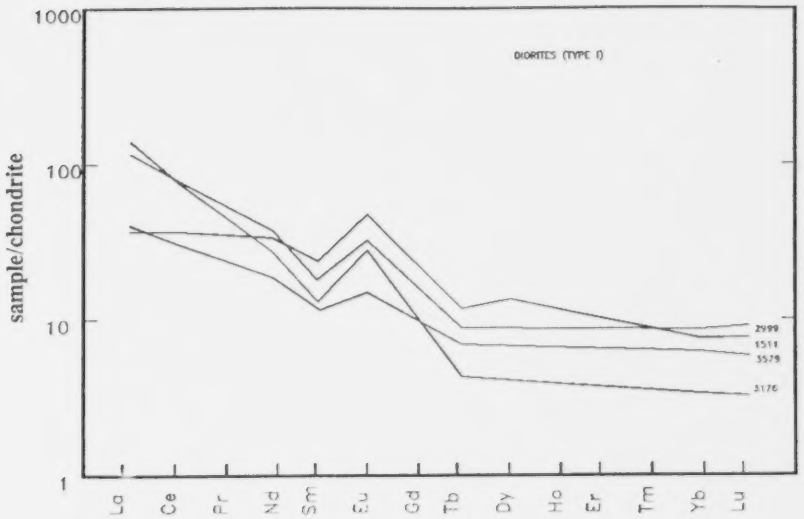

Figure 43. REE diagram for the synvolcanic diorites exhibiting type I patterns.

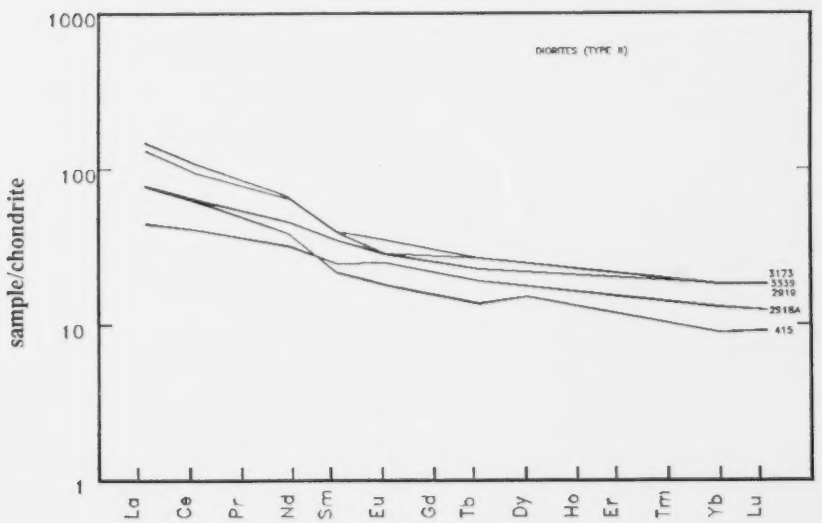

Figure 44a). REE diagram for the synvolcanic diorites exhibiting type II patterns.

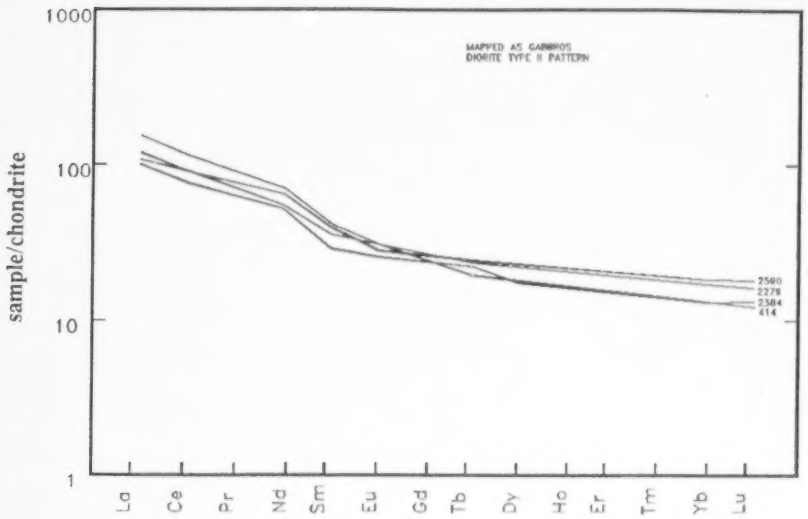

Figure 44b). REE diagram for the gabbros from the synvolcanic complex exhibiting type II patterns.

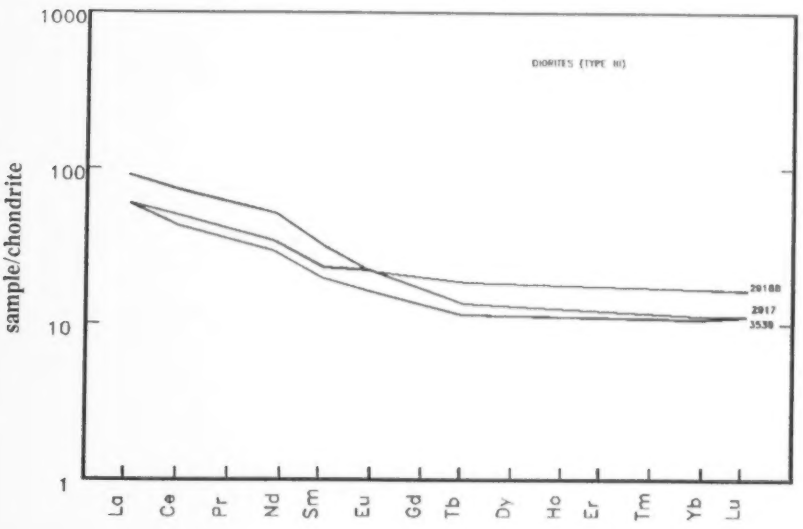

Figure 45. REE diagram for the type III pattern synvolcanic diorites.

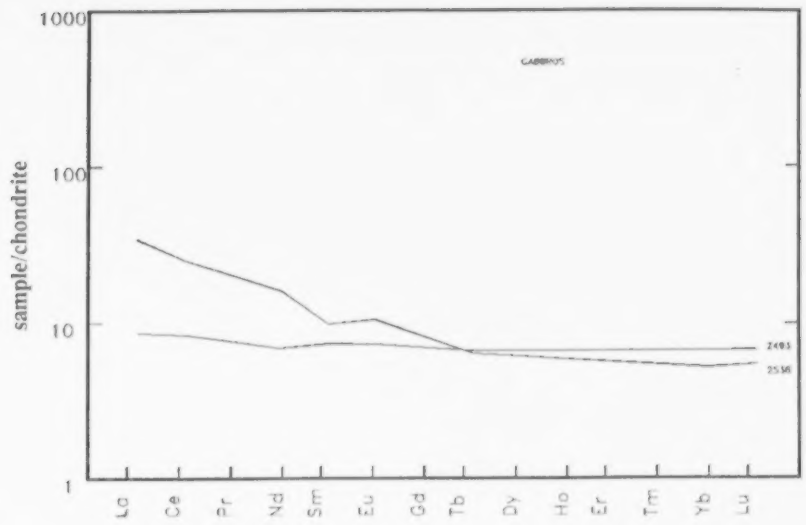

Figure 46. REE diagram for gabbros from the synvolcanic complex displaying patterns similar to the type I mafic volcanics.

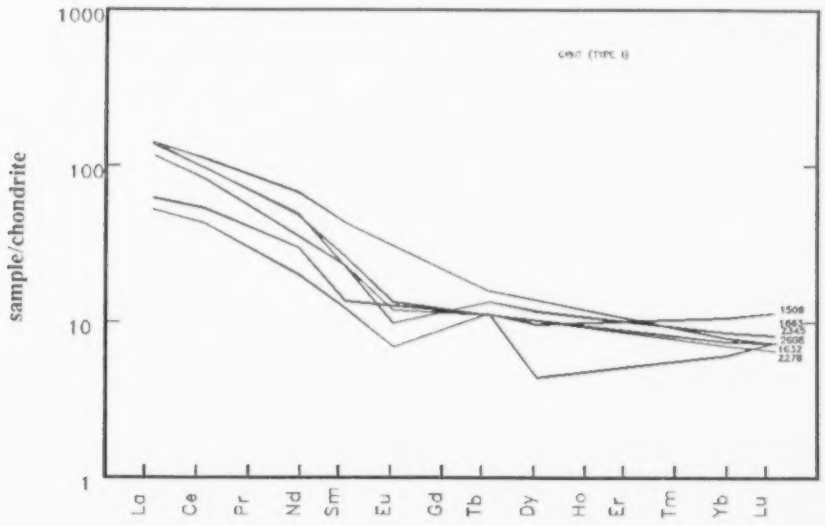

Figure 47. REE diagram of type I granitoids.

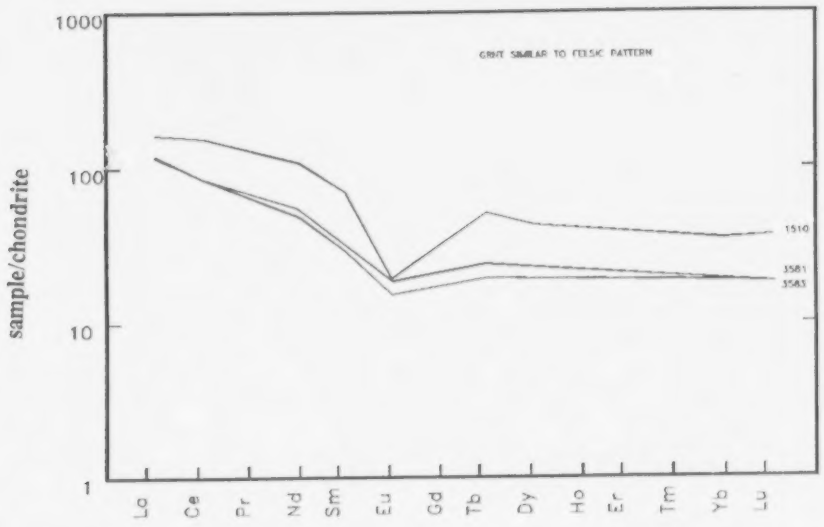

Figure 48. REE diagram of granites with large negative Eu anomalies.

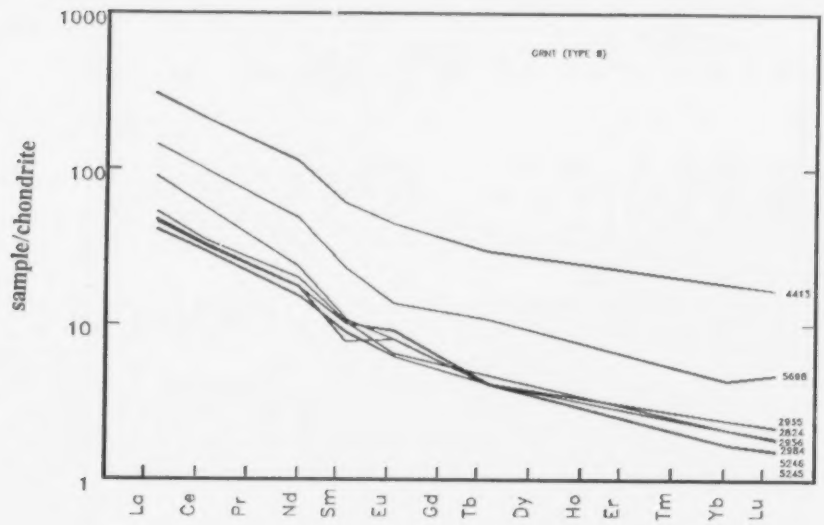

Figure 49a). REE diagram of the type II granites.

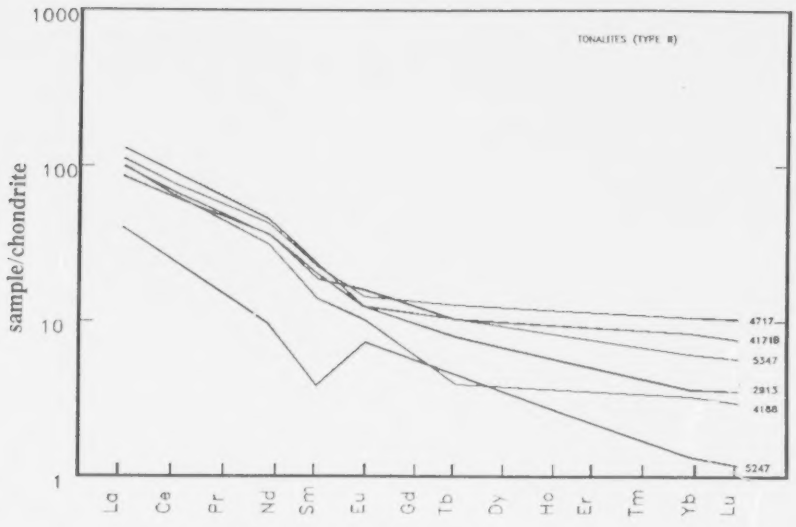

Figure 49b) REE diagram of tonalites having type II granitic patterns.

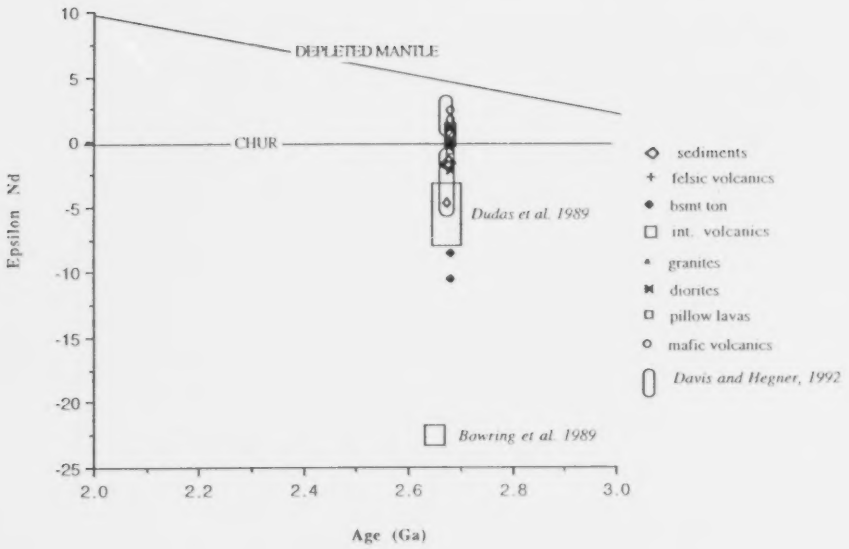

Figure 50. ϵNd vs. time plot.

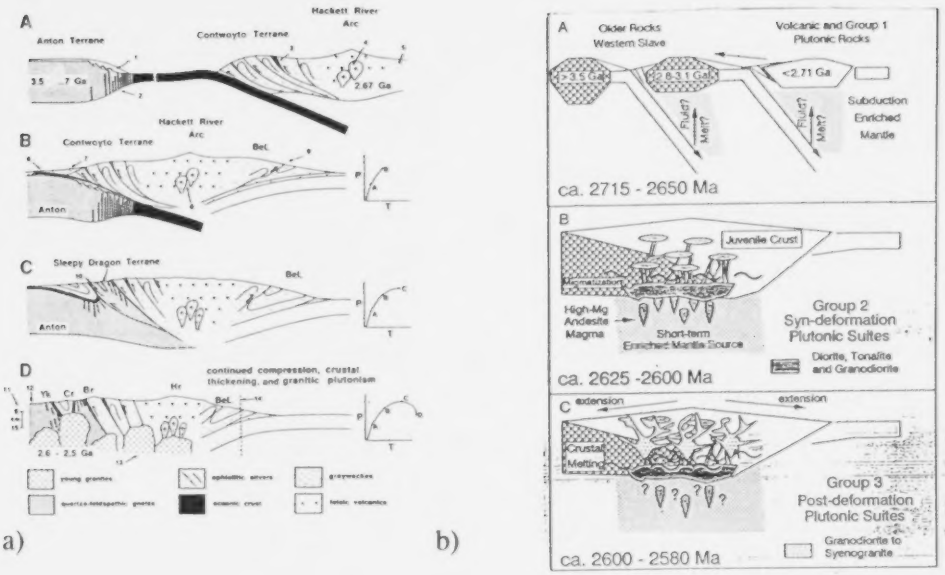

Figure 51. Proposed tectonic models for the Slave Structural Province. a) accretionary model (from Kusky (1989)) b) accretionary model (from Davis *et al.*, 1994) c) Andean-type (from Fyson and Helmstaedt, 1988) d) ensialic rift (from Easton, 1985).

SAMPLE	Age (Ma)	Sample Type	Comments
JG91-1663	>2420	Tak Granite, NW of ABVB	metamict zircons, high Pb loss
JG91-1510	ca. 2550	Rim Granite, S of Hanikahimajuk L.	U-rich zircons, highly discordant
JG91-1923	ca. 2560	mafic gneiss, W of ABVB	discordant, imprecise age
JG91-1657	2572	musc-rich pegmatite, western ABVB	many metamict zircons, rare clear zircons
JG91-1930	2583,2900	zircons from qtz-pebble conglomerate	zircons with different ages
JG91-1295	>2620	felsic volcanic, eastern ABVB	single highly discordant analysis
JG91-0414	2673	diorite, N of Hanikahimajuk L.	two analyses, slightly discordant
JG91-1655	2675	felsic volcanic at Hood-10 deposit	discordant with complex systematics
JG91-1666	2680	felsic volcanic, E of Hanikahimajuk L.	complex discordance
JG91-1511	2680	diorite, S of Hanikahimajuk L.	slightly discordant, one concordant age 2680 Ma
JG91-2767	2681	felsic volcanic from the southern zone	discordant
JG91-1660	ca. 3350	tonalite, N of Hanikahimajuk L.	slightly discordant

Table 1. Preliminary U-Pb geochronological data (granted from S. Bowring, unpublished).

CONDIE'S AVERAGE COMPOSITIONS (1981)						STUDY AREA AVERAGE COMPOSITIONS				
	TH1	TH2	A1	A11	A111		INT	TYPE II	TYPE I	FVLC
SiO2	50.2	49.5	56.7	58.9	55.1	SiO2	56.26	50.74	49.91	72.99
TiO2	0.94	1.49	0.92	0.65	0.95	TiO2	0.91	1.44	1.02	0.17
Al2O3	15.5	15.2	14	15.5	15.9	Al2O3	15.48	13.64	14.89	12.47
Fe2O3	1.63	2.8	2.3	1.5	1.99	Fe2O3	2.21	2.93	3.18	0.68
FeO	9.26	9.17	7	1.5	5.86	Fe (tot)	6.67	10.83	9.86	2.32
MgO	7.53	6.82	5.4	4.5	4.3	MgO	3.22	3.62	5.66	1.60
CaO	11.6	8.79	6.6	4.5	5.9	CaO	6.37	7.32	9.49	1.34
Na2O	2.15	2.7	3.4	5.1	3.9	Na2O	3.14	2.79	2.51	2.20
K2O	0.22	0.69	0.67	4	1.1	K2O	1.25	0.60	0.42	2.85
P2O5	0.1	0.17				P2O5	0.32	0.53	0.16	0.06
MnO	0.22	0.18				MnO	0.14	0.12	0.25	0.02
H2O	1.62	2.04	3	3	2.8	LOI	4.87	5.39	2.86	2.08
Cr	490	250	125	88	105	Cr	133.33	131.67	275.88	186.11
Ni	140	125	70	60	55	Ni	25.56	25.83	71.82	2.78
V	260	365								
Co	52	55	25	23	29	Co	25.00	49.33	47.87	0.78
Cu	110	100	60	36	64	Cu	46.02	32.90	160.00	4.81
Zn	80	120	97	81	77	Zn	62.09	151.17	137.49	55.51
Zr	53	135	150	190	104	Zr	203.75	171.00	83.18	254.00
Ba	80	90	230	547	361	Ba	312.22	261.67	174.44	477.78
Sr	100	190	278	580	210	Sr	<500	<500	<500	<500
La	3.6	13	13	34	12	La	26.24	23.58	5.01	52.98
Ce	9.2	30	31	70	30	Ce	54.56	53.00	13.12	108.22
Nd	6.6	17	17	35	22	Nd	26.00	27.83	8.41	47.33
Sm	2	4	3.6	6.7	7.3	Sm	5.15	6.12	2.41	9.48
Eu	0.73	1.3	1.1	1.9	2	Eu	1.51	2.00	0.95	1.45
Dy	3.1	4.2	3.8	5.8	11	Dy	4.60	4.05	3.70	5.31
Yb	1.9	2.2	1.8	2.4	6.1	Yb	2.47	2.84	2.18	5.34
Lu	0.31	0.38	0.3	0.3	1.1	Lu	0.36	0.43	0.35	0.80
Y	20	30	25	35	35	Y	26.00	24.00	20.50	45.00

Table 2. Comparison table of Condie (1981) Archean average compositions and Hanikahimajuk Lake area averages.

BIBLIOGRAPHY

Barrie, C.T.,and Davis, W.J.,1990: Timing of magmatism and deformation in the Kamiskotia-Kidd Creek area, western Abitibi Subprovince, Canada; Precambrian Research, v. 46, p. 217-240.

Barrie, C.T.,Ludden, J.N.,and Green, T.H.,1993: Geochemistry of volcanic rocks associated with Cu-Zn and Ni-Cu deposits in the Abitibi Subprovince, Economic Geology, v. 88, p. 1341-1358.

Barrie, C.T.,and Shirey, S.B.,1991: Nd and Sr isotope systematics for the Kamiskotia-Montcalm area: implications for the formation of late Archean crust in the western Abitibi Subprovince, Canada; Canadian Journal of Earth Sciences, v. 28, p. 58-76.

Barker, F., and Arth, J.G.,1976: Generation of trondhjemitic-tonalitic liquids and Archean bimodal trondhjemite-basalt suites; Geology, v. 4, p. 596-600.

Bau, A.F.S.,Aspler, L.B.,and Hurdle, E.J.,1978: Preliminary geology of NTS 86H/14,15,16; DIAND EGS 1978-4

Bostock, H.H.,1980: The Itchen Lake Area, District of Mackenzie: Geological Survey of Canada, Memoir 391, 101 p.

Bowring, S.A.,King, J.E.,Housh, T.B.,Isachsen, C.E.,and Podosek, F.A.,1989: Neodymium and lead isotope evidence for enriched early Archaean crust in North America; Nature, v. 340, p. 222-225.

Campbell, I.H.,Coad, P., Franklin, J.M.,Gorton, M.P.,and Thurston, P.C.,1982: Rare-earth elements in volcanic rocks associated with Cu-Zn massive sulphide mineralization: A preliminary report; Canadian Journal of Earth Sciences, v. 19, p. 619-623.

Condie, K.C.,1981: Archean Greenstone Belts; Developments in Precambrian Geology, v. 3; Elsevier Scientific Publishing Company, 434 p.

Davis, W.J.,Fryer, B.J.,and King, J.E.,1994: Geochemistry and evolution of Late Archean plutonism and it's significance to the tectonic development of the Slave Craton; Precambrian Research, v. 67, p. 1-35.

Davis, W.J.,and Hegner, E., 1992: Neodymium isotopic evidence for the tectonic assembly of Late Archean crust in the Slave Province, northwest Canada; Contributions to Mineralogy and Petrology, v. 111, p. 493-504.

DePaolo, D.J.,1988: Neodymium Isotope Geochemistry: An Introduction; Springer-Verlag, 187 p.

Drury, S.A.,1978: Rare-earth and other trace-element data bearing on the origin of Archaean granitic rocks from Yellowknife, Northwest Territories; Canadian Journal of Earth Sciences, v. 16, p. 809-815.

Dudas, F.O.,1989: Nd isotopic compositions from the Slave craton: the case of the missing mantle; Geological Association of Canada, Program with Abstracts, 14, Montreal, A24.

Easton, R.M.,1985: The nature and significance of pre-Yellowknife Supergroup rocks in the Point Lake area, Slave Structural Province, Canada; in Evolution of Supracrustal Sequences, Geological Association of Canada, Special Paper 28, p. 153-167.

Ewing, T.E.,1979: Two calc-alkaline volcanic trends in the Archean: Trace element evidence, Contributions to Mineralogy and Petrology, v. 48, p. 1-7.

Fraser, J.A.,1960: North-central District of Mackenzie, Northwest Territories; Geological Survey of Canada, Preliminary Map 18-1960.

Frith, R.A.,1987: Precambrian geology of the Hackett River area, District of Mackenzie, N.W.T.,Geological Survey of Canada, Memoir 417, 61 p.

Frith, R.A.,and Fryer, B.J.,1985: Geochemistry and origin of the Regan Intrusive Suite and other granitoids in the northeastern Slave Province, northwest Canadian Shield; Canadian Journal of Earth Sciences, v. 22, p. 1048-1065.

Fyson, W.K.,and Helmstaedt, H., 1988: Structural patterns and tectonic evolution of supracrustal domains in the Archean Slave Province, Canada; Canadian Journal of Earth Sciences, v. 25, p. 301-315

Fyson, W.K.,and Padgham, W.A.,1993: Geology of the Slave Structural Province, 1:1,000,000scale map; DIAND EGS 1993-8.

Gebert, J.S.,1995: Archean geology of the Hanikahimajuk Lake area, northern Point Lake volcanic belt, west-central Slave Structural Province, District of Mackenzie, N.W.T.;DIAND EGS 1995-3, 27 p.

Gill, J.W.,1976: The Takiyuak metavolcanic belt, geology, geochemistry, and mineralization; unpublished Ph.D. thesis, Carleton University, Ottawa, Ontario, 210 p.

Goodwin, A.M.,1988: Geochemistry of Slave Province volcanic rocks, Yellowknife belt; in Contributions to the Geology of the Northwest Territories, v. 3, Department of Indian and Northern Development, Yellowknife, N.W.T.,p. 13-25.

Hanson, G.N.,1980: Rare-earth elements in petrogenetic studies of igneous systems; Annual Review, Earth and Planetary Science, v. 8, p. 371-406.

Henderson, J.B.,1970: Stratigraphy of the Archean Yellowknife Supergr[illegible]p, Yellowknife Bay-Prosperous Lake area, District of Mackenzie, Geological Survey Of Canada, Paper 70-26, 12 p.

Henderson, J.B.,1981: Archaean basin evolution in the Slave Province, Canada; in Precambrian Plate Tectonics, Developments in Precambrian Geology v. 4, A. Kroner ed.; p. 213-235.

Henderson, J.B.,1988: Geology, Keskarrah Bay area, District of Mackenzie, N.W.T.;Geological Survey of Canada, Map 1679A.

Henderson, J.B.,and Easton, R.M.,1977: Archean supracrustal-basement rock relationships in the Keskarrah Bay map area, Slave Structural Province, District of Mackenzie; in Current Research, Geological Survey of Canada, Paper 77-1A, p. 217-221.

Hyde, R.S.,McLeod, H.A.,Scribbins, B.T.,and Taylor, S.L.,1976a: Preliminary geology of NTS 86I/1, part of the Takijuq Lake area; DIAND EGS 1976-17.

Hyde, R.S.,McLeod, H.A.,Scribbins, B.T.,and Taylor, S.L.,1976b: Preliminary geology of NTS 86I/2, part of the Takijuq Lake area; DIAND EGS 1976-18.

Irvine, T.N.,and Barager, W.R.A.,1971: A guide to the chemical classification of the common volcanic rocks; Canadian Journal of Earth Sciences, v. 8, p. 523-548.

Isachsen, C.E.,and Bowring, S.A.,1994: Evolution of the Slave craton; Geology, v. 22, p. 917-920.

Jahn, B., Glikson, A.Y.,Peucat, J.J.,and Hickman, A.H.,1981: REE geochemistry and isotopic data of Archean silicic volcanics and granitoids from the Pilbara Block, Western Australia: implication for the early crustal evolution; Geochimica et Cosmochimica Acta, v. 45, p. 1633-1652.

Jenner, G.A.,Fryer, B.J. Fryer, and McLennan, S.M.,1981: Geochemistry of the Archean Yellowknife Supergroup, Geochimica et Cosmochimica Acta, v. 45, p. 1111-1129.

Jensen, L.S., 1976: A new cation plot for classifying subalkalic volcanic rocks; Ontario Division of Mines, MP 66, 22 p.

Jensen, L.S., 1985: Stratigraphy and petrogenesis fo Archean metavolcanic sequences southwestern Abitibi Subprovince, Ontario; in Evolution of Archean Supracrustal Sequences, L.D. Ayres, P.C. Thurston, K.D. Card and W. Weber eds.; Geological Association of Canada, Special Paper 28, p. 65-87.

King, J.E., Davis, W.J., and Relf, C., 1989: Comment and reply on "Accretion of the Archean Slave province"; Geology, v. 17, p. 963-966.

King, J.E., Davis, W.J., and Relf, C., 1992: Late Archean tectono-magmatic evolution of the central Slave Province, Northwest Territories; Canadian Journal of Earth Sciences, v. 29, p. 2156-2170.

King, J.E., Davis, W.J., Relf, C., and Van Nostrand, T., 1990: Geology of the Contwoyto - Nose Lakes map area, central Slave Province, District of Mackenzie, N.W.T.; in Current Research, Part C, Geological Survey of Canada, Paper 90-1C, p. 177-187.

King, J.E., Davis, W.J., Van Nostrand, T., and Relf, C., 1989: Archean to Proterozoic deformation and plutonism of the western Contwoyto Lake map area, central Slave Province, District of Mackenzie, N.W.T.; in Current Research, Geological Survey of Canada, Paper 89-1C, p. 81-94.

King, J.E., and Helmstaedt, H., 1989: Deformation history of an Archean fold belt, eastern Point Lake area, Slave Structural Province, N.W.T.; Canadian Journal of Earth Sciences, v. 26, p. 106-118.

Krogh, T.E., and Davis, G.L., 1974: Alteration in zircons with discordant U-Pb ages; Carnegie Institute, Washington, Year Book, v. 73, p. 560-567.

Krogh, T.E., and Gibbins, W.A., 1978: U-Pb isotopic ages of basement and supracrustal rocks in the Point Lake area of the Slave Province, Canada; GAC/MAC program with abstracts, v. 3, p. 438.

Kusky, T.M., 1989: Accretion of the Archean Slave Province; Geology, v. 17, p. 63-67.

Kusky, T.M., 1990: Evidence for Archean ocean opening and closing in the southern Slave Province; Tectonics, v. 9, p. 1533-1563.

Kusky, T.M., 1991: Structural development of an Archean Orogen, western Point Lake, Northwest Territories; Tectonics, v. 10, p. 820-841.

LeMaitre, R.W.,1989: A Classification of Igneous Rocks and Glossary of Terms; Blackwell, Oxford, 183 p.

Lesher, C.M.,**Goodwin, A.M.**,**Campbell, I.H.**,**and Gorton, M.P.**,1986: Trace-element geochemistry of ore-associated and barren, felsic metavolcanic rocks in the Superior Province, Canada; Canadian Journal of Earth Sciences, v. 23, p. 222-237.

Mortensen, J.K.,**Thorpe, R.I.**,**Padgham, W.A.**,**King, J.E.**,**and Davis, W.J.**,1988: U-Pb zircon ages for felsic volcanism in the Slave Province, N.W.T.; in Radiogenic and Isotopic Studies: Report 2, Geological Survey of Canada, Paper 88-2, p. 85-95.

Mullen, E.D.,1983: $MnO/TiO_2/P_2O_5$: a minor element discriminant for basaltic rocks of oceanic environments and its implications for petrogenesis; Earth and Planetary Science Letters, v. 62, p.53-62.

Padgham, W.A.,1985: Observations of supracrustal successions in the Slave Structural Province; in Evolution of Archean Supracrustal Sequences, L.D. Ayres, P.C. Thurston, K.D. Card and W. Weber eds.; Geological Association of Canada, Special Paper 28, p. 133-151.

Pagdham, W.A.,1990: The Slave Province, an overview; in Mineral Deposits of the Slave Province, Northwest Territories, W.A. Padgham and D. Atkinson, eds.; Geological Survey of Canada, Open File 2168, p. 1-40.

Padgham, W.A.,**and Fyson, W.K.**,1992: The Slave Province: a distinct Archean craton; Canadian Journal of Earth Sciences, v. 29, p. 2702-2086.

Pearce, J.A.,1983: Role of the sub-continental lithosphere in magma genesis at active continental margins; in Continental Basalts and Mantle Xenoliths, C.J. Hawkesworth and M.J. Norry, eds.; Shiva Geology Series, p. 230-249.

Pearce, J.A.,**and Cann, J.R.**,1973: Tectonic setting of basic volcanic rocks determined using trace element analyses; Earth and Planetary Science Letters, v. 19, p. 290-300.

Pearce, T.H.,**Gorman, B.E.**,**and Birkett, T.C.**,1977: The relationship between major element chemistry and tectonic environment of basic and intermediate volcanic rocks; Earth and Planetary Science Letters, v. 36, p. 121-132.

Pearce, J.A.,**Harris, N.B.W.**,**and Tindle, A.G.**,1984: Trace element discrimination diagrams for the tectonic interpretation of granitic rocks; Journal of Petrology, v.25, p. 956-983.

Relf, C., 1992: Two distinct shortening event during late Archean orogeny in the west-central Slave Province, Northwest Territories, Canada; Canadian Journal of Earth Sciences, v. 29, p. 2104-2117.

Rockingham, C.J., 1979: Metamorphism and metal zoning of the Hood River - 41 massive sulfide deposit, Slave Structural Province, N.W.T.; unpublished M.Sc. thesis, University of Western Ontario, London, Ontario, 125 p.

Shirey, S.B., and Hanson, G.N., 1986: Mantle heterogeneity and crustal recycling in Archean granite-greenstone belts: Evidence from Nd isotopes and trace elements in the Rainy Lake area, Superior Province, Ontario, Canada; Geochimica et Cosmochimica Acta, v. 50, p. 2631-2651.

Stockwell, C.H., 1933: Great Slave Lake-Coppermine River area, N.W.T.; Geological Survey of Canada, Summary Report 1932, Part C, p. 37-63.

Taylor, S.R., and McLennan, S.M., 1985: The Continental Crust: its Composition and Evolution, an examination of the geochemical record preserved in sedimentary rocks; Blackwell Scientific Publications, 312 p.

Thorpe, R.I., Cumming, G.L., and Mortensen, J.K., 1992: A major Pb-isotope boundary in the Slave Province and its probable relation to ancient basement in the western Slave; in Canada-NWT MDA Summary Volume, Geological Survey of Canada, Open File 2484, p. 179-184.

van Breemen, O., Davis, W.J., and King, J.E., 1992: Temporal distribution of granitoid plutonic rocks of the Archean Slave Province, northwestern Canadian Shield; Canadian Journal of Earth Sciences, v. 29, p. 2186-2199.

APPENDIX A

GEOCHEMICAL DATA

The geochemical analyses were contracted out to different laboratories for each of the three years. The 1991 samples were analyzed by Barringer Magenta Laboratories Ltd. of Calgary, AB. The 1992 and 1993 samples were analyzed by X-RAL Assay Laboratories of Don Mills, Ont. The major elements were analyzed using neutron activation (NA) techniques or x-ray fluorescence (XRF) and the trace element methods and detection limits are listed here.

ABBREVIATIONS
NA (NAA) - neutron activation
XRF - x-ray fluorescence
wet - wet chemistry
FAA - fire assay
DCP - direct coupled plasma

1991 GEOCHEMICAL SAMPLE ANALYSES METHODS

	METHOD	DETECTION LIMIT		METHOD	DETECTION LIMIT
Au ppb	NA	5	La ppm	NA	0.1
Na ppm	NA	50	Ce ppm	NA	1
Ca %	NA	1	Nd ppm	NA	5
Sc ppm	NA	0.1	Sm ppm	NA	0.5
Cr ppm	NA	10	Eu ppm	NA	0.2
Fe %	NA	0.1	Tb ppm	NA	0.5
Co ppm	NA	5	Yb ppm	NA	0.2
Ni ppm	NA	50	Lu ppm	NA	0.05
Zn ppm	NA	50	Hf ppm	NA	1
As ppm	NA	2	Ta ppm	NA	1
Se ppm	NA	5	W ppm	NA	4
Br ppm	NA	1	Ir ppb	NA	5
Rb ppm	NA	30	Hg ppb	NA	1
Sr ppm	NA	500	Th ppm	NA	0.5
Mo ppm	NA	5	U ppm	NA	0.5
Ag ppm	NA	5			
Sb ppm	NA	0.2			
Cs ppm	NA	2			
Ba ppm	NA	100			
Sn %	NA	0.02			

1992 GEOCHEMICAL SAMPLE ANALYSES METHODS

	METHOD	DETECTION LIMIT
Au ppb	FADCP	1
Au ppb	NA	5
Na ppm	NA	500
WRMAJ %	WR	0.01
Ca %	NA	1
Sc ppm	NA	0.1
Cr ppm	NA	10
Mn ppm	DCP	100
Fe ppm	NA	0.1
Fe %	NA	0.1
Co ppm	DCP	1
Co ppm	NA	5
Ni ppm	DCP	1
Ni ppm	NA	100
Cu ppm	DCP	0.5
Zn ppm	DCP	0.5
Zn ppm	NA	50
As ppm	FAA	1
As ppm	NA	2
Se ppm	NA	5
Br ppm	NA	1
Rb ppm	NA	30
Sr ppm	NA	500
Mo ppm	DCP	1
Mo ppm	NA	5
Ag ppm	DCP	0.5
Ag ppm	NA	5
Sb ppm	NA	0.2
Cs ppm	NA	3
Ba ppm	NA	100
La ppm	NA	1

	METHOD	DETECTION LIMIT
La ppm	NA	0.1
Ce ppm	NA	3
Ce ppm	NA	1
Nd ppm	NA	10
Nd ppm	NA	3
Sm ppm	NA	0.5
Sm ppm	NA	0.01
Eu ppm	NA	0.2
Eu ppm	NA	0.05
Tb ppm	NA	0.5
Tb ppm	NA	0.1
Yb ppm	NA	0.2
Yb ppm	NA	0.05
Lu ppm	NA	0.05
Lu ppm	NA	0.01
Hf ppm	NA	1
Ta ppm	NA	1
W ppm	NA	4
Ir ppb	NA	20
Hg ppb	WET	5
Pb ppm	DCP	2
Th ppm	NA	0.5
Th ppm	NA	0.2
U ppm	NA	0.5
U ppm	NA	0.1

1993 GEOCHEMICAL SAMPLE ANALYSES METHODS

	METHOD	DETECTION LIMIT
Au ppb	NA	5
Na ppm	NA	500
WRMAJ %	XRF–F	0.01
Ca %	NA	1
Sc ppm	NA	0.1
Ti ppm	XRF	5
Cr ppm	NA	10
Fe %	NA	0.1
FeO %	WET	0.1
Co ppm	NA	5
Ni ppm	NA	100
Zn ppm	NA	50
As ppm	NA	2
Se ppm	NA	5
Br ppm	NA	1
Rb ppm	NA	30
Sr ppm	NA	500
Y ppm	XRF	2
Zr ppm	XRF	3
Nb ppm	XRF	2
Mo ppm	NA	5
Ag ppm	NA	5
Sb ppm	NA	0.2
Cs ppm	NA	3
Ba ppm	NA	100
La ppm	NA	1

	METHOD	DETECTION LIMIT
La ppm	NA	0.1
Ce ppm	NA	3
Ce ppm	NA	1
Nd ppm	NA	10
Nd ppm	NA	3
Sm ppm	NA	0.5
Sm ppm	NA	0.01
Eu ppm	NA	0.2
Eu ppm	NA	0.05
Tb ppm	NA	0.5
Tb ppm	NA	0.1
Yb ppm	NA	0.2
Yb ppm	NA	0.05
Lu ppm	NA	0.05
Lu ppm	NA	0.01
Hf ppm	NA	1
Ta ppm	NA	1
W ppm	NA	4
Ir ppb	NA	20
Hg ppb	WET	5
Th ppm	NA	0.5
Th ppm	NA	0.2
U ppm	NA	0.5
U ppm	NA	0.1

Yr	No.		ROCK	MAJOR OXIDES											
				SiO2	TiO2	Al2O3	Fe2O3	Fe (tot)	MnO	MgO	CaO	Na2O	K2O	P2O5	LOI
JG91-	0079	A	DIA	47.05	1.620	15.24		17.16	0.184	4.48	6.75	4.05	1.55	0.69	2.13
JG91-	0266	A	PLLV	48.01	0.589	15.11		15.87	0.215	3.38	8.51	2.72	0.83	0.50	6.01
JG91-	0267	A	PLLV	53.61	0.647	14.54		14.00	0.240	2.50	7.00	3.64	0.76	0.48	5.27
JG91-	0268	A	PLLV	51.34	0.350	14.92		13.73	0.191	7.25	7.16	2.79	0.31	0.39	3.14
JG91-	0288	A	IVLC	47.22	0.641	18.89		13.30	0.197	4.61	11.00	2.48	0.73	0.50	4.19
JG91-	0289	A	FVLC	73.86	0.088	11.33		3.00	0.028	1.38	0.50	3.61	1.18	0.04	1.06
JG91-	0414	A	DIO	52.80	0.577	17.19		13.58	0.156	4.39	6.56	2.85	2.11	0.59	1.35
JG91-	0415	A	DIO	56.29	0.334	18.13		9.72	0.110	4.00	7.44	3.77	1.05	0.31	1.99
JG91-	1295	A	FVLC	69.10	0.055	13.41		1.43	0.027	0.60	0.61	1.24	8.10	0.08	1.19
JG91-	1439	A	FVLC	64.45	0.167	16.43		8.58	0.064	5.45	0.35	0.10	3.00	0.33	4.09
JG91-	1509	A	GRNT	68.73	0.033	15.23		0.57	0.008	0.45	0.31	3.40	6.75	0.03	0.73
JG91-	1510	A	GRNT	72.85	0.042	13.22		1.38	0.011	0.16	0.33	4.23	4.22	0.07	0.01
JG91-	1511	A	DIO	50.84	0.872	20.77		14.33	0.183	2.71	8.66	3.74	0.24	1.03	0.13
JG91-	1604	A	PLLV	46.98	0.440	15.49		15.44	0.250	6.03	7.55	2.20	0.06	0.38	7.44
JG91-	1632	A	GRNT	71.52	0.118	14.88		2.00	0.033	0.64	1.08	4.51	1.82	0.10	0.56
JG91-	1654	A	IVLC	52.83	0.367	14.73		10.01	0.209	4.47	6.73	2.78	1.05	0.36	8.14
JG91-	1655	A	FVLC	74.26	0.047	12.08		1.29	0.016	1.20	0.59	3.44	1.63	0.04	1.32
JG91-	1656	A	FVLC	76.45	0.068	11.40		1.36	0.011	0.69	0.21	1.85	3.01	0.04	1.04
JG91-	1657	A	PEG	73.14	0.008	14.90		0.55	0.010	0.14	0.26	4.04	3.12	0.07	0.14
JG91-	1659	A	UM	37.64	0.093	2.83		12.87	0.141	32.50	0.32	0.06	0.08	0.27	10.42
JG91-	1660	A	TON	65.17	0.144	15.46		2.86	0.032	0.96	2.00	4.13	2.16	0.17	2.22
JG91-	1663	A	GRNT	67.28	0.126	14.77		3.15	0.024	0.67	1.15	3.67	4.30	0.15	0.73
JG91-	1666	A	FVLC	70.20	0.093	13.22		2.72	0.023	0.48	0.95	3.28	3.83	0.06	1.17
JG91-	1702	A	FVLC	71.66	0.053	12.24		5.00	0.024	2.40	0.10	0.09	2.64	0.08	1.54
JG91-	1719	A	IVLC	58.37	0.533	17.54		11.30	0.154	3.61	6.01	3.58	0.78	0.50	1.20
JG91-	1754	A	TON	71.00	0.080	15.43		2.03	0.023	0.50	1.73	4.60	1.35	0.13	1.21
JG91-	1758	A	GAB	47.88	0.477	16.06		16.02	0.218	7.26	10.00	1.96	0.78	0.48	1.18
JG91-	1786	A	IVLC	52.00	0.360	18.50		10.01	0.148	7.05	2.04	3.77	1.60	0.40	2.68
JG91-	1793	A	IVLC	60.03	0.377	17.75		10.16	0.097	3.26	5.60	3.66	1.23	0.38	1.44
JG91-	1924	A	CLAST	72.20	0.038	13.38		2.06	0.029	0.66	1.51	3.85	1.39	0.04	0.96

NO.	TRANSITION METALS							GRANITOID			PRECIOUS AND PRECIOUS PATHFINDER						
	Cr NAA	Ni	Co	Sc	Cu	Pb	Zn	Sn NAA	W	Mo	As	Se	Sb	Ag	Ir	Au (FAA)	Hg
0079	120	<50	37	19			114	<260	<4	<5	40	<5	<0.2	<5	<5	13	<1
0266	140	<50	58	20			149	<200	<4	<5	30	<5	<0.2	<5	<5	<5	<1
0267	120	<50	52	20			172	<200	<4	<5	15	<5	0.3	<5	<5	<5	<1
0268	300	<50	36	34			<50	<200	<4	<5	<2	<5	0.4	<5	<5	5	<1
0288	170	<50	25	21			<50	<200	<4	<5	11	<5	0.9	<5	<5	<5	<1
0289	300	<50	6	3			<50	<200	<4	<5	4	<5	<0.2	<5	<5	<5	<1
0414	170	<50	29	20			153	<200	<4	<5	13	<5	<0.2	<5	<5	<5	<1
0415	230	280	25	15			<50	<200	<4	7	3	<5	<0.2	<5	<5	<5	<1
1295	240	<50	<5	2			<50	<200	<4	<5	10	<5	<0.2	<5	<5	<5	<1
1439	140	<50	8	8			166	<200	<4	<5	<2	<5	0.7	<5	<5	<5	<1
1509	280	<50	<5	2			<50	<200	<4	<5	7	<5	<0.2	<5	<5	<5	<1
1510	250	<50	<5	2			<50	<200	<4	<5	<2	<5	3.0	<5	<5	<5	<1
1511	190	<50	28	14			<50	<200	<4	<5	5	<5	<0.2	<5	<5	5	<1
1604	290	<50	58	39			<50	<200	<4	<5	7	<5	0.8	<5	<5	8	<1
1632	420	<50	6	4			<50	<200	<4	<5	8	<5	<0.2	<5	<5	<5	<1
1654	190	<50	22	17			<50	<200	<4	<5	5	<5	1.7	<5	<5	<5	<1
1655	360	<50	<5	3			<50	<200	<4	<5	4	<5	0.7	<5	<5	<5	<1
1656	260	<50	<5	4			<50	<200	<4	<5	<2	<5	0.7	<5	<5	<5	<1
1657	320	<50	<5	7			<50	<200	<4	<5	<2	<5	<0.2	<5	<5	5	<1
1659	3800	1300	110	10			115	<200	<4	5	5	<5	4.1	<5	<5	<5	<1
1660	460	<50	7	2			<50	<200	<4	<5	4	<5	0.5	<5	<5	6	<1
1663	260	<50	<5	3			118	<200	<4	<5	<2	<5	<0.2	<5	<5	<5	<1
1666	290	<50	<5	3			62	<200	<4	<5	190	<5	0.4	<5	<5	<5	<1
1702	190	<50	<5	3			51	<200	<4	<5	3	<5	0.2	<5	<5	6	<1
1719	220	<50	28	18			<50	<200	<4	5	33	<5	<0.2	<5	<5	<5	<1
1754	270	<50	<5	2			<50	<200	<4	<5	9	<5	0.6	<5	<5	<5	<1
1758	320	<50	47	34			110	<200	<4	<5	15	<5	2.4	<5	<5	<5	<1
1786	120	<50	28	16			<50	<200	<4	<5	<2	<5	<0.2	<5	<5	<5	<1
1793	170	<50	21	16			<50	<200	<4	<5	13	<5	<0.2	<5	<5	<5	<1
1924	360	<50	<5	1			<50	<200	<4	<5	<2	<5	0.5	<5	<5	<5	<1

	LOW FIELD STRENGTH				HIGH FIELD STRENGTH							RARE EARTH ELEMENTS								
NO.	Rb	Cs	Ba	Sr	Ta	Nb	Hf	Zr	Y	Th	U	La NAA	Ce NAA	Nd NAA	Sm NAA	Eu NAA	Tb NAA	Dy NAA	Yb NAA	Lu NAA
0079	64		640	<500	3	35	n.a.	242	40	5.0	0.5	25.9	66	38	7.6	2.5	1.2	6.2	2.0	0.29
0266	<30		340	<500	<1	15	n.a.	132	16	2.0	1.7	19.7	44	24	4.0	1.4	0.6	4.7	1.6	0.28
0267	<30		430	<500	<1	15	n.a.	129	17	2.3	5.9	18.5	44	21	4.3	1.4	0.8	3.4	1.6	0.25
0268	<30		110	<500	<1	12	n.a.	70	16	1.9	0.9	5.4	15	6	1.9	0.7	0.6	3.5	1.8	0.29
0288	<30		340	<500	3	16	n.a.	133	19	2.4	0.9	14.2	36	19	4.1	1.8	0.8	3.9	2.0	0.32
0289	<30		190	<500	<1	27	n.a.	272	40	19.0	5.1	45.8	102	44	8.2	1.3	1.3	8.3	5.1	0.70
0414	77		520	<500	<1	19	n.a.	174	21	4.8	0.5	29.0	63	28	4.9	1.6	0.9	4.9	2.4	0.34
0415	34		290	<500	3	16	n.a.	163	17	4.8	1.1	22.4	48	21	3.9	1.2	0.6	4.5	1.7	0.27
1295	200		770	<500	5	53	n.a.	172	79	21.0	8.6	36.6	88	37	9.1	1.2	1.8	11.9	6.2	1.02
1439	62		330	<500	1	26	n.a.	450	37	11.0	3.6	33.9	73	33	5.9	1.8	1.2	6.1	3.7	0.51
1509	170		290	<500	4	30	n.a.	81	22	19.0	4.2	15.8	34	12	2.3	0.5	0.5	3.0	2.1	0.34
1510	76		540	<500	<1	36	n.a.	187	75	21.0	3.8	50.8	123	63	13.0	1.4	2.3	13.6	7.0	1.12
1511	<30		110	<500	<1	16	n.a.	62	16	1.0	0.9	10.4	27	18	4.0	3.1	0.5	3.9	1.4	0.22
1604	<30		20	<500	<1	8	n.a.	61	15	0.6	0.5	2.6	10	8	1.9	0.7	0.6	3.7	1.9	0.31
1632	65		310	<500	4	27	n.a.	131	13	8.3	3.0	18.6	42	17	2.5	0.6	0.5	1.4	1.2	0.23
1654	<30		220	<500	3	14	n.a.	183	22	4.4	1.1	23.4	55	23	4.6	1.7	0.9	4.5	2.3	0.35
1655	<30		220	<500	1	18	n.a.	191	37	20.0	5.5	40.6	87	34	6.2	0.8	1.0	6.4	3.3	0.55
1656	63		400	<500	2	16	n.a.	237	36	16.0	4.0	37.6	80	33	5.9	1.1	1.0	4.9	3.9	0.53
1657	320		10	<500	9	60	n.a.	32	34	7.5	3.9	8.3	21	8	2.9	0.2	0.8	4.8	2.5	0.34
1659	<30		10	<500	<1	4	n.a.	30	2	0.6	1.0	1.5	6	5	0.4	0.2	0.5	2.0	0.4	0.05
1660	79		380	<500	<1	11	n.a.	171	9	9.1	1.8	26.8	48	14	2.0	0.7	0.5	1.9	0.8	0.12
1663	150		540	<500	5	16	n.a.	160	24	26.0	4.2	40.7	80	29	4.1	0.7	0.6	3.6	1.7	0.25
1666	62		1050	<500	<1	36	n.a.	397	75	17.0	4.3	54.4	129	56	11.0	2.2	2.1	13.0	6.0	1.04
1702	55		340	<500	<1	17	n.a.	178	41	18.0	4.4	46.0	102	43	7.5	0.8	1.1	7.0	4.2	0.56
1719	<30		250	<500	<1	14	n.a.	211	25	4.8	2.0	20.5	48	25	4.9	1.6	0.9	5.4	2.3	0.41
1754	<30		270	<500	<1	3	n.a.	125	2	4.6	0.5	16.2	30	10	1.2	0.5	0.5	0.5	0.2	0.05
1758	<30		30	<500	<1	7	n.a.	75	20	0.6	0.5	3.1	11	8	2.3	1.0	0.6	4.8	2.4	0.38
1786	56		560	<500	<1	11	n.a.	194	23	5.8	1.8	21.1	49	23	4.3	1.4	0.9	4.0	2.5	0.33
1793	<30		300	<500	<1	13	n.a.	213	29	6.6	1.9	22.9	52	28	4.9	1.5	1.0	4.4	2.9	0.38
1924	83		410	<500	4	27	n.a.	124	65	33.0	6.4	17.8	49	21	6.0	0.9	1.4	9.2	6.0	1.04

MAJOR OXIDES

				SiO2 XRF	TiO2 XRF	Al2O3 XRF	Fe2O3 XRF	FeO wet	MnO XRF	MgO XRF	CaO XRF	Na2O XRF	K2O XRF	P2O5 XRF	LOI XRF
JG91-	0166	A	MVLC	50.7	2.680	14.5	5.5	11.1		3.74	1.36	1.63	2.38	0.41	3.95
JG91-	0722	A	SED	53.5	1.710	16.4	5.4	11.0		3.26	4.16	1.45	1.53	0.15	0.95
JG92-	2507	A	IVLC	51.6	1.450	14.0	3.3	6.9		3.89	6.39	2.33	1.03	0.32	7.60
JG92-	2918	A	DIO	47.5	1.680	14.6	4.1	8.0		7.90	9.18	1.90	1.32	0.32	2.35
JG92-	2918	B	DIO	61.2	1.130	14.1	2.9	5.4		3.31	5.35	3.56	1.03	0.23	1.80
JG92-	2278	A	GRNT-D	75.1	0.148	12.6	0.5	1.3		0.34	1.20	3.72	3.92	0.03	0.60
JG92-	2279	A	GAB	51.0	1.650	15.0	4.5	9.2		4.58	8.03	2.91	0.83	0.37	1.50
JG92-	2345	A	GRNT	68.1	0.626	14.7	1.2	3.0		1.32	0.88	3.61	3.64	0.28	1.65
JG92-	2384	A	GAB	49.4	2.030	13.6	5.6	10.0		4.69	8.25	2.31	0.62	0.62	1.35
JG92-	2477	A	LAM	56.2	1.400	14.4	3.6	5.4		3.12	4.81	3.12	1.02	0.07	6.85
JG92-	2478	A	EPI	78.6	0.091	10.9	0.6	0.8		0.38	0.31	0.20	5.25	0.02	1.30
JG92-	2479	A	FVLC	73.4	0.242	12.9	1.1	2.0		2.43	1.37	3.30	1.07	0.04	2.45
JG92-	2480	A	SED	61.3	0.710	17.5	2.5	5.1		3.05	0.37	4.57	1.51	0.10	3.30
JG92-	2481	A	IRON	52.6	0.127	4.0	11.0	22.0		2.31	1.15	<0.01	1.44	0.07	5.70
JG92-	2482	A	FVLC	76.0	0.215	12.6	1.0	1.6		1.54	0.59	2.81	1.85	0.03	2.20
JG92-	2483	A	EPI	77.0	0.237	11.3	1.2	1.9		0.87	0.28	0.07	3.07	0.03	2.20
JG92-	2484	A	EPI	58.4	1.410	13.1	2.4	4.9		3.59	5.44	4.13	0.29	0.31	5.45
JG92-	2485	A	LAM	48.0	1.570	13.9	4.5	8.9		4.58	7.20	2.42	0.08	0.28	8.60
JG92-	2493	A	MVLC	50.0	0.756	14.6	3.8	7.0		8.65	9.50	2.56	0.19	0.04	1.95
JG92-	2494	A	PLLV	49.4	0.936	16.0	3.4	6.1		3.54	12.40	2.43	0.14	0.08	5.20
JG92-	2495	A	PLLV	59.0	1.020	14.7	2.8	5.4		3.91	5.86	3.51	0.45	0.24	2.45
JG92-	2496	A	PLLV	46.8	1.850	10.8	5.1	9.6		2.19	10.50	0.51	0.93	0.86	10.20
JG92-	2538	A	IVLC	50.6	0.480	16.8	2.5	5.4		6.38	9.45	2.43	1.28	0.07	2.75
JG92-	2590	A	GAB	53.7	1.630	15.5	4.1	8.2		3.47	7.78	3.07	1.05	0.44	0.80
JG92-	2601	A	SED	56.8	0.817	20.0	2.8	5.8		3.22	0.81	1.12	2.57	0.14	4.55
JG92-	2608	A	GRNT	73.0	0.161	14.4	0.6	1.2		0.48	0.73	4.04	4.68	0.07	0.85
JG92-	2824	A	GRNT	71.7	0.222	14.8	0.6	1.4		0.57	2.22	5.25	2.41	0.06	0.65
JG92-	2913	A	GNEISS	64.5	0.374	16.6	1.0	2.3		1.86	2.06	4.72	3.06	0.04	2.75
JG92-	2914	A	SED	78.9	0.499	10.4	1.2	2.5		0.78	0.27	0.08	2.22	0.06	2.05
JG92-	2915	A	FVLC	72.6	0.217	13.4	1.0	1.8		0.88	1.51	4.68	1.83	0.03	1.30
JG92-	2917	A	DIO	50.7	0.897	16.9	3.8	6.2		6.42	8.09	2.40	1.87	0.19	2.85
JG92-	2919	A	DIO	50.5	2.110	13.9	5.1	9.5		4.03	7.54	2.54	1.03	0.32	1.80
JG92-	2931	A	PLLV	48.4	0.919	15.4	4.7	8.2		7.03	10.00	1.58	0.56	0.08	2.20
JG92-	2932	A	PLLV	49.1	0.962	15.6	4.1	8.4		7.94	9.79	2.23	0.50	0.09	1.50
JG92-	2933	A	PLLV	48.6	0.854	14.4	3.9	7.2		5.77	12.50	2.30	0.71	0.07	2.15
JG92-	2935	A	GRNT	71.3	0.249	15.1	0.6	1.4		0.82	0.89	5.75	2.51	0.07	1.10
JG92-	2936	A	GRNT	71.0	0.287	14.8	0.7	1.5		0.98	1.00	5.40	2.82	0.08	1.35
JG92-	2984	A	GRNT	70.6	0.301	15.7	0.7	1.7		0.66	3.00	5.69	1.44	0.08	0.55
JG92-	2999	A	DIO	62.6	0.458	18.2	1.9	3.4		1.14	4.91	5.08	1.17	0.14	1.00
JG92-	3173	A	DIO	61.3	1.000	15.7	2.3	4.8		1.31	4.73	3.85	1.88	0.26	1.00
JG92-	3176	A	DIO	69.2	0.498	14.3	1.7	3.2		0.65	3.58	4.10	1.41	0.13	0.60
JG92-	3270	A	FVLC	63.5	0.451	10.9	2.2	3.8		4.50	7.00	0.34	0.54	0.15	6.95
JG92-	3271	A	LAM	62.9	0.523	14.3	3.9	5.2		3.53	2.13	0.54	3.48	0.31	3.10
JG92-	3272	A	EPI	74.0	0.197	12.2	0.6	0.9		0.77	0.99	0.11	5.44	0.04	2.40

	TRANSITION METALS							GRANITOID			PRECIOUS AND PRECIOUS PATHFINDER						
	Cr NAA	Ni NAA	Co NAA	Sc NAA	Cu	Pb	Zn	Sn	W	Mo	As FAA ppm	Se	Sb	Ag	Ir	Au FA	Hg
0166	30	63	n.a.	21.9	157.0	<2	198.0	n.a.	4	1	34	<5	0.7	<0.5	<20	<1	9
0722	470	60	n.a.	54.1	84.3	<2	75.7	n.a.	<4	6	5	<5	<0.2	0.6	<20	7	8
2507	100	44	n.a.	23.3	28.9	7	261.0	n.a.	<4	<1	2	<5	0.7	<0.5	<20	2	5
2918	460	82	n.a.	27.1	35.4	<2	52.2	n.a.	<4	2	1	<5	0.3	<0.5	<20	5	6
2918	240	37	n.a.	16.0	14.4	<2	38.3	n.a.	<4	4	<1	<5	<0.2	<0.5	<20	2	9
2278	360	8	n.a.	4.0	6.1	<2	18.4	n.a.	<4	6	<1	<5	<0.2	<0.5	<20	3	<5
2279	150	49	n.a.	25.7	49.5	<2	62.7	n.a.	5	2	2	<5	<0.2	<0.5	<20	160	8
2345	270	13	n.a.	7.0	7.3	<2	56.2	n.a.	<4	8	1	<5	<0.2	<0.5	<20	<1	<5
2384	150	40	n.a.	25.0	47.4	<2	87.6	n.a.	<4	3	<1	<5	0.2	<0.5	<20	28	9
2477	170	122	n.a.	16.1	58.2	<2	82.5	n.a.	<4	1	34	<5	0.3	<0.5	<20	8	<5
2478	210	6	n.a.	2.7	8.2	7	68.2	n.a.	<4	7	2	<5	0.4	<0.5	<20	2	<5
2479	130	5	n.a.	4.7	25.2	<2	92.7	n.a.	<4	2	<1	<5	0.2	<0.5	<20	1	<5
2480	240	84	n.a.	16.6	13.9	<2	78.6	n.a.	<4	3	30	<5	0.8	<0.5	<20	<1	6
2481	120	12	n.a.	3.3	7.2	<2	67.6	n.a.	<4	2	<1	<5	0.6	<0.5	<20	<1	10
2482	120	3	n.a.	3.6	1.3	<2	56.6	n.a.	<4	3	<1	<5	0.3	<0.5	<20	<1	<5
2483	90	5	n.a.	3.1	6.5	<2	32.3	n.a.	<4	1	1	<5	0.2	<0.5	<20	3	<5
2484	110	58	n.a.	18.5	53.6	<2	103.0	n.a.	<4	2	<1	<5	0.3	<0.5	<20	<1	<5
2485	100	136	n.a.	24.1	77.6	<2	138.0	n.a.	<4	1	<1	<5	0.4	<0.5	<20	<1	<5
2493	200	29	n.a.	39.7	9.7	<2	31.9	n.a.	<4	2	1	<5	0.9	<0.5	<20	2	7
2494	370	154	n.a.	40.6	162.0	<2	78.0	n.a.	<4	2	15	<5	<0.2	0.7	<20	3	<5
2495	110	38	n.a.	16.7	7.7	<2	107.0	n.a.	<4	3	<1	<5	<0.2	<0.5	<20	<1	<5
2496	40	6	n.a.	29.4	25.9	<2	177.0	n.a.	<4	<1	1	<5	0.3	<0.5	<20	1	<5
2538	150	56	n.a.	26.4	5.4	<2	96.6	n.a.	<4	1	<1	<5	<0.2	<0.5	<20	8	10
2590	150	29	n.a.	23.0	78.8	<2	72.1	n.a.	<4	4	<1	<5	0.9	0.5	<20	2	6
2601	210	86	n.a.	22.1	19.8	25	98.2	n.a.	5	2	32	<5	0.6	<0.5	<20	3	6
2608	330	9	n.a.	1.4	4.5	14	26.2	n.a.	<4	5	<1	<5	<0.2	<0.5	<20	2	<5
2824	380	11	n.a.	2.3	8.6	<2	58.6	n.a.	<4	6	<1	<5	<0.2	<0.5	<20	3	<5
2913	230	38	n.a.	6.5	10.3	12	45.1	n.a.	<4	3	<1	<5	<0.2	<0.5	<20	5	<5
2914	360	28	n.a.	7.0	37.3	3	35.5	n.a.	<4	8	34	<5	0.7	<0.5	<20	2	5
2915	150	9	n.a.	5.8	5.7	15	39.3	n.a.	<4	5	2	<5	2.5	<0.5	<20	1	<5
2917	280	80	n.a.	19.7	66.0	<2	62.2	n.a.	<4	3	1	<5	<0.2	<0.5	<20	<1	10
2919	80	12	n.a.	25.6	64.8	<2	70.3	n.a.	<4	3	1	<5	0.5	<0.5	<20	<1	22
2931	320	65	n.a.	34.8	165.0	<2	58.8	n.a.	4	2	5	<5	0.3	<0.5	<20	2	<5
2932	350	80	n.a.	34.9	118.0	<2	98.4	n.a.	<4	2	<1	<5	<0.2	<0.5	<20	<1	<5
2933	370	73	n.a.	36.4	167.0	24	91.8	n.a.	<4	2	<1	<5	<0.2	0.6	<20	4	6
2935	250	8	n.a.	2.1	12.0	<2	34.2	n.a.	<4	4	<1	<5	<0.2	<0.5	<20	2	<5
2936	260	7	n.a.	2.5	7.3	<2	40.2	n.a.	<4	7	<1	<5	0.2	<0.5	<20	2	<5
2984	330	8	n.a.	2.3	8.9	<2	55.5	n.a.	<4	8	<1	<5	0.2	<0.5	<20	<1	<5
2999	190	9	n.a.	5.9	12.6	<2	75.2	n.a.	<4	6	1	<5	<0.2	<0.5	<20	2	<5
3173	240	7	n.a.	13.0	68.5	<2	81.8	n.a.	<4	11	1	<5	0.4	0.5	<20	2	15
3176	300	9	n.a.	4.7	5.9	<2	72.6	n.a.	<4	5	1	<5	<0.2	<0.5	<20	120	9
3270	100	8	n.a.	6.6	22.6	<2	188.0	n.a.	<4	4	<1	<5	0.5	<0.5	<20	2	<5
3271	60	4	n.a.	11.8	27.5	<2	142.0	n.a.	<4	3	<1	<5	0.6	0.5	<20	<1	<5
3272	110	5	n.a.	3.6	13.9	23	122.0	n.a.	<4	2	1	<5	0.3	<0.5	<20	6	<5

	LOW FIELD STRENGTH				HIGH FIELD STRENGTH							RARE EARTH ELEMENTS								
	Rb	Cs	Ba	Sr	Ta	Nb	Hf	Zr	Y	Th	U	La	Ce	Nd	Sm	Eu	Tb	Dy	Yb	Lu
0166	30	<3	1700	<500	1	n.a.	7	n.a.	n.a.	5.8	2.1	43.6	82	35	7.23	2.01	1.0		3.21	0.47
0722	<30	7	300	<500	<1	n.a.	2	n.a.	n.a.	0.6	0.3	6.4	16	10	3.05	1.19	0.7		3.37	0.54
2507	30	<3	200	<500	<1	n.a.	4	n.a.	n.a.	3.2	0.9	20.5	44	22	5.04	1.30	0.8		2.67	0.41
2918	40	<3	200	<500	<1	n.a.	2	n.a.	n.a.	1.1	0.5	12.8	30	17	4.24	1.64	0.8		2.37	0.35
2916	<30	<3	200	<500	1	n.a.	6	n.a.	n.a.	6.8	1.4	29.0	61	31	6.20	1.61	0.9		3.60	0.55
2278	70	<3	900	<500	<1	n.a.	5	n.a.	n.a.	14.0	1.7	42.4	75	28	4.82	0.90	0.5		1.39	0.20
2279	40	<3	400	<500	1	n.a.	6	n.a.	n.a.	2.4	0.6	32.3	63	33	6.49	1.81	1.0		3.33	0.50
2345	130	3	600	<500	<1	n.a.	7	n.a.	n.a.	29.0	12.6	43.0	87	39	7.95	0.98	0.7		1.57	0.22
2364	<30	<3	200	<500	<1	n.a.	6	n.a.	n.a.	2.4	1.4	26.5	53	27	5.95	1.90	0.8		2.36	0.36
2477	30	<3	400	<500	<1	n.a.	2	n.a.	n.a.	1.3	0.4	5.9	13	7	1.77	0.80	0.3		1.46	0.24
2478	90	<3	700	<500	1	n.a.	5	n.a.	n.a.	20.0	7.3	27.0	59	32	8.30	1.05	1.5		6.32	0.94
2479	50	<3	400	<500	1	n.a.	9	n.a.	n.a.	17.0	5.6	60.5	115	46	9.14	1.25	1.2		5.57	0.87
2480	60	<3	200	<500	<1	n.a.	3	n.a.	n.a.	6.6	2.5	28.0	51	21	4.16	1.22	0.6		1.46	0.22
2481	100	17	100	<500	<1	n.a.	2	n.a.	n.a.	6.8	1.9	17.3	31	13	2.42	0.67	0.2		1.13	0.18
2482	70	<3	300	<500	1	n.a.	9	n.a.	n.a.	21.0	6.6	69.0	135	61	12.10	1.23	1.9		5.54	0.80
2483	<30	<3	200	<500	1	n.a.	7	n.a.	n.a.	19.0	4.8	61.6	120	50	9.64	1.21	1.4		5.90	0.90
2484	<30	<3	200	<500	1	n.a.	4	n.a.	n.a.	4.1	1.1	26.6	51	24	5.29	1.70	0.8		2.52	0.38
2485	<30	<3	<100	<500	<1	n.a.	4	n.a.	n.a.	2.9	0.8	20.6	44	23	5.11	1.92	0.9		3.05	0.46
2493	<30	<3	<100	<500	<1	n.a.	<1	n.a.	n.a.	0.6	1.1	2.7	7	4	1.39	0.52	0.3		1.32	0.21
2494	<30	<3	100	<500	<1	n.a.	1	n.a.	n.a.	0.3	<0.1	3.9	10	6	2.05	0.81	0.4		2.03	0.32
2495	<30	<3	200	<500	<1	n.a.	6	n.a.	n.a.	5.6	1.8	31.1	62	29	6.04	1.69	0.9		2.88	0.44
2496	30	<3	200	<500	<1	n.a.	5	n.a.	n.a.	2.2	0.3	23.5	57	33	8.37	3.01	1.6		4.02	0.60
2538	60	<3	200	<500	<1	n.a.	1	n.a.	n.a.	2.9	0.7	10.3	20	9	1.85	0.75	0.3		1.05	0.17
2590	<30	<3	500	<500	1	n.a.	8	n.a.	n.a.	2.8	1.1	43.3	84	38	7.16	1.98	1.0		3.24	0.47
2601	70	3	600	<500	<1	n.a.	3	n.a.	n.a.	9.9	3.2	18.0	35	15	2.88	0.83	0.6		2.29	0.34
2608	170	<3	1000	<500	2	n.a.	3	n.a.	n.a.	19.0	17.2	34.4	65	21	4.24	0.85	0.5		1.46	0.22
2824	<30	<3	600	<500	<1	n.a.	2	n.a.	n.a.	3.8	1.0	13.0	24	9	1.77	0.46	0.2		0.44	0.06
2913	80	<3	700	<500	2	n.a.	5	n.a.	n.a.	32.0	9.7	41.1	75	28	5.09	0.96	0.4		0.81	0.12
2914	70	<3	400	<500	<1	n.a.	4	n.a.	n.a.	14.0	4.9	34.6	61	24	4.04	0.87	0.5		1.90	0.29
2915	<30	<3	800	<500	1	n.a.	8	n.a.	n.a.	20.0	6.4	74.6	145	64	13.00	1.57	1.9		5.64	0.82
2917	70	<3	200	<500	<1	n.a.	3	n.a.	n.a.	2.0	0.8	17.5	38	19	4.17	1.50	0.6		2.23	0.34
2919	<30	<3	300	<500	<1	n.a.	2	n.a.	n.a.	3.3	1.4	21.3	44	24	5.85	1.82	1.1		3.35	0.50
2931	<30	<3	<100	<500	<1	n.a.	1	n.a.	n.a.	<0.2	<0.1	2.9	7	5	1.74	0.77	0.4		1.95	0.32
2932	<30	<3	<100	<500	<1	n.a.	1	n.a.	n.a.	0.4	0.4	4.0	10	6	1.82	0.87	0.4		1.95	0.31
2933	<30	<3	100	<500	<1	n.a.	1	n.a.	n.a.	0.2	0.8	3.6	9	6	1.78	0.91	0.4		1.84	0.28
2935	70	3	500	<500	<1	n.a.	4	n.a.	n.a.	4.1	2.7	15.4	28	11	1.98	0.66	0.2		0.51	0.07
2936	80	<3	500	<500	<1	n.a.	3	n.a.	n.a.	7.4	1.8	16.4	29	12	2.06	0.48	0.2		0.45	0.06
2984	60	<3	600	<500	<1	n.a.	4	n.a.	n.a.	4.0	1.3	14.6	26	10	1.55	0.58	0.2		0.36	0.05
2999	<30	3	700	<500	<1	n.a.	5	n.a.	n.a.	7.6	2.1	34.8	61	21	3.36	2.26	0.4		1.73	0.28
3173	<30	<3	800	<500	<1	n.a.	10	n.a.	n.a.	12.0	1.9	43.3	84	35	7.19	1.93	1.0		3.46	0.52
3176	<30	<3	1100	<500	<1	n.a.	5	n.a.	n.a.	8.0	1.0	42.3	59	16	2.46	1.93	0.2		0.68	0.10
3270	<30	<3	100	<500	1	n.a.	5	n.a.	n.a.	9.6	3.9	26.9	59	34	8.87	2.96	1.8		6.26	0.92
3271	80	<3	500	<500	1	n.a.	7	n.a.	n.a.	9.6	3.3	42.3	89	44	9.74	2.03	1.6		5.67	0.86
3272	70	<3	600	<500	1	n.a.	5	n.a.	n.a.	18.0	3.9	47.3	93	40	8.01	1.24	1.4		5.08	0.74

MAJOR OXIDES

				SiO2 XRF	TiO2 XRF	Al2O3 XRF	Fe2O3 XRF	FeO wet	MnO XRF	MgO XRF	CaO XRF	Na2O XRF	K2O XRF	P2O5 XRF	LOI XRF
JG92-	3273	A	FVLC	75.5	0.158	11.3	0.9	1.2		1.26	1.38	0.47	4.94	0.03	2.80
JG92-	3275	A	FVLC	73.2	0.194	13.9	1.0	1.5		2.01	0.58	1.13	3.89	0.03	2.50
JG92-	3276	A	LAM	56.3	1.060	14.1	2.8	4.8		3.61	6.02	3.10	0.84	0.26	6.65
JG92-	3277	A	LAM	55.0	1.060	14.6	3.2	7.1		3.37	5.07	2.59	0.43	0.23	5.45
JG92-	3278	A	LAM	51.1	1.410	14.2	2.6	3.9		2.14	9.98	2.05	2.28	0.40	9.45
JG92-	3279	A	EPI	54.9	1.170	15.6	2.4	3.9		1.46	8.80	2.36	1.91	0.25	7.30
JG92-	3280	A	FVLC	77.3	0.169	11.0	0.9	1.3		1.80	0.73	0.14	3.74	0.02	2.35
JG92-	3282	A	SED	62.2	0.701	18.0	2.2	4.1		2.72	1.91	2.31	2.27	0.12	3.50
JG92-	3283	A	LAM	72.7	0.219	12.8	1.0	1.6		0.49	1.85	2.73	2.72	0.04	2.55
JG92-	3284	A	LAM	52.9	1.140	14.4	2.3	3.8		1.75	9.45	3.24	1.32	0.24	9.25
JG92-	3285	A	LAM	48.3	1.130	13.7	3.2	5.9		2.68	10.60	2.44	1.02	0.25	10.80
JG92-	3339	A	DIO	51.3	1.850	14.3	4.5	9.2		4.58	6.75	3.11	1.20	0.44	1.55
JG92-	3368	A	DIO	60.9	0.761	16.1	1.9	4.4		2.78	4.31	5.20	1.35	0.21	1.55
JG92-	3539	A	DIO	51.1	2.030	14.9	4.6	8.4		4.43	8.07	2.76	1.10	0.11	2.45
JG92-	3544	A	FVLC	77.4	0.185	11.9	0.7	1.3		0.46	1.17	2.00	2.65	0.02	2.20
JG92-	3579	A	DIO	50.5	0.638	18.2	2.1	5.2		5.43	8.86	2.86	1.50	0.14	2.70
JG92-	3581	A	GRANO	68.6	0.615	13.8	1.5	3.4		0.86	3.32	4.87	1.41	0.13	1.60
JG92-	3583	A	GRANO	70.6	0.533	13.6	1.1	2.8		1.97	0.64	6.05	0.98	0.10	1.75
JG92-	3584	A	FVLC	75.6	0.154	12.7	0.4	0.7		0.24	1.02	4.24	3.00	0.02	1.45
JG92-	3586	A	PLLV	56.8	1.150	15.2	2.9	6.2		3.24	5.65	3.43	1.15	0.26	3.80
JG92-	3587	A	PLLV	60.0	1.320	14.7	2.6	5.9		2.13	3.65	2.96	1.46	0.35	3.35
JG92-	3588	A	PLLV	49.5	1.980	11.1	5.7	9.0		5.31	6.21	2.16	0.18	0.55	7.00
JG92-	3589	A	PLLV	54.8	1.710	15.7	3.4	6.3		3.68	4.54	4.40	0.57	0.37	2.70

	TRANSITION METALS							GRANITOID			PRECIOUS AND PRECIOUS PATHFINDER						
	Cr NAA	Ni NAA	Co NAA	Sc NAA	Cu	Pb	Zn	Sn	W	Mo	As FAA ppm	Se	Sb	Ag	Ir	Au FA	Hg
3273	110	5	n.a.	3.1	8.7	11	109.0	n.a.	<4	2	<1	<5	0.5	<0.5	<20	2	<5
3275	100	5	n.a.	4.0	6.6	<2	54.9	n.a.	4	2	<1	<5	0.5	<0.5	<20	<1	<5
3276	70	41	n.a.	16.2	49.5	<2	95.8	n.a.	<4	2	1	<5	<0.2	<0.5	<20	1	5
3277	60	41	n.a.	17.6	44.8	<2	102.0	n.a.	<4	<1	1	<5	0.4	<0.5	<20	1	<5
3278	100	49	n.a.	17.1	41.7	<2	77.7	n.a.	<4	6	1	<5	2.2	<0.5	<20	<1	<5
3279	130	42	n.a.	18.9	57.9	<2	90.9	n.a.	<4	1	<1	<5	<0.2	<0.5	<20	<1	<5
3280	90	3	n.a.	2.4	8.0	<2	44.9	n.a.	<4	4	<1	<5	<0.2	<0.5	<20	<1	<5
3282	300	91	n.a.	16.6	15.4	<2	92.4	n.a.	<4	4	34	<5	0.5	<0.5	<20	7	<5
3283	100	6	n.a.	3.8	16.7	<2	41.4	n.a.	<4	2	1	<5	0.3	<0.5	<20	2	<5
3284	100	40	n.a.	16.2	32.1	<2	75.2	n.a.	<4	<1	1	<5	<0.2	<0.5	<20	3	<5
3285	110	88	n.a.	18.3	49.2	<2	111.0	n.a.	<4	<1	<1	<5	0.2	<0.5	<20	2	<5
3339	170	45	n.a.	24.2	52.5	<2	76.9	n.a.	<4	2	1	<5	0.2	<0.5	<20	13	19
3368	190	21	n.a.	12.3	14.9	4	129.0	n.a.	<4	5	<1	<5	<0.2	<0.5	<20	2	5
3539	80	42	n.a.	26.5	46.5	<2	42.5	n.a.	<4	2	1	<5	<0.2	0.6	<20	16	14
3544	180	6	n.a.	2.2	3.2	<2	17.4	n.a.	<4	2	<1	<5	0.3	<0.5	<20	3	<5
3579	110	50	n.a.	22.4	72.7	3	32.1	n.a.	<4	2	6	<5	0.6	<0.5	<20	3	<5
3581	260	9	n.a.	9.2	5.9	<2	26.2	n.a.	<4	7	<1	<5	<0.2	<0.5	<20	<1	12
3583	240	7	n.a.	7.5	4.6	<2	25.0	n.a.	<4	6	<1	<5	<0.2	<0.5	<20	1	<5
3584	160	6	n.a.	3.2	5.2	<2	7.3	n.a.	<4	3	<1	<5	<0.2	<0.5	<20	3	<5
3586	110	40	n.a.	16.7	6.7	<2	128.0	n.a.	<4	3	2	<5	0.2	0.5	<20	2	<5
3587	90	13	n.a.	18.4	58.1	<2	102.0	n.a.	<4	2	<1	<5	<0.2	<0.5	<20	2	<5
3588	250	106	n.a.	26.2	36.9	<2	132.0	n.a.	<4	1	<1	<5	<0.2	<0.5	<20	2	<5
3589	100	43	n.a.	20.7	35.9	<2	107.0	n.a.	<4	4	<1	<5	<0.2	<0.5	<20	<1	<5

	LOW FIELD STRENGTH				HIGH FIELD STRENGTH							RARE EARTH ELEMENTS								
	Rb	Cs	Ba	Sr	Ta	Nb	Hf	Zr	Y	Th	U	La	Ce	Nd	Sm	Eu	Tb	Dy	Yb	Lu
3273	90	<3	400	<500	1	n.a.	6	n.a.	n.a.	16.0	5.3	44.4	89	38	7.85	1.29	1.4		4.38	0.63
3275	80	<3	300	<500	1	n.a.	7	n.a.	n.a.	20.0	7.6	52.7	105	45	9.24	1.32	1.5		5.47	0.82
3276	<30	<3	100	<500	<1	n.a.	4	n.a.	n.a.	5.5	1.2	29.6	56	27	4.96	1.36	0.7		2.70	0.42
3277	<30	<3	100	<500	<1	n.a.	4	n.a.	n.a.	5.4	1.4	29.4	57	26	5.35	1.48	0.8		2.67	0.41
3278	40	<3	500	<500	1	n.a.	5	n.a.	n.a.	3.1	1.1	35.9	72	34	6.63	1.83	1.0		2.63	0.38
3279	40	<3	<100	<500	<1	n.a.	4	n.a.	n.a.	5.1	1.4	30.6	63	29	5.92	1.35	0.8		2.27	0.34
3280	90	4	300	<500	1	n.a.	7	n.a.	n.a.	21.0	6.5	72.7	140	63	12.70	1.32	1.9		6.66	1.00
3282	50	4	600	<500	<1	n.a.	3	n.a.	n.a.	7.1	2.2	33.5	61	24	4.69	1.19	0.5		1.40	0.22
3283	110	4	800	<500	2	n.a.	7	n.a.	n.a.	20.0	3.1	91.7	165	66	11.10	1.66	1.8		5.48	0.81
3284	50	<3	600	<500	<1	n.a.	4	n.a.	n.a.	3.3	0.9	24.6	50	23	4.64	1.59	0.7		1.99	0.29
3285	30	<3	200	<500	<1	n.a.	4	n.a.	n.a.	3.5	1.2	25.4	50	24	5.04	1.37	0.9		2.91	0.44
3339	40	<3	400	<500	1	n.a.	6	n.a.	n.a.	4.7	1.0	35.8	69	35	6.73	2.28	1.1		3.37	0.50
3368	30	<3	400	<500	3	n.a.	5	n.a.	n.a.	4.2	2.2	18.0	39	21	5.04	1.33	0.5		1.18	0.17
3539	30	<3	200	<500	<1	n.a.	3	n.a.	n.a.	4.4	1.1	16.8	33	16	3.50	1.09	0.5		2.09	0.33
3544	40	<3	500	<500	2	n.a.	9	n.a.	n.a.	16.0	4.9	68.4	138	68	14.50	1.86	2.2		8.14	1.21
3579	50	<3	300	<500	<1	n.a.	2	n.a.	n.a.	2.9	0.4	11.4	23	10	2.03	0.99	0.3		1.18	0.17
3581	30	<3	600	<500	1	n.a.	10	n.a.	n.a.	12.0	2.9	36.4	69	32	6.43	1.34	1.1		3.82	0.57
3583	<30	<3	200	<500	1	n.a.	9	n.a.	n.a.	15.0	3.1	35.9	69	29	5.60	1.13	0.9		3.75	0.57
3584	50	<3	900	<500	<1	n.a.	6	n.a.	n.a.	23.0	6.7	71.1	129	52	9.77	1.24	1.4		5.07	0.77
3586	40	<3	200	<500	<1	n.a.	4	n.a.	n.a.	6.9	1.9	28.6	54	26	5.22	1.52	0.7		2.47	0.38
3587	<30	<3	400	<500	<1	n.a.	6	n.a.	n.a.	6.3	1.8	29.4	60	28	6.17	1.57	0.9		3.19	0.50
3588	<30	<3	100	<500	<1	n.a.	5	n.a.	n.a.	4.1	1.2	26.8	62	32	7.13	2.49	1.1		3.57	0.55
3589	<30	<3	300	<500	1	n.a.	5	n.a.	n.a.	4.2	1.4	27.4	56	28	6.11	1.81	1.0		3.07	0.46

MAJOR OXIDES

			SiO2	TiO2	Al2O3	Fe2O3	FeO	MnO	MgO	CaO	Na2O	K2O	P2O5	LOI
			XRF	XRF	XRF	XRF	wet	XRF	XRF	XRF	XRF	XRF	XRF	XRF
JG93-	4171 B	TON	71.6	0.204	14.5	0.9	1.4	0.05	1.23	2.48	4.86	1.27	0.04	1.65
JG93-	4188 A	TON	70.3	0.322	15.2	0.9	2.2	0.08	1.05	2.53	5.10	1.18	0.11	0.75
JG93-	4205 A	FVLC	73.9	0.251	11.8	1.5	1.7	0.06	0.97	3.04	3.24	2.49	0.04	1.25
JG93-	4237 B	LAM-MVLC	51.0	1.000	15.1	3.0	8.8	0.29	3.97	10.10	2.90	0.58	0.10	2.20
JG93-	4259 A	MVLC-flow	63.6	0.751	13.6	2.6	5.0	0.16	2.78	4.98	2.92	1.38	0.15	1.60
JG93-	4296 C	DIA-TREME	45.6	2.130	13.5	5.9	11.4	0.23	5.77	9.56	1.74	0.84	0.27	1.85
JG93-	4350 A	BIO-DIO	48.1	1.710	14.5	4.4	10.9	0.22	6.72	10.40	2.09	0.55	0.27	0.60
JG93-	4413 A	GRNT-parph	62.0	1.150	14.6	3.0	4.7	0.12	1.68	3.76	3.39	2.75	0.43	1.20
JG93-	4691 A	LAM	51.0	1.290	16.2	2.2	8.6	0.18	7.84	2.14	3.90	0.02	0.11	5.55
JG93-	4692 A	LAM	49.6	0.868	14.2	3.5	9.6	0.23	6.12	10.90	2.37	0.81	0.08	1.50
JG93-	4693 B	LAM	47.5	1.070	14.9	4.9	7.0	0.27	4.48	15.20	2.06	0.33	0.10	2.15
JG93-	4693 C	LAM	52.6	1.200	13.8	3.4	7.1	0.32	5.19	11.20	3.71	0.45	0.11	1.40
JG93-	4697 A	CNT rock	56.1	0.758	19.2	2.0	6.3	0.18	4.50	0.88	4.94	1.40	0.10	3.30
JG93-	4717 A	CNT rock	63.0	0.668	16.3	1.8	4.5	0.06	3.48	0.97	1.41	3.19	0.06	3.60
JG93-	4718 A	MVLC-foli	51.2	1.670	14.3	4.3	11.6	0.45	3.89	7.84	2.47	0.51	0.17	1.30
JG93-	4742 A	MVLC-foli	51.7	1.850	14.6	3.4	10.2	0.24	4.64	7.13	3.33	0.32	0.39	1.15
JG93-	4792 A	AMPH	52.7	2.460	13.9	5.2	7.6	0.17	3.91	6.44	3.54	1.17	0.54	1.45
JG93-	5132 A	FVLC	75.5	0.263	12.0	1.6	1.4	0.05	0.44	2.48	3.69	1.93	0.05	0.55
JG93-	5159 A	MVLC	48.8	1.100	13.5	4.1	11.4	0.22	6.77	11.00	1.59	0.25	0.10	0.75
JG93-	5245 A	GRNT	70.8	0.221	15.1	1.2	0.8	0.05	0.65	2.30	5.34	2.37	0.06	0.65
JG93-	5246 A	GRNT	72.7	0.236	14.0	1.0	1.2	0.04	0.60	1.90	4.23	3.31	0.06	0.50
JG93-	5247 A	TON	72.1	0.218	14.6	1.0	1.1	0.04	0.52	2.95	5.19	1.02	0.06	0.30
JG93-	5347 A	TON	72.1	0.256	14.5	0.8	1.8	0.05	0.55	2.77	4.77	1.59	0.09	0.65
JG93-	5417 A	DIO	46.4	2.420	15.1	6.5	6.9	0.15	5.29	8.86	2.51	1.65	1.50	1.55
JG93-	5609 A	DIO	44.4	3.560	13.5	5.5	13.3	0.27	6.15	9.95	1.98	0.50	0.03	1.00
JG93-	5648 A	MVLC	53.2	1.280	12.8	3.7	7.5	0.19	4.49	11.80	2.22	0.45	0.20	2.45
JG93-	5663 A	MVLC-lam	50.3	1.200	13.9	4.1	10.3	0.22	5.70	8.32	2.92	0.29	0.11	1.80
JG93-	5672 A	MVLC	48.7	0.976	13.7	4.2	10.2	0.21	6.50	11.60	1.88	0.18	0.09	0.80
JG93-	5695 A	MVLC	63.2	0.773	12.6	2.0	6.3	0.14	4.24	4.16	3.11	0.91	0.14	1.45
JG93-	5697 A	MVLC	49.1	1.250	12.8	4.5	12.4	0.23	6.21	10.30	1.96	0.43	0.13	0.65
JG93-	5698 A	GRANO	66.5	0.584	15.8	1.6	2.9	0.08	1.13	3.78	4.68	1.80	0.15	0.80
JG93-	5719 A	AMPH	50.6	2.170	12.6	6.0	10.5	0.29	4.75	7.54	2.28	1.56	0.24	1.15
JG93-	5726 A	AMPH	50.5	0.949	14.4	4.6	8.4	0.24	6.06	9.90	2.74	1.21	0.08	0.75
JG93-	5735 A	AMPH	54.9	1.040	14.4	3.0	7.1	0.18	4.57	8.20	3.44	0.40	0.23	1.85

	TRANSITION METALS							GRANITOID			PRECIOUS AND PRECIOUS PATHFINDER						
	Cr NA	Ni	Co	Sc	Cu	Pb	Zn	Sn	W	Mo	As	Se	Sb	Ag	Ir	Au	Hg
4171	230	<100	8	4.3			<50		4	<5	<2	<5	<0.2	<5	<20	<5	<5
4188	200	<100	5	3.2			100		<4	<5	<2	<5	<0.2	<5	<20	<5	<5
4205	180	<100	<5	4.7			<50		4	<5	<2	<5	<0.2	<5	<20	<5	<5
4237	440	<100	57	39.4			200		<4	<5	39	<5	0.3	<5	<20	<5	5
4259	190	<100	23	15.2			110		4	<5	<2	<5	<0.2	<5	<20	<5	<5
4296	180	<100	64	40.2			210		<4	<5	<2	<5	<0.2	<5	<20	<5	<5
4350	340	<100	57	37.9			90		6	<5	<2	<5	<0.2	<5	<20	<5	<5
4413	160	<100	17	12.4			160		6	<5	<2	<5	<0.2	<5	<20	<5	<5
4691	270	<100	45	45.6			140		<4	<5	8	<5	<0.2	<5	<20	<5	<5
4692	330	<100	54	41.4			140		<4	<5	7	<5	<0.2	<5	<20	<5	<5
4693	260	<100	35	35.9			130		<4	<5	<2	<5	0.5	<5	20	<5	<5
4693	350	<100	52	47.3			130		<4	<5	<2	<5	0.6	<5	<20	<5	<5
4697	360	300	24	23.1			150		<4	<5	<2	<5	<0.2	<5	<20	<5	<5
4717	350	<100	12	20.1			100		<4	<5	17	<5	<0.2	<5	<20	<5	<5
4718	230	<100	51	41.7			300		8	<5	13	<5	0.3	<5	<20	<5	<5
4742	140	<100	38	27.4			170		<4	<5	<2	<5	<0.2	<5	<20	<5	<5
4792	120	<100	35	22.6			90		<4	<5	<2	<5	<0.2	<5	<20	<5	<5
5132	250	<100	<5	5.8			110		<4	<5	<2	<5	<0.2	<5	<20	<5	<5
5159	260	300	59	40.9			180		<4	<5	<2	<5	<0.2	<5	<20	<5	<5
5245	240	<100	5	2.5			<50		<4	10	<2	<5	<0.2	<5	<20	<5	<5
5246	160	<100	<5	0.8			<50		<4	<5	<2	<5	<0.2	<5	<20	<5	<5
5247	230	<100	6	0.8			90		<4	<5	<2	<5	<0.2	<5	<20	<5	<5
5347	290	<100	7	2.4			110		<4	<5	<2	<5	<0.2	<5	<20	<5	<5
5417	130	<100	40	26.7			150		<4	<5	<2	<5	<0.2	<5	<20	<5	<5
5609	70	<100	53	39.8			240		<4	<5	<2	<5	<0.2	<5	<20	<5	<5
5648	250	<100	36	26.7			120		<4	<5	<2	<5	0.2	<5	<20	<5	<5
5663	210	300	50	38.3			220		6	<5	2	<5	0.7	<5	<20	<5	<5
5672	200	<100	56	39.2			110		<4	<5	<2	<5	<0.2	<5	<20	<5	<5
5695	380	200	27	19.1			80		<4	<5	3	<5	1.1	<5	<20	<5	<5
5697	170	200	48	37.7			110		<4	<5	<2	<5	<0.2	<5	<20	<5	<5
5698	150	<100	8	5.5			60		<4	<5	<2	<5	<0.2	<5	<20	<5	<5
5719	220	<100	54	43.3			140		9	<5	<2	<5	<0.2	<5	<20	<5	<5
5726	310	200	42	33.6			130		<4	<5	<2	<5	<0.2	<5	<20	<5	<5
5735	210	200	33	24.7			110		<4	<5	<2	<5	0.3	<5	<20	8	<5

	LOW FIELD STRENGTH				HIGH FIELD STRENGTH							RARE EARTH ELEMENTS								
	Rb	Cs	Ba	Sr	Ta	Nb	Hf	Zr	Y XRF	Th	U	La	Ce	Nd	Sm	Eu	Tb	Dy	Yb	Lu
4171	<30	<3	<200	<500	<1	7	6	225	20	12.0	2.4	31.4	58	22	3.69	1.17	0.5		1.83	0.25
4188	80	6	200	<500	<1	14	3	181	13	5.6	1.6	31.3	54	19	2.79	0.74	0.2		0.72	0.10
4205	80	<3	600	<500	<1	25	9	326	57	19.0	5.8	56.0	110	47	9.46	1.56	1.4		5.21	0.78
4237	<30	<3	200	<500	<1	3	2	78	23	0.9	0.3	6.7	16	10	2.60	1.16	0.5		2.07	0.32
4259	60	<3	300	<500	<1	9	5	197	27	7.2	2.2	24.6	49	22	4.40	1.15	0.7		2.43	0.36
4296	50	3	400	<500	<1	11	4	153	35	1.5	0.5	19.4	42	24	5.63	2.02	0.8		3.16	0.49
4350	<30	<3	300	<500	<1	8	2	69	25	0.5	0.5	9.0	22	15	4.17	1.53	0.8		2.40	0.35
4413	100	4	1300	<500	<1	18	9	349	45	20.0	3.3	94.4	171	67	11.40	3.13	1.4		3.67	0.52
4691	<30	<3	<200	<500	<1	6	1	88	17	0.3	0.1	2.5	7	4	1.39	0.51	0.4		2.05	0.33
4692	<30	<3	<200	<500	<1	5	1	66	21	0.3	0.2	3.5	10	7	2.06	0.85	0.4		1.91	0.32
4693	<30	<3	200	<500	<1	7	2	81	23	0.5	0.2	4.6	12	9	2.62	1.01	0.5		2.37	0.38
4693	<30	<3	200	<500	<1	4	2	83	25	0.4	0.2	5.0	12	9	2.69	0.98	0.5		2.35	0.35
4697	170	4	400	<500	<1	8	4	134	32	15.0	3.5	54.1	94	37	6.20	1.52	0.8		2.21	0.31
4717	190	6	500	<500	<1	12	4	156	28	16.0	4.6	35.3	65	26	4.54	1.05	0.6		2.29	0.34
4718	<30	3	300	<500	<1	6	3	121	36	0.8	0.2	6.8	18	13	3.95	1.36	1.0		3.40	0.51
4742	<30	<3	200	<500	<1	18	5	252	39	3.7	0.9	25.6	55	29	6.79	1.90	1.0		3.15	0.46
4792	<30	<3	400	<500	<1	16	5	203	33	4.9	1.3	37.7	77	36	7.46	2.07	0.9		2.99	0.44
5132	<30	<3	700	<500	<1	22	9	277	56	24.0	8.6	62.5	122	54	10.20	1.30	1.5		5.71	0.78
5159	<30	3	<200	<500	<1	4	2	77	22	0.5	0.3	4.2	11	8	2.53	0.99	0.5		2.28	0.37
5245	110	<3	800	<500	<1	7	3	124	5	4.3	1.4	12.8	25	10	1.90	0.61	0.2		0.40	0.05
5246	60	<3	900	<500	<1	8	3	119	3	7.2	2.0	27.9	47	14	2.08	0.60	0.2		0.35	0.05
5247	<30	<3	400	<500	<1	9	4	144	4	3.1	2.5	12.6	21	6	0.80	0.55	<0.1		0.30	0.04
5347	100	4	500	<500	<1	21	5	192	15	6.9	2.9	27.3	52	22	3.86	0.94	0.5		1.34	0.19
5417	70	3	800	1000	<1	14	5	243	42	6.6	2.6	70.8	153	77	16.80	4.01	1.7		2.82	0.40
5609	<30	<3	<200	<500	<1	6	<1	39	5	0.2	0.3	1.5	4	3	0.91	0.85	0.1		0.80	0.13
5648	<30	<3	200	<500	<1	8	2	119	23	2.1	0.9	11.6	27	15	3.60	1.25	0.5		2.01	0.31
5663	<30	<3	200	<500	<1	7	2	85	25	0.4	0.4	4.5	12	9	2.67	1.06	0.5		2.42	0.39
5672	<30	<3	<200	<500	<1	5	2	66	23	<0.2	<0.1	3.5	10	7	2.16	0.70	0.5		2.07	0.33
5695	30	<3	300	<500	<1	12	7	345	36	5.3	2.4	18.8	41	22	5.06	1.47	0.8		3.16	0.50
5697	<30	<3	200	<500	<1	5	2	93	30	0.6	0.5	5.0	14	10	3.08	1.05	0.7		3.01	0.46
5698	<30	3	400	<500	<1	14	7	260	15	7.3	2.1	44.8	82	29	4.46	0.98	0.5		0.93	0.15
5719	<30	3	400	<500	<1	10	5	145	44	2.8	1.8	12.1	30	20	5.76	1.53	1.3		4.47	0.67
5726	<30	<3	200	<500	<1	5	2	66	21	0.4	0.9	4.4	11	7	2.15	0.78	0.4		2.01	0.33
5735	<30	<3	<200	<500	<1	12	4	188	22	3.5	1.3	19.2	41	21	4.74	1.71	0.7		2.40	0.36

APPENDIX B

UTM COORDINATES FOR SAMPLE LOCATIONS

Sample No.	ROCK CODE	Easting	Northing	Rock Descript
0079 A	DIABASE	422789	7331762	NW trending diabase dyke chill margin
0266 A	PLLV	421614	7331273	small pillows, non variolitic
0267 A	PLLV	421753	7331063	small pillows, variolitic
0268 A	PLLV	422070	7330729	small pillows, non variolitic
0288 A	IVLC	419197	7329831	large pillows, plag phenos
0289 A	FVLC	423222	7329843	felsic fragmental rock – volcaniclastic
0414 A	DIO	422855	7335114	diorite near contact of Stock A (mappe
0415 A	DIO	425836	7335249	diorite central portion of Stock A
1295 A	FVLC	435026	7334508	qtz–eye rhyolite
1439 A	IVLC	420082	7328233	massive altered volcanic, chloritized
1509 A	GRNT	414610	7325715	granite west of ABVB
1510 A	GRNT	419887	7325799	Rim Granite – red weathering, qtz–rich
1511 A	DIO	418827	7323540	balck and white diorite
1604 A	PLLV	428712	7331003	small pillows
1632 A	GRNT	434200	7327397	foliated GRNT, east contact of ABVB
1654 A	AMYGD	420490	7327825	ore host to Hood–10, marker unit (Gill, 1976)
1655 A	FVLC	420536	7327634	massive rhyolite at Hood–10
1656 A	FVLC	418641	7330021	massive rhyolite
1657 A	PEG	417580	7331326	qtz–Kspar–musc pegmatite dyke, western ABVB
1659 A	ULTRA	425485	7332838	ultramafic dyke cutting basement
1660 A	BAS–TON	422799	7332337	basement tonalite – 3.35 Ga.
1663 A	GRNT	420308	7334297	foliated rapakivi granite (Tak Granite)
1666 A	FVLC	427718	7329424	qtz–eye rhyolite
1702 A	FVLC	418861	7327845	massive altered volcanic rock
1719 A	IVLC	424214	7329993	mapped as massive mafic volcanic
1754 A	BAS–TON	423226	7331484	basement tonalite
1758 A	BAS–GAB	423714	7331996	gabbro body within basement tonalite
1786 A	Volcani	426241	7329623	intermediate volcani, mafic fragments
1793 A	IVLC	425665	7330013	mapped as massive volcanic
1924 A	CLAST	420691	7333418	feldspar porphyry clast from west cong
0166 A	MVLC	420649	7331652	massive mafic volcanic
0722 A	MAF–LAM	419338	7332874	laminated mafic volcanic
2278 A	GRNT	429311	7333456	granitic dyke cutting diorite
2279 A	DIO	429270	7333517	diorite, mapped as gabbro
2345 A	GRNT	440886	7339124	granite
2384 A	DIO	430388	7338658	diorite, mapped as gabbro
2477 A	MVLC	433148	7333585	pillowed mafic interbedded with lam–int
2478 A	FVLC	432256	7333367	white rhyolite, rare qtz eyes
2479 A	FVLC	432320	7333266	grey qtz–eye rhyolite
2480 A	SED	432333	7333043	
2481 A	IRON	432424	7332851	iron formation
2482 A	FVLC	432428	7332777	qtz–eye rhyolite
2483 A	FVLC	432456	7332735	volcaniclastic
2484 A	INT–LAM	432609	7332646	grey intermediate volcaniclastic, carb
2485 A	INT–LAM	432583	7332898	carb alt intermediate volcaniclastic
2493 A	SYN–GAB	434097	7332547	gabbro sill
2494 A	PLLV	434211	7332844	small pillows

Sample No.	ROCK CODE	Easting	Northing	Rock Descript
2495 A	PLLV	434134	7332948	small pillows
2496 A	PLLV	434096	7333026	small pillows
2507 A	PLLV	428772	7328878	large pillows, plag phenos
2538 A	SYN–GAB	430083	7327070	leucogabbro
2590 A	DIO	425494	7336324	diorite, mapped as gabbro
2601 A	LAM	423698	7338809	strongly laminated volcanic rock
2608 A	GRNT	422369	7339568	granite
2824 A	GRNT	423302	7317473	
2913 A	GNEISS	412307	7322341	melanosome of geochron sample
2914 A	SED	421692	7333750	qtz–wacke matrix of qtz pebble cong
2915 A	FVLC	424702	7323598	massive rhyolite
2917 A	DIO	426379	7323362	black and white diorite
2918 A	DIO	426382	7323114	black and white diorite
2918 B	DIO	426382	7323114	leucocratic diorite
2919 A	DIO	426656	7322717	black and white diorite
2931 A	PLLV	426212	7321920	glomeroporphyritic, small pillows
2932 A	PLLV	426585	7321878	small pillows
2933 A	PLLV	426914	7321714	small pillows
2935 A	GRNT	427592	7321118	contact of Rockinghorse Batholith
2936 A	GRNT	429933	7322162	contact of Rockinghorse Batholith
2984 A	GRNT	431658	7321373	contact of Rockinghorse Batholith
2999 A	DIO	428320	7336686	black and white diorite
3173 A	DIO	424348	7335221	black and white diorite
3176 A	DIO	425873	7335471	mapped as diorite
3270 A	IVLC	433535	7334921	altered volcanic
3271 A	FVLC	433497	7334834	carb filled pockets
3272 A	FVLC	433723	7334698	
3273 A	FVLC	433823	7334669	
3275 A	FVLC	433911	7334582	
3276 A	INT–LAM	433957	7334557	carb altered intermediate volcaniclastic
3277 A	INT–LAM	433989	7334502	carb altered intermediate volcaniclastic
3278 A	INT–LAM	433996	7334472	carb altered intermediate volcaniclastic
3279 A	INT–LAM	434637	7334194	carb altered intermediate volcaniclastic
3280 A	FVLC	434695	7334147	
3282 A	SED	434136	7334439	
3283 A	FVLC	434463	7334605	
3284 A	INT–LAM	434579	7334511	carb altered intermediate volcaniclastic
3285 A	INT–LAM	434709	7334433	carb altered intermediate volcaniclastic
3339 B	DIO	427189	7338464	diorite
3368 A	DIO in GR	439558	7330576	diorite within granite east of ABVB
3539 A	DIO	427536	7323732	black and white diorite
3544 A	FVLC	430984	7323691	qtz–eye rhyolite
3579 A	DIO	427256	7325050	black and white diorite
3581 A	GRANO	428214	7324923	granodiorite
3583 A	GRANO	428803	7325150	granodiorite
3584 A	FVLC	429599	7325098	QFP with Q>P
3586 A	PLLV	430118	7323759	mapped as mafic pillows

Sample No.	ROCK CODE	Easting	Northing	Rock Descript
3587 A	PLLV	430430	7323784	mapped as mafic pillows
3588 A	PLLV	430094	7323481	mapped as mafic pillows
3589 A	PLLV	430770	7323438	mapped as mafic pillows
4171 B	TON	411746	7317829	foliated tonalite within gnessic area
4188 A	TON	403095	7306941	
4205 A	FVLC	403882	7304644	
4237 B	MAF–LAM	404213	7307513	
4259 A	MVLC	405153	7309825	
4296 C	DIATREME	402574	7305159	mafic intrusive with grnt xenoliths
4318 A	HB–GAB	397625	7305889	hornblende gabbro along edge of Slave
4350 A	AMPH	415450	7310249	volcanic belt caught up in diorite
4413 A	GRNT	421052	7305528	porphyritic granite
4616 A	TON	410834	7305340	biotite bearing tonalite
4691 A	MAF–LAM	415410	7325031	laminated mafic rock, west ABVB
4692 A	MAF–LAM	415285	7325213	laminated mafic rock, west ABVB
4693 B	MAF–LAM	415082	7325130	laminated mafic rock, west ABVB
4693 C	MAF–LAM	415082	7325130	laminated mafic rock, west ABVB
4697 A	CNT rock	414980	7325361	sheared granite at west ABVB contact
4717 A	CNT rock	401932	7296129	sheared granite at west PLVB contact
4718 A	MVLC–foli	402170	7296485	strongly foliated mafic volcanic rock
4742 A	MVLC–foli	401879	7295619	strongly foliated mafic volcanic rock
4792 A	AMPH	398708	7297295	amphibolite west of PLVB
5132 A	FVLC	405741	7307677	
5159 A	MVLC	404827	7302338	
5228 A	HB–GAB	399415	7304253	hornblende gabbro along edge of Slave
5245 A	GRNT	419012	7306441	
5246 A	GRNT	420091	7306113	
5247 A	TON	420204	7306631	
5347 A	TON	414877	7309875	
5417 A	DIO in GR	420958	7304181	magnetite–rich diorite in granite
5609 A	DIO	417266	7313153	
5648 A	MVLC	404599	7301545	
5663 A	MAF–LAM	403891	7300009	
5672 A	MVLC	403989	7298295	
5695 A	MVLC	402229	7294936	
5697 A	MVLC	403158	7294413	
5698 A	GRANO	404235	7293896	
5719 A	AMPH	395596	7301429	
5726 A	AMPH	397680	7299797	
5735 A	AMPH	396451	7297553	

LEGEND

15 Quaternary Sediments

14 Diabase Intrusions (classified on the basis of trend)

14a Northeast–trending diabase dykes.
14b East to southeast–trending non–magnetic diabase dykes, commonly plagioclase porphyritic.
14c North–trending diabase dykes.
14d Morel Sills.
14e North–northwest trending Mackenzie diabase dykes, strongly magnetic.

13 Proterozoic Rocks of the Wopmay Orogen

13a Odjick Formation.
13b Rocknest Formation.

12 Mafic Intrusive Rocks of Unknown Age – age relationship to enclosing granitoids obscure.

12a Mafic intrusive rocks composed of hornblende, Kspar and clinopyroxene. (near margin of Slave Province in 86 H/14).
12b Strongly magnetic gabbro, relation to enclosing granitoids unknown.
12c Mafic intrusion containing granitoid xenoliths.
12d Biotite–bearing lamprophyre dyke.

11 Muscovite–bearing Pegmatite Dykes

Quartz–Kspar–muscovite dykes, along the western margin of supracrustal rocks in 86 I/2
Note: muscovite–free pegmatitic dykes are related to unit 9

10 Mixed rocks, locally gneissic (Hybrid Rocks of Bostock, 1980) – amphibolite–facies supracrustal rocks enveloped by dioritic and granitoid rocks.

10a Amphibolites intruded by granitic and pegmatitic rocks; probably derived from volcanic rocks.
10b Coarse–grained amphibolites probably derived from mafic intrusive rocks, mixed with granitoid rocks.
10c Metasedimentary rocks and paragneiss

9 Plutonic Rocks – predominantly granitoid rocks (granite and granodiorite, minor tonalite), and associated pegmatite.

9a Non–to weakly–foliated biotite–granite to granodiorite.
9b Weakly porphyritic biotite–granite to granodiorite.
9c Porphyritic biotite–granite to granodiorite.
9d Foliated rapakivi granite (Tak Granite of Hyde et al., 1976).
9e Red–weathering granite with up to 30% subrounded quartz eyes (Rim Granite of Hyde et al., 1976).
9f Granodiorite to tonalite; appears to be an early phase of 9c in 86 H/15.
9g Mixed foliated granitoids (granite to tonalite), locally with minor amounts of diorite.
9h Strongly deformed granitoids, locally mylonitic, locally includes supracrustal rocks.

8 Synvolcanic Diorite Complex (Western Pluton of Bostock, 1980) – gradational contacts between differing subunits, locally cut by granitic and pegmatitic dykes.

8a Black and white weathering hornblende diorite, locally grading into quartz diorite.
8b Pegmatitic diorite.
8c Agmatite – leucocratic diorite cutting gabbro (unit 1a).
8d Monzogabbro.
8e Granodiorite, commonly transitional to diorite.
8f Fine–grained mafic rocks lacking diagnostic structures, may include fine–grained diorite. and mafic volcanic rocks.
8g Mixed diorite and granite, may contain minor amounts of volcanic–derived amphibolite.

7 Synvolcanic Mafic Intrusions cutting supracrustal rocks

Gabbro, leucogabbro and plagioclase–porphyritic gabbros intruding the Yellowknife Supergroup.

Yellowknife Supergroup – Supracrustal Rocks

6 Metasedimentary Rocks – Mudstones, siltstones, wackes and conglomerates and their metamorphic equivalents

6a Fine–grained clastic rocks, shale, siltstone, commonly as interflow sediments
6b Magnetite–bearing siltstones, iron formation
6c Interbedded mudstones, siltstones, minor wacke beds (predominantly pelite).
6d Interbedded wackes, siltstones and mudstones (predominantly psammite).

EGS 1995-03 Sheet 1 - Geology of

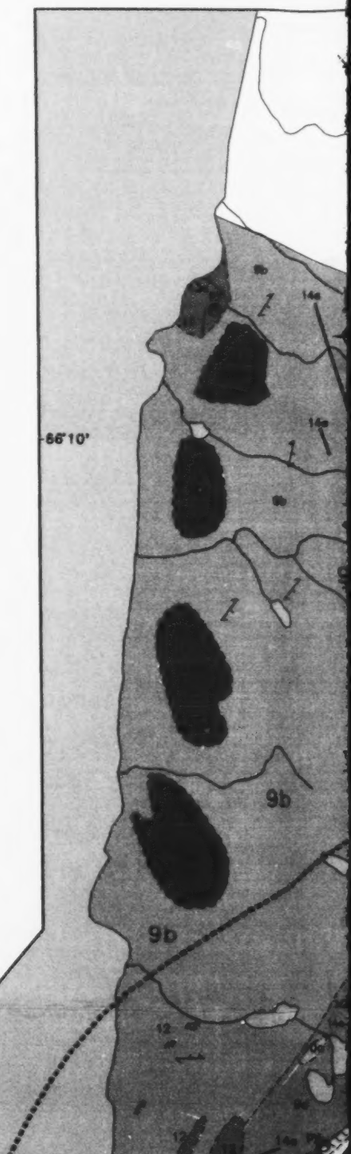

GS 1995-03 Sheet 1 - Geology of the northern Point Lake volcanic belt, par

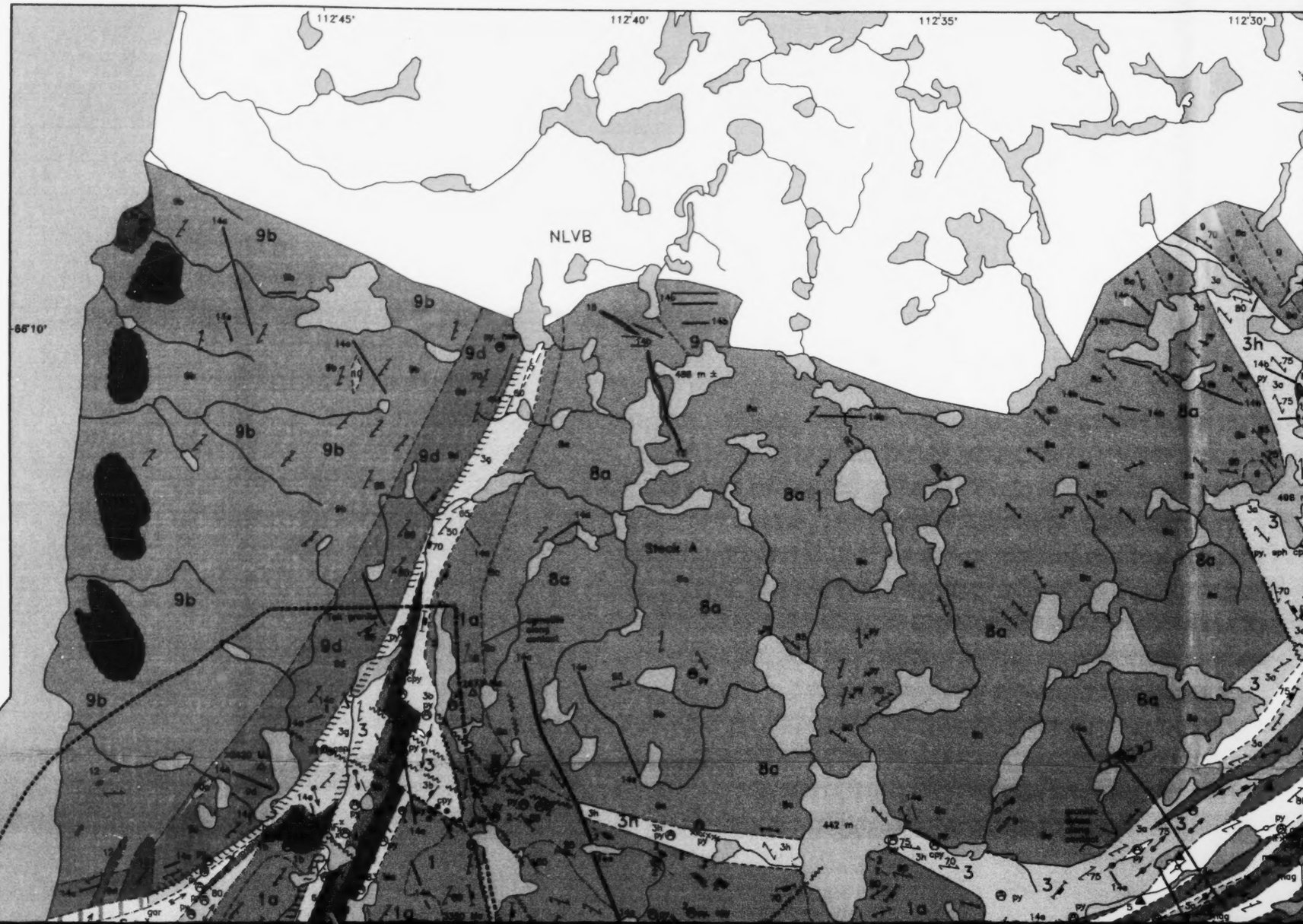

of the northern Point Lake volcanic belt, parts of NTS 86 I/1,2; 86 H/14,15.

8 Synvolcanic Diorite Complex (Western Pluton of Bostock, 1980) – gradational contacts between differing subunits, locally cut by granitic and pegmatitic dykes.

8a Black and white weathering hornblende diorite, locally grading into quartz diorite.
8b Pegmatitic diorite.
8c Agmatite – leucocratic diorite cutting gabbro (unit 1a).
8d Monzogabbro.
8e Granodiorite, commonly transitional to diorite.
8f Fine-grained mafic rocks lacking diagnostic structures, may include fine-grained diorite. and mafic volcanic rocks.
8g Mixed diorite and granite, may contain minor amounts of volcanic-derived amphibolite.

7 Synvolcanic Mafic Intrusions cutting supracrustal rocks

Gabbro, leucogabbro and plagioclase-porphyritic gabbros intruding the Yellowknife Supergroup.

Yellowknife Supergroup – Supracrustal Rocks

6 Metasedimentary Rocks – Mudstones, siltstones, wackes and conglomerates and their metamorphic equivalents

6a Fine-grained clastic rocks, shale, siltstone, commonly as interflow sediments
6b Magnetite-bearing siltstones, iron formation
6c Interbedded mudstones, siltstones, minor wacke beds (predominantly pelite).
6d Interbedded wackes, siltstones and mudstones (predominantly psammite).
6e Quartzite and quartz-wacke
6f Quartz-pebble dominated polymictic conglomerate, grades into units 6e and 6g
6g Polymictic conglomerate with minor quartz-pebbles.
6h Mixed zone of metasedimentary rock and granitoids.

5 Felsic Volcanic Rocks – Massive, phyric, fragmental, volcaniclastic and tuffaceous rocks. Tuffaceous rocks are commonly interbedded with intermediate volcanic rocks.

5a Aphyric, massive felsic volcanic rocks, massive rhyolite.
5b Phyric felsic volcanic rocks with quartz eyes and less commonly feldspar phenocrysts, rhyolite and dacite.
5c Fragmental felsic rocks of possible pyroclastic origin.
5d Fragmental felsic rocks of possible volcaniclastic orgin.
5e Foliated felsic rocks and quartz-eye sericite schists: of probable tuffaceous origin.
5f Felsic volcanic rocks intermixed with mafic and intermediate volcanic rocks.

4 Intermediate Volcanic Rocks – Pillowed and massive flows, and volcaniclastic deposits. Includes interbedded mafic and felsic volcanic rocks.

4a Light-green weathering flows with plagioclase and quartz phenocrysts.
4b Massive flows with up to 50% quartz-filled amygdules (marker unit of Gill, 1976).
4c Light-grey weathering laminated rocks of possible tuffaceous origin, carbonate amygdules, minor felsic volcanic rocks, possible distal volcanic deposits.
4d Mixed intermediate fragmental rocks and felsic volcanic material, more proximal deposits than 4c
4e Fragmental rocks consisting of light coloured fragments set in a mafic-to-intermediate matrix.

3 Mafic to Intermediate Volcanic Rocks – Pillowed and massive flows, and associated gabbroic sills, may locally include minor intermediate and felsic volcanic rocks. Flows are commonly variolitic. Includes laminated rocks of epiclastic or tuffaceous origin.

3a Undivided supracrustal rocks of predominantly mafic composition.
3b Medium- to dark-green pillowed flows with a light-orange weathered surface. Pillows are generally smaller than 40 cm and have 1–2 cm thick selvages. Flows are locally variolitic.
3c Medium- to light-green pillowed flows. Pillows are up to 1 m in length, have irregular amoeboid outlines, thick selvages (3–4 cm) and local clusters of coalesced varioles to 4 cm.
3d Sparsely plagioclase porphyritic and glomeroporphyritic flows.
3e Banded volcanic rocks of the western Point Lake volcanic Belt, includes foliated mafic volcanic rocks, laminated intermediate volcanic rocks, and sedimentary rocks derived from mafic volcanics.
3f Laminated rocks of mafic composition, banding is of sedimentary origin (tuffaceous or epiclastic).
3g Banded mafic rocks of uncertain origin, probably includes both sedimentary and volcanic protoliths.
3h Amphibolite-facies mafic volcanic rocks.
3i Mixed zone containing volcanic rock and granitoids.

Pre-Yellowknife Supergroup

2 Ultramafic Dykes

Red-weathering ultramafic dykes cutting unit 1.

1 Mixed Intrusive Unit – Tonalite and gabbro, minor granitoid bodies; locally strongly foliated and. partially intruded by unit 8. Note: Only the tonalite phase has been dated (ca. 3350 Ma).

1a Gabbro dominated, minor tonalite.
1b Tonalite dominated (tonalite is in places trondhjemitic), minor gabbro.
1c Tonalite dominated with numerous granitoid bodies, minor gabbro.

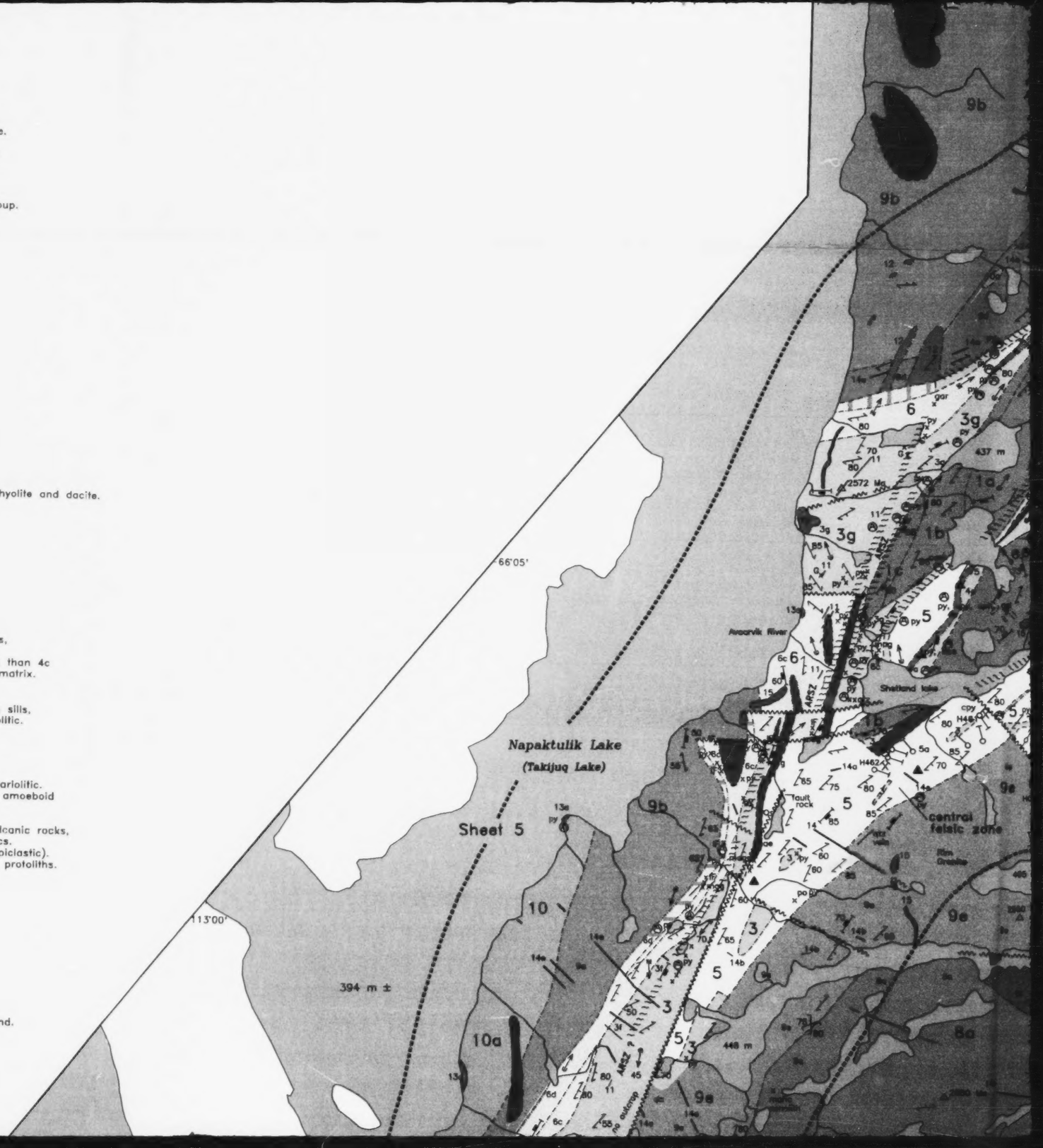

66°05'

Napaktulik Lake
(Takijuq Lake)

Sheet 5

394 m ±

Awarnik River

Shallond lake

central felsic zone

Tault rock

Rim Granite

Hanbechimajuk L.

aeromag anomaly

Stock C

sand bar

clean outcrop

3c large poeson var x

approximate amphibolite isograd

ABVB

no outcrop

mag IF

431 m ±

437 m

448 m

442 m

429 m ±

465 m ± 14b

2572 Mo

2680 Mo

2675 Mo

H462

H48

H-41

H-41A

HCOD-10

no outcrop

aeromag anomaly

mag IF

431 m ±

ABVB

2680 Ma

2675 Ma

2681 Ma

approximate amphibolite isograd

441 m ±

Stack C

66°00'

1 **Mixed Intrusive Unit** – Tonalite and gabbro, minor granitoid bodies; locally strongly foliated and partially intruded by unit 8. Note: Only the tonalite phase has been dated (ca. 3350 Ma).

1a Gabbro dominated, minor tonalite.
1b Tonalite dominated (tonalite is in places trondhjemitic), minor gabbro.
1c Tonalite dominated with numerous granitoid bodies, minor gabbro.

394 m ±
65°00'
65°55'
no outcrop
438±
501±
481±
545±
Sheet 5
Stock 8
10a
9a
9b
8a
8f
3h

Sheet 5
Sheet 8
southern
felsic zone
441 m ±
112°30'
65°35'

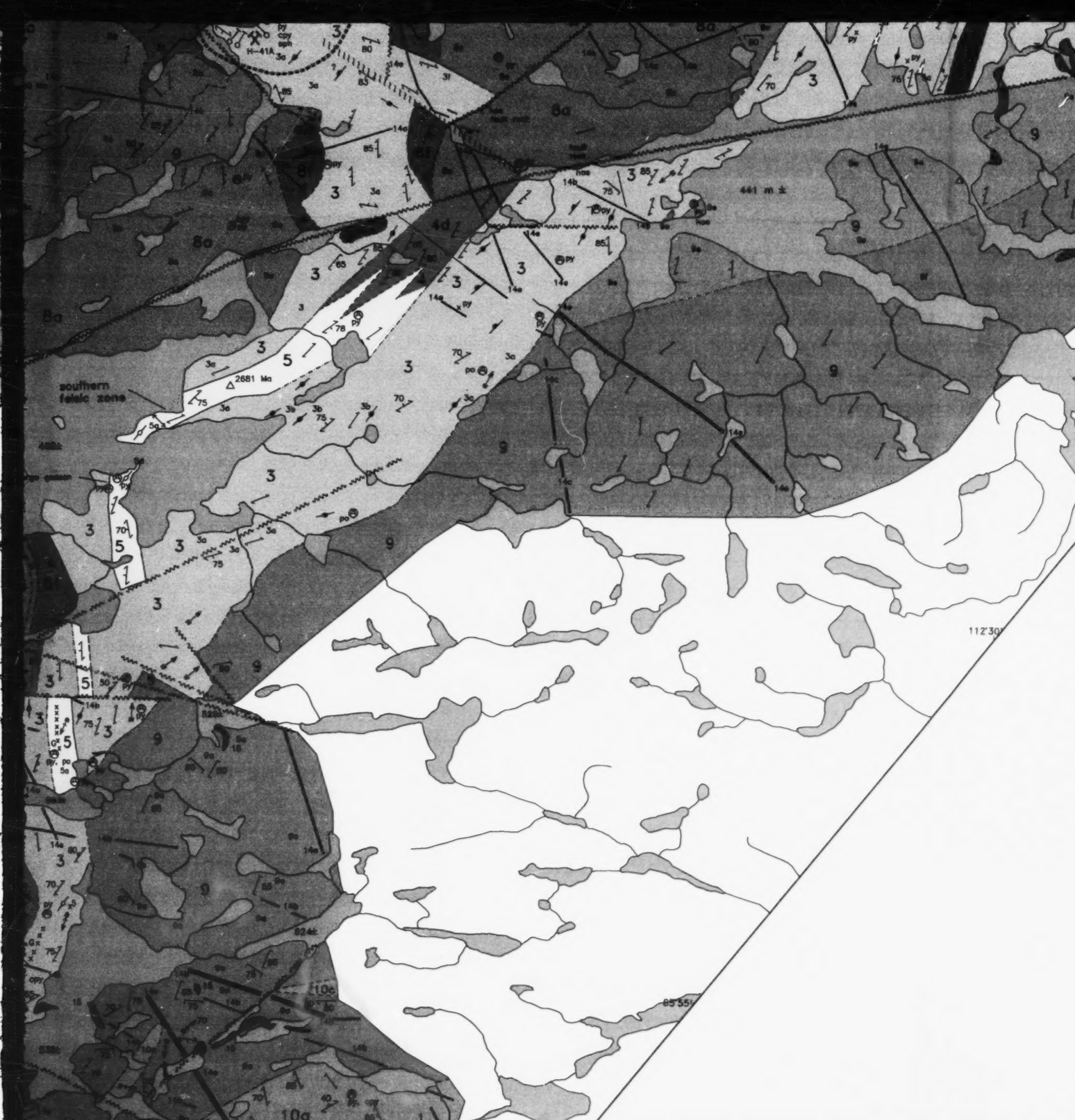

REFERENCES

Bau, A.F.S., Aspler, L.B., and Hurdle, E.J., 1978: Preliminary geology of NTS 86 H/14, 15, 16 District of Mackenzie NWT; DIAND EGS 1978–4.

Bostock, H.H., 1980: Geology of the Itchen Lake area; District of Mackenzie, Geological Survey of Canada, Memoir 391, 101 p.

Craig, B.G., Davison, W.L., Fraser, J.A., Fulton, R.J., Heywood, W.W., and Irvine, T.N., 1960: Geology north-central District of Mackenzie, Northest Territories; Geological Survey of Canada, Map 18–1960.

Fyson, W.K., and Padgham, W.A., 1993: Geology of the Slave Structural Province, 1:1,000,000 scale map; DIAND EGS 1993–8.

Gill, J.W., 1976: The Takiyuak metavolcanic belt, geology, geochemistry and mineralization; unpublished PhD Thesis, Carleton University, Ottawa Ontario, 210 p.

Hyde, R.S., McLeod, H.A., Scribbins, B.T., and Taylor, S.L., 1976: Preliminary geology of NTS 86 I/2, part of the Takiljuq Lake area; DIAND EGS 1976–17.

Hyde, R.S., McLeod, H.A., Scribbins, B.T., and Taylor, S.L., 1976: Preliminary geology of NTS 86 I/1, part of the Takiljuq Lake area; DIAND EGS 1976–18.

GEOCHRONOLOGY

Preliminary data (unpublished) provided by S. Bowring (MIT).

Mortensen, J.K., Thorpe, R.I., Padgham, W.A., King, J.E., and Davis, W.J., 1988: U–Pb zircon ages for felsic volcanism in the Slave Province, NWT; In Radiogenic and Isotopic Studies: Report 2, Geological Survey of Canada, Paper 88–2, pp. 85–95.

Aeromagnetic contour lines from Geological Survey of Canada Aeromagnetic Map 8233G

PLVB

PLVB

PLVB

no outcrop

Roadrunner lake

Outcrop

Geological contact (assu

LEGEND

granitoid rocks
gneissic granitoids

migmatites and gneisses

metasedimentary rocks

felsic/intermediate volca
mafic volcanic rocks

synvolcanic intrusions

pre-2.8 Ga rocks

AL–Aylmer Lake
CCL–Clinton–Colden Lake
CL–Contwoyto Lake
LdG–Lac de Gras
ML–MacKay Lake
NL–Napaktulik Lake
PL–Point Lake

Abbreviations

asp	arsenopyrite
bn	bornite
cpy	chalcopyrite
hae	haematite
gal	galena
mag	magnetite
mo	molybdenite
py	pyrite
po	pyrrhotite
sph	sphalerite
Au	gold
Ag	silver
Cu	copper
Ni	nickel
Pb	lead
Zn	zinc
and	andalusite
gar	garnet
sil	sillimanite
carb	carbonate
gab	gabbro
iF	iron formation
lamp	lamprophyre
qtz	quartz
var	varioles
xeno	xenolith

ABVB	Amooga Booga volcanic belt
ARSZ	Avaarvik River shear zone
ILVB	Izok Lake volcanic belt
NLVB	Napaktulik Lake volcanic belt
PLVB	Point Lake volcanic belt
YK	Yellowknife

MAP SYMBOLS

Outcrop

Geological contact (assumed, transitional)

Aeromagnetic contour lines from Geological Survey of Canada Aeromagnetic Map 8233G

Abbreviations

asp	arsenopyrite
bn	bornite
cpy	chalcopyrite
hae	haematite
gal	galena
mag	magnetite
mo	molybdenite
py	pyrite
po	pyrrhotite
sph	sphalerite
Au	gold
Ag	silver
Cu	copper
Ni	nickel
Pb	lead
Zn	zinc
and	andalusite
gar	garnet
sil	sillimanite
carb	carbonate
gab	gabbro
IF	iron formation
lamp	lamprophyre
qtz	quartz
var	varioles
xeno	xenolith

ABVB	Amooga Booga volcanic belt
ARSZ	Avaarvik River shear zone
ILVB	Izok Lake volcanic belt
NLVB	Napaktulik Lake volcanic belt
PLVB	Point Lake volcanic belt
YK	Yellowknife

MAP SYMBOLS

x

act (assumed, transitional)

LOCATION MAP

Simplified from Fyson and Padgham (1993) – EGS 1993–8

LEGEND

- granitoid rocks
- gneissic granitoids
- migmatites and gneisses
- metasedimentary rocks
- felsic/intermediate volcanic rocks
- mafic volcanic rocks
- synvolcanic intrusions
- pre–2.8 Ga rocks

AL–Aylmer Lake
CCL–Clinton–Colden Lake
CL–Contwoyto Lake
LdG–Lac de Gras
ML–MacKay Lake
NL–Napaktulik Lake
PL–Point Lake

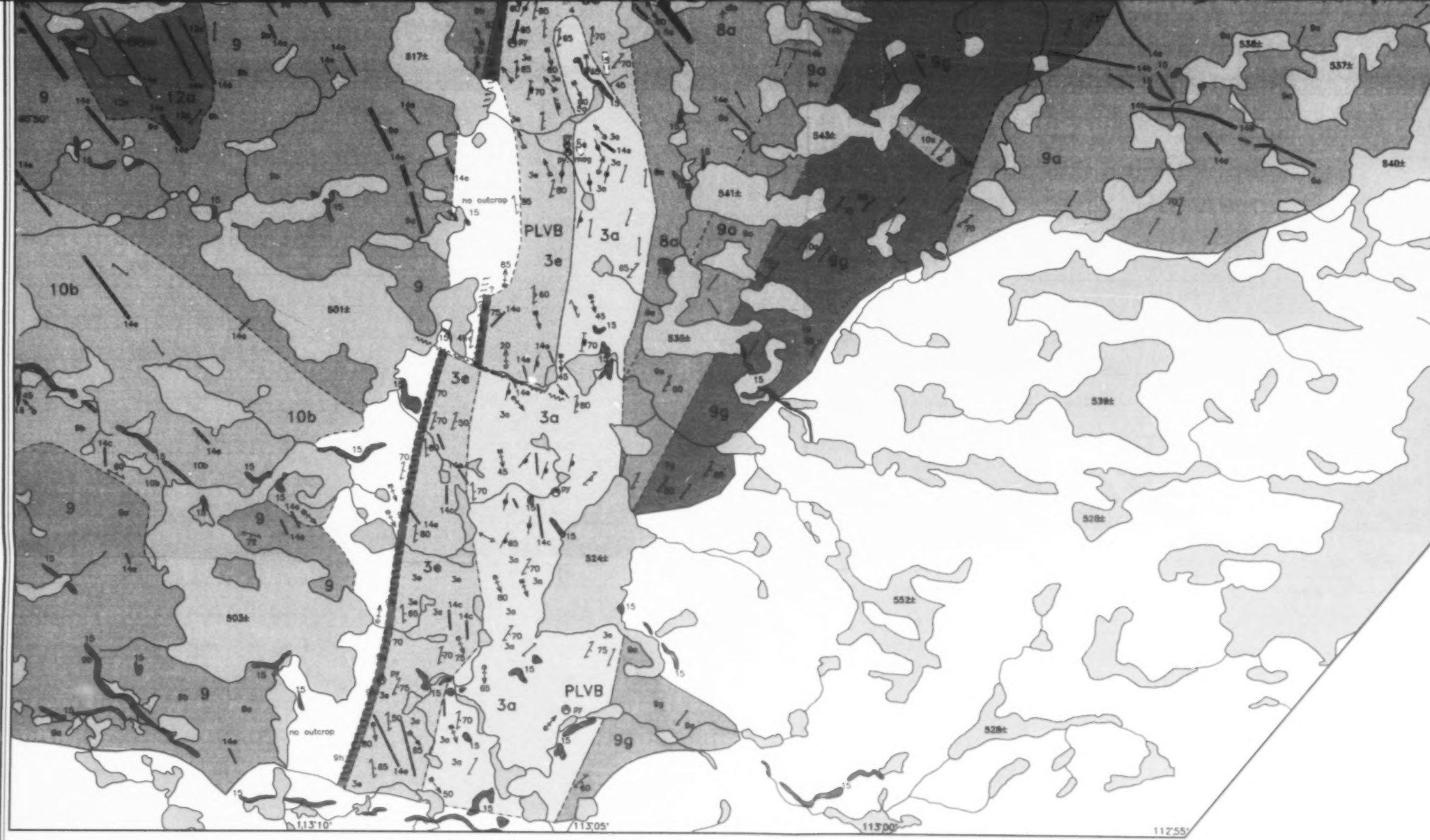

Scale 1 : 50,000

1000 0 1000 2000 3000 4000 metres

Outcrop

Geological contact (a

Bedding (top unknow

Pillows (tops known,

Igneous layering (top

Foliation (local first

Foliation (generation

Syncline

Approximate amphibo

Shearing (displacemen

Clast flattening, fragm

Minor fold (symmetric

Joint

Vein

Fault (known, interp

Shear zone

Glacial striae (directio

Thin dyke (<10 m)

Thick dyke (>10 m)

Gossan

Mineral occurrence, pr

Mineral occurrence tes

Area tested by diamon

Geochronology sample

Geochronology site an

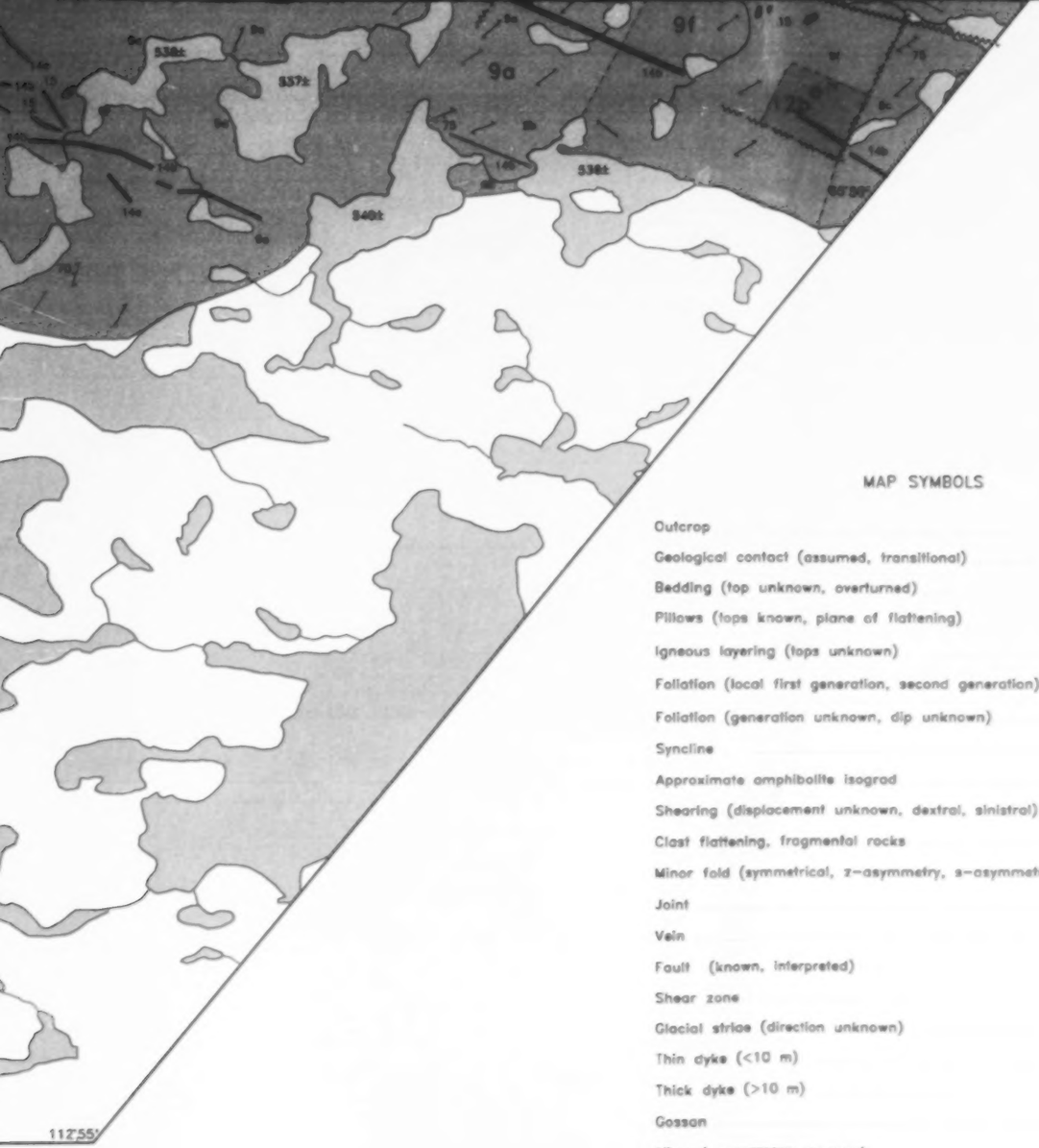

MAP SYMBOLS

- Outcrop
- Geological contact (assumed, transitional)
- Bedding (top unknown, overturned)
- Pillows (tops known, plane of flattening)
- Igneous layering (tops unknown)
- Foliation (local first generation, second generation)
- Foliation (generation unknown, dip unknown)
- Syncline
- Approximate amphibolite isograd
- Shearing (displacement unknown, dextral, sinistral)
- Clast flattening, fragmental rocks
- Minor fold (symmetrical, z-asymmetry, s-asymmetry)
- Joint
- Vein
- Fault (known, interpreted)
- Shear zone
- Glacial striae (direction unknown)
- Thin dyke (<10 m)
- Thick dyke (>10 m)
- Gossan — xG
- Mineral occurrence, prospect — xPy
- Mineral occurrence tested by assay
- Area tested by diamond drilling
- Geochronology sample site and age (Bowring, unpub.) — △ 2680 Ma
- Geochronology site and age (Mortensen et al., 1988) — ▽ 2694 Ma

Cu copper
Ni nickel
Pb lead
Zn zinc

and andalusite
gar garnet
sil sillimanite

carb carbonate
gab gabbro
IF iron formation
lamp lamprophyre
qtz quartz
var varioles
xeno xenolith

ABVB Amooga Booga volcanic belt
ARSZ Avaarvik River shear zone
ILVB Izok Lake volcanic belt
NLVB Napaktulik Lake volcanic belt
PLVB Point Lake volcanic belt
YK Yellowknife

pre-2.6 Ga rocks

AL–Aylmer Lake
CCL–Clinton-Colden Lake
CL–Contwoyto Lake
LdG–Lac de Gras
ML–MacKay Lake
NL–Napaktulik Lake
PL–Point Lake

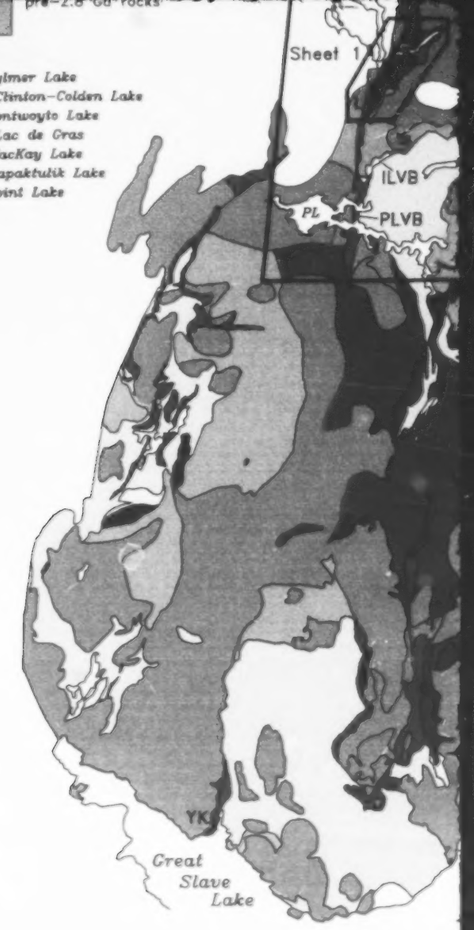

The base map was digitized from 1:50,000 topographic base maps 86 I/1,2; H/14,15 (Transverse Mercator Projection, NAD 1927) produced by the Surveys and Mapping Branch of Energy, Mines and Resources, Ottawa, 1979. Further enlargement of this map may enhance inaccuracies of manual digitization. The 1979 magnetic bearing for the centre of sheet 86 H/15 is 38° 15' east decreasing 9' 3" per year.

Mapping project implemented and managed by Energy, Mines and Petroleum Resources (GNWT) as a contribution to the Canada/NWT Mineral Initiatives.
Mapped between 1991 and 1993 by J. Geberl, T. Faraghar, J. Jensen and D. Stephenson with assistance from R. Gau, L. Gourdine, D. Hanak, C. King, G. Stretch, and J. Tyler.

Cu copper
Ni nickel
Pb lead
Zn zinc

and andalusite
gar garnet
sil sillimanite

carb carbonate
gab gabbro
IF iron formation
lamp lamprophyre
qtz quartz
var varioles
xeno xenolith

ABVB Amooga Booga volcanic belt
ARSZ Avaarvik River shear zone
ILVB Izok Lake volcanic belt
NLVB Napaktulik Lake volcanic belt
PLVB Point Lake volcanic belt
YK Yellowknife

MAP SYMBOLS

- ...act (assumed, transitional)
- ...nknown, overturned)
- ...nown, plane of flattening)
- ...g (tops unknown)
- ... first generation, second generation)
- ...ration unknown, dip unknown)
- ...mphibolite isograd
- ...lacement unknown, dextral, sinistral)
- ..., fragmental rocks
- ...mmetrical, z-asymmetry, s-asymmetry)
- ...
- ...
- ... interpreted)
- ...
- ...direction unknown)
- ... m)
- ...0 m)
- ...
- ...nce, prospect
- ...nce tested by assay
- ... diamond drilling
- ...sample site and age (Bowring, unpub.) △ 2680 Ma
- ...ite and age (Mortensen et al., 1988) ▽ 2694 Ma

pre-2.8 Ga rocks

AL–Aylmer Lake
CCL–Clinton-Colden Lake
CL–Contwoyto Lake
LdC–Lac de Gras
ML–MacKay Lake
NL–Napaktulik Lake
PL–Point Lake

Sheet 1

ABVB
ILVB
PLVB
PL
CL
LdC
AL
CCL
ML
SLAVE PROVINCE
YK
Great Slave Lake

100 km

The base map was digitized from 1:50,000 topographic base maps 86 I/1,2; H/14,15 (Transverse Mercator Projection, NAD 1927) produced by the Surveys and Mapping Branch of Energy, Mines and Resources, Ottawa, 1979. Further enlargement of this map may enhance inaccuracies of manual digitization. The 1979 magnetic bearing for the centre of sheet 86 H/15 is 38° 15' east decreasing 9' 3'' per year.

Mapping project implemented and managed by Energy, Mines and Petroleum Resources (GNWT) as a contribution to the Canada/NWT Mineral Initiatives. Mapped between 1991 and 1993 by J. Gebert, T. Faroghar, J. Jensen and D. Stephenson with assistance from R. Gau, L. Gourdine, D. Hanak, C. King, G. Stretch, and J. Tyler.

MINERAL INITIATIVES
1991-1996 CANADA-NWT ECONOMIC DEVELOPMENT AGREEMENT

NWT GEOLOGICAL MAPPING DIVISION
Box 1500 – Yellowknife

Indian and Northern Affairs Canada
Affaires indiennes et du Nord Canada

EGS 1995–03 Sheet 1 – Geology of the northern Point Lake volcanic belt, parts of NTS 86 I/1,2; 86 H/14,15.

Mineral Initiatives 1991–1996
Canada–NWT Economic Development Agreement
by J.S. Gebert

1 map ($15.00)

EGS 1995-03 Sheet 3 - Geochemical sample location overlay for g

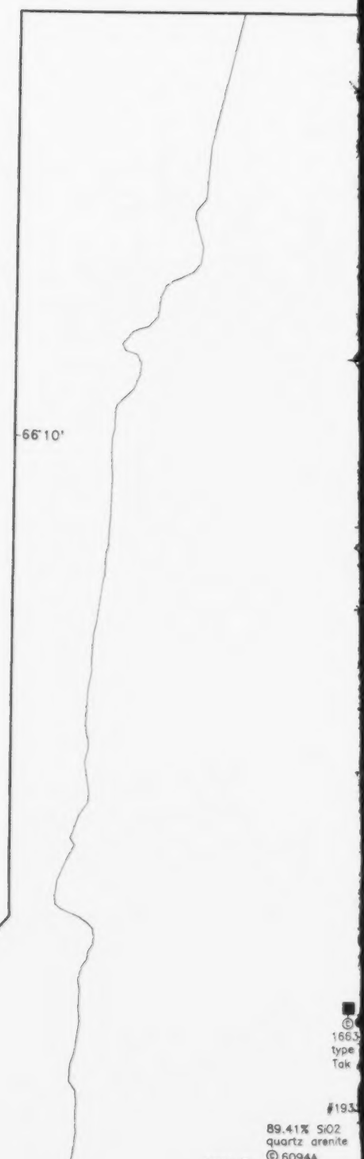

al sample location overlay for geology map (Sheet 1)

geology map (Sheet 1)

112°45' 112°40' 112°35' 112°30' 112°25' 112°20'

2608
© type I granite

©2601
int pattern
56.8% SiO2

©3339B
type II diorite
51.3% SiO2

©2384
type II diorite
49.4% SiO2

©2345
type I granite

66°10'

(3305)
©2999
type I diorite
62.6% SiO2

53.7% SiO2
type III diorite
©2590

69.2% SiO2
type I diorite
©3176

2673 Ma
©3173
type II diorite
61.3% SiO2
©0415
type II diorite
56.29% SiO2
©0414
type II diorite
52.80% SiO2

LREE enriched pattern
low Na2O
©3270 ©3273 low Na2O
low Na2O ©3271 3275 felsic pattern
low Na2O ©3272 3276 LREE enriched pattern
LREE enriched pattern ©3277 3283 felsic pattern
LREE enriched pattern ©3278 ©3282 3284 LREE enriched pattern
©3279 ©3280 3285 LREE enriched pattern
low Na2O
1295 high K2O
>2620 Ma

1663
type I granite
Tak Granite

84.15% SiO2
©7036A
©2914
LREE enriched pattern
78.9% SiO2

#1931 ©2924
similar to felsic pattern
clast from conglomerate

#1930
2583 Ma

65.17% SiO2
1660
3350 Ma

7077A ©
tonalite

©1659
32.50% MgO
high LOI

51.0% SiO2
type III diorite
©2279

©2278
type I granite

low Na2O
felsic pattern
2478 ©2479 felsic pattern
©2477
flat pattern
high LOI
2480 ©
iron formation 2481 ©2485 LREE enriched
felsic pattern 2482 ©2483 low Na2O
2484 ©
LREE enriched pattern
high LOI

2496 LREE enriched pattern
2495 LREE enriched pattern
©2494 flat pattern
©2493 flat pattern

89.41% SiO
quartz aren
©6094A
0722 ©
flat pattern
©6086A
1657
©
2572 Ma
clast from congl. 6106A
quartz wacke 6106B ©
75.64% SiO2
66°05'
©6105A gabbro
61058 tonalite
©1656
felsic pattern
©0288
LREE enriched patte
©
6066A
6066B
6066C
©
6074A
6074B
1439©
©6121A
sil+cord+and schist
©
1702
felsic pattern
low Na2O
LREE enriched
hi
amygda
113°00'
1509 ©
type I granite
4697A ©
sheared contact rock
6.12% MgO
flat pattern
©4692A
4693C ©
4693B
flat pattern
©4691A
flat pattern
7.85% MgO
high LOI
2550 Ma
©1510
similar
Rim Gr
2680 Ma
©1511
type I diorite
50.84% SiO2

66°05'

2560 Ma

6121A
all+cord+and schist

1509 E
type I granite

4697A E
sheared contact rock

4693C C
4693B
flat pattern

6.12% MgO
flat pattern
C 4692A

C 4691A
flat pattern
7.85% MgO
high LOI

6066A
6066B
6066C

6074A
6074B

1657
C
2572 Ma

clast from congl. 6106A
quartz wacke 6106B
75.64% SiO2

6105A gabbro
6105B tonalite

C 1656
felsic pattern

C 7011A
tonalite

C 0288
LREE enriched pattern

1702
felsic pattern
low Na2O

low Na2O
1439 E LREE enriched pattern

1654 E
LREE enriched pattern
high LOI
amygdal. unit

2675 Ma
C 1655
felsic pattern

2550 Ma
C 1510
similar to felsic pattern
Rim Granite

2680 Ma
C 1511
type I diorite
50.84% SiO2

2673 Ma
C
0414
type II diorite
52.80% SiO2

1653
C
type I granite
Tak Granite

84.15% SiO2
C 7036A
2914
LREE enriched pattern
78.9% SiO2

#1931 C 2924
similar to felsic pattern
clast from conglomerate

89.41% SiO2
quartz arenite
E 6094A

#1930
2583 Ma

0722 C
flat pattern

65.17% SiO2
1660
C
3350 Ma

7077A C
tonalite

6086A

0079 E
diabase

flat pattern
E 1758

LREE enriched pattern
0166 C

C 1754
71.00% SiO2

high LOI
LREE enriched pattern
E 0266

C 0267
LREE enriched pattern
high LOI

tonalite
C 6130A

C 0268
flat pattern

tonalite
7072A C

C 6131A
gabbro

C 7059A
tonalite

C 0289
felsic pattern
fragmental rock

C 1719
LREE enriched pattern
58.37% SiO2

C 1793
LREE enriched pattern
60.03% SiO2

C 1788
LREE enriched pattern
fragmental rock

1666 C
2680 Ma
felsic pattern

2694 Ma
C 6155A
LREE enriched pattern

C 2507
LREE enriched pattern

C 2999
type I diorite
62.6% SiO2

53.7% SiO2
type III diorite
C 2590

69.2% SiO2
type I diorite
C 3176

C 3173
type II diorite
61.3% SiO2

C
0415
type II diorite
56.29% SiO2

LREE enriched pattern
low Na2O
3270
low Na2O 3271
low Na2O 3272
LREE enriched pattern 3277
LREE enriched pattern 3278
LREE enriche

51.0% SiO2
type III diorite
C 2279

C 2278
type I granite

low Na2O
felsic pattern
2478
C 2479
felsic pattern
2480
C

C 2477
flat pattern
high LOI

iron formation 2481 C
felsic pattern 2482 C
C 2485 LREE enriched
2483 low Na2O
2484
LREE enriched pattern
high LOI

C 1859
32.50% MgO
high LOI

C 1604
flat pattern
high LOI

#7081

#7082

C 7080A

C 7079A

#7078

C 2538
LREE enriched

similar to type I granite
similar setting to Rim Granite
3583 E

3579 C
type I diorite
50.5% SiO2

C 3581
similar to type I granite
similar setting to Rim Granite

E 3584
felsic pattern

felsic pattern
C 3515

50.7% SiO2
type III diorite
C 2917

C 3539
type III diorite
51.1% SiO2

2918A C 2918B
type II diorite
47.5% SiO2
type III diorite
61.2% SiO2

C 2919
type III diorite
50.5% SiO2

LREE enriched pattern
3586 E

3588 E
LREE enriched pattern

LREE enriched pattern
E 3587

C 3544
felsic pattern

3589 E
LREE enriched pattern

#2937

+ Eu anomaly

+ Eu anomaly

C 2936
type II granite

53.7% SiO2
type III diorite
© 2590

type I diorite
62.6% SiO2

69.2% SiO2
type I diorite
© 3176

2673 Ma
0414
type II diorite
52.80% SiO2

©3173
type II diorite
61.3% SiO2

0415
type II diorite
56.29% SiO2

LREE enriched pattern
low Na2O
3270
low Na2O 3271
low Na2O 3272
low Na2O
3273
3275 felsic pattern
3276 LREE enriched pattern
3283 felsic pattern
3284 LREE enriched pattern
3285 LREE enriched pattern
1295 high K2O
>2620 Ma
LREE enriched pattern 3277
LREE enriched pattern 3278
3282
3279
LREE enriched pattern
3280
low Na2O

1663
type I granite
Tak. Granite

84.15% SiO2
7036A
2914
LREE enriched pattern
78.9% SiO2

#1931
2924
similar to felsic pattern
clast from conglomerate

51.0% SiO2
type III diorite
©2279

©2278
type I granite

low Na2O
felsic pattern
2478
2479
felsic pattern
2480
2477
flat pattern
high LOI

iron formation 2481
felsic pattern 2482
2485 LREE enriched
2483 low Na2O
2484
LREE enriched pattern
high LOI

2496 LREE enriched pattern
2495 LREE enriched pattern
2494 flat pattern
©2493 flat pattern

#1930
2583 Ma

65.17% SiO2
1660
3350 Ma
7077A
tonalite

©1659
32.50% MgO
high LOI

0079
diabase
flat pattern
©1758

LREE enriched pattern
0166

©1754
71.00% SiO2

high LOI
LREE enriched pattern
©0266

©0267
LREE enriched pattern
high LOI

©0268
flat pattern

tonalite
©6130A
tonalite
7072A
©6131A
gabbro
©7059A
tonalite

©1604
flat pattern
high LOI

©3368
similar to diorite II
60.9% SiO2

©7011A
tonalite

pattern

©0289
felsic pattern
fragmental rock

©1719
LREE enriched pattern
58.37% SiO2

©1793
LREE enriched pattern
60.03% SiO2

©1786
LREE enriched pattern
fragmental rock

1686
2680 Ma
felsic pattern

2694 Ma
©6155A
LREE enriched pattern

©2507
LREE enriched pattern

66°05'

low Na2O
LREE enriched pattern

#7081

#7082

©7080A

1654
high LOI
mygdal. unit

2675 Ma
©1655
felsic pattern

©7079A

©1632
type I granite

#7078

©2538
LREE enriched

0 Ma
©1510
similar to felsic pattern
Rim Granite

similar to type I granite
similar setting to Rim Granite
3583
3579
type I diorite
50.5% SiO2
©3581
similar to type I granite
similar setting to Rim Granite
©3584
felsic pattern

felsic pattern
©2915

©3539
type III diorite
51.1% SiO2

50.7% SiO2
type III diorite
©2917

LREE enriched pattern
3586
3588
LREE enriched pattern

LREE enriched pattern
©3587
©3544
felsic pattern
3589
LREE enriched pattern

2918A
type II diorite
47.5% SiO2
©2918B
type III diorite
61.2% SiO2
©2919
type III diorite
50.5% SiO2

#2937

©2936
type II granite

+ Eu anomaly
flat pattern
+ Eu anomaly

113°00'

66°00'

65°55'

1509 ©
type I granite

4697A ©
sheared contact rock

6.12% MgO
flat pattern
© 4692A

4693C ©
4693B ●
flat pattern

© 4691A
flat pattern
7.85% MgO
high LOI

2560 Ma
2913 ©
mafic portion of amphibolite gneiss

2550
sim
Rim

2580 Ma
© 1511
type I diorite
50.84% SiO2

● © 4171B
type II granite pattern

● © 5609
44.4% SiO2

type I granite

4697A ©
sheared contact rock

6.12% MgO
flat pattern
© 4692A

4693C ©
4693B ●

© 4691A
flat pattern
7.85% MgO
high LOI

■ 2560 Ma
2913 ©
mafic portion of amphibolite gneiss

similar to felsic pattern
Rim Granite

2680 Ma
■
© 1511
type I diorite
50.84% SiO2

3583 ©

© 3584
felsic pattern

3579 ©
type I diorite
50.5% SiO2

© 3581
similar to type I granite
similar setting to Rim Granite

LREE enriched pattern
3586 ©

LREE enriched pattern
© 3587

© 3544
◪ felsic pattern

felsic pattern
© 2915
◪

© 3539
type III diorite
51.1% SiO2

50.7% SiO2
type III diorite
● © 2917

3588 ©
LREE enriched pattern

3589 ©
LREE enriched pattern

2918A © 2918B
type II diorite
47.5% SiO2
type III diorite
61.2% SiO2

© 2919
type III diorite
50.5% SiO2

#2937
◪

© 2936
type II granite

+ Eu anomaly
flat pattern
2931 ◪ ●

+ Eu anomaly
flat pattern
© 2932

stratigraphic base of ABVB ?

© 2933
+ Eu anomaly
flat pattern

© 2984
type II granite

●© 2935
type II granite

● ■ 2681 Ma
#2767

● © 41718
type II granite pattern

© 2824
type II granite

● © 5609
44.4% SiO2

112°30'

65°55'

similar setting to Rim Granite

felsic pattern
© 2915

50.7% SiO2
type III diorite
●© 2917

© 3539
type III diorite
51.1% SiO2

2918A © 2918B
type II diorite
47.5% SiO2
type III diorite
61.2% SiO2

© 2919
type III diorite
50.5% SiO2

+ Eu anomaly
flat pattern
2931 ©●

+ Eu anomaly
flat pattern
© 2932

stratigraphic base of ABVB ? ©2933
+ Eu anomaly
flat pattern

●© 2935
type II granite

LREE enriched pattern
3586 ©
3588 ©
LREE enriched pattern

LREE enriched pattern
© 3587
©3544
felsic pattern
3589©
LREE enriched pattern

© 2936
type II granite

#2937

© 2984
type II granite

66°00'

2681 Ma
#2767

© 2824
type II granite

112°30'

65°55'

65°55'

© 5609
44.4% SiO2

© 4350
similar to LREE enriched pattern

© 5347
type II granite

© 4259
LREE enriched pattern

© 5132
felsic pattern

© 4237B
flat pattern

© 4188
type II granite pattern

type II

5245 ©

type I

© 5246

12.42% MgO
© 6161A
Ⓟ4318

© 4616
type II granite

mafic intrusive with grnt xenoliths
© 4296C
similar to LREE enriched pattern

© 4205
felsic pattern

similar

© 5228
6160A ©
7.22% MgO

65°50'

© 5159

112°30'

65°55'

© 5609
44.4% SiO2

© 4350
similar to LREE enriched pattern

© 5347
type II granite

type II granite

type II granite

5245 ©

© 5248

5247 type II granite

© 4413
type II granite

© 4616
type II granite

5417A © 5417B
similar to LREE enriched pattern
46.4% SiO2

65°50'

112°30'

65°55'

type II granite

type II granite

© 5246

5247 type II granite

© 4413
type II granite

5417A © 5417B
similar to LREE enriched pattern
46.4% SiO2

12.42% MgO
6161A
4318

mafic intrusive with grnt xenoliths
4296C
similar to LREE enriched pattern

4616
type II granite

4205
felsic pattern

5228
6160A
7.22% MgO

5246

similar to LRE

65°50'

5159
flat pattern
6.77% MgO

65°50

2100 m to sample 5719 (395596,7301429)

5648
LREE enriched pattern
4.49% MgO

5726
flat pattern

5663
flat pattern
5.70% MgO

5708

5672
flat pattern
6.50% MgO

1240 m to sample 5735 (396451,7297553)

4792
LREE enriched pattern

3.89% MgO
flat pattern
4718

4717
sheared granite at belt contact

4742
LREE enriched pattern
4.64% MgO

5695
LREE enriched pattern
4.24% MgO

4752

5697
flat pattern
6.21% MgO

5698
type II granite

113°10'
113°05'
113°00'
112°55'

© 4413
type II granite

5417A © 5417B
similar to LREE enriched pattern
46.4% SiO2

65°50'

112°55'

© geochemical sample

◆ geochron sample: Mortensen et al. 1988

■ geochron sample: Boering unpublished (MIT)

◪ geochron sample: not yet analyzed

● Nd/Sm sample site: Jensen (1995)

© geochemical sample

◆ geochron sample: Mortensen et al. 1988

■ geochron sample: Bowring unpublished (MIT)

◪ geochron sample: not yet analyzed

● Nd/Sm sample site: Jensen (1995)

MINERAL INITIATIVES

1991-1996 CANADA-NWT ECONOMIC DEVELOPMENT AGREEMENT

NWT GEOLOGICAL MAPPING DIVISION
Box 1500 – Yellowknife

Indian and Northern Affairs Canada | Affaires indiennes et du Nord Canada

EGS 1995-03 Sheet 3 – Geochemical sample location overlay for geology map (Sheet 1)

Mineral Initiatives 1991–1996
Canada–NWT Economic Development Agreement
by J.S. Gebert

Assay data overlay ($5.00)